Identification of Expansive Soils Using Remote Sensing and In-Situ Field Measurements – Phase I

Dr. Richard A. Coffman, P.E., PLS
and Cyrus D. Garner, MSCE, EIT

MBTC DOT 3031
October 2012

Prepared for
Mack-Blackwell Rural Transportation Center
University of Arkansas
The National Transportation Security Center of Excellence:
A Department of Homeland Security
Science and Technology Center of Excellence

ACKNOWLEDGEMENT
This material is based upon work supported by the U.S. Department of Transportation under Grant Award Number DTRT07-G-0021. The work was conducted through the Mack-Blackwell Rural Transportation Center at the University of Arkansas.

REPORT DOCUMENTATION PAGE

Form Approved
OMB No. 0704-0188

1. AGENCY USE ONLY *(Leave Blank)*	2. REPORT DATE	3. REPORT TYPE AND DATES COVERED
	October 2012	Technical 7/1/2011 – 9/1/2012

4. TITLE AND SUBTITLE
Identification of Expansive Soils Using Remote Sensing and In-situ Field Measurements – Phase I

5. FUNDING NUMBERS

6. AUTHOR(S)
Dr. Richard A. Coffman, PE, PLS and Cyrus D. Garner, MSCE, EIT

7. PERFORMING ORGANIZATION NAME(S) AND ADDRESS(ES)
Mack-Blackwell Rural Transportation Center
4190 Bell Engineering Center
University of Arkansas
Fayetteville, AR 72701

8. PERFORMING ORGANIZATION REPORT NUMBER
MBTC DOT 3031

9. SPONSORING/MONITORING AGENCY NAME(S) AND ADDRESS(ES)
US Department of Transportation
Research and Special Programs Administration
400 7th Street, S.W.
Washington, DC 20590-0001

10. SPONSORING/ MONITORING AGENCY REPORT NUMBER

11. SUPPLEMENTARY NOTES

Supported by a grant from the U.S. Department of Transportation University Transportation Centers program

12a. DISTRIBUTION/AVAILABILITY STATEMENT

12b. DISTRIBUTION CODE
N/A

13. ABSTRACT (MAXIMUM 200 WORDS)

Researchers at the University of Arkansas have conducted research on the suitability of using remote sensing techniques (radar and LIDAR) to monitor the shrink-swell behavior of an expansive clay material in a field test site as part of the Mack Blackwell Rural Transportation Center Project 3031. The field test site consisted of two 5,000 square foot compacted clay pads installed at the University of Arkansas' Cato Springs Research Center (CSRC). In Phase I-A of the project four LIDAR scans and 335 radar scans were captured over an eight month period. The pads were constructed of eight inches of compacted clay material sourced from a local supplier overlying a two inch sand blanket. One pad was amended by the addition of three percent sodium bentonite (by dry weight) to increase the expansive behavior of the material. Radar scans were conducted on a weekly basis or after significant precipitation events. Additionally in Phase I-B, an additional three percent bentonite was added to the expansive pad and both pads were reconstructed. Results generated by this research project indicate that the LIDAR was able to detect the presence of ground movement due to expansive material. However, processing limitations severely curtailed the accuracy of this method. There were several issues encountered with the installation of the in-situ monitoring equipment in the compacted clay. Further research is required to determine the optimum method of installing TDR probes in compacted clay. TDR probes and tensiometers were used to develop the soil water characteristic curve. However, the pads did not experience a large enough change in volumetric water content to develop a large portion of the curve.

14. SUBJECT TERMS

15. NUMBER OF PAGES
168

16. PRICE CODE
N/A

17. SECURITY CLASSIFICATION OF REPORT	18. SECURITY CLASSIFICATION OF THIS PAGE	19. SECURITY CLASSIFICATION OF ABSTRACT	20. LIMITATION OF ABSTRACT
none	none	none	N/A

Standard Form 298

1. Report Number	2. Government Access No.	3. Recipient's Catalog No.
MBTC DOT 3031		

4. Title and Subtitle	5. Report Date
Identification of Expansive Soils Using Remote Sensing and In-situ Field Measurements – Phase I	October 2012
	6. Performance Organization Code

7. Author(s)	8. Performing Organization Report No.
Dr. Richard A. Coffman, PE, PLS and Cyrus D. Garner, MSCE, EIT	

9. Performing Organization Name and Address	10. Work Unit No. (TRAIS)
Mack-Blackwell Rural Transportation Center 4190 Bell Engineering Center University of Arkansas Fayetteville, AR 72701	11. Contract or Grant No.
	13. Type of Report and Period Covered
12. Sponsoring Agency Name and Address US Department of Transportation Research and Special Programs Administration 400 7th Street, S.W. Washington, DC 20590-0001	Technical 7/1/2011 – 9/1/2012
	14. Sponsoring Agency Code

15. Supplementary Notes

Supported by a grant from the U.S. Department of Transportation University Transportation Centers program

16. Abstract

Researchers at the University of Arkansas have conducted research on the suitability of using remote sensing techniques (radar and LIDAR) to monitor the shrink-swell behavior of an expansive clay material in a field test site as part of the Mack Blackwell Rural Transportation Center Project 3031. The field test site consisted of two 5,000 square foot compacted clay pads installed at the University of Arkansas' Cato Springs Research Center (CSRC). In Phase I-A of the project four LIDAR scans and 335 radar scans were captured over an eight month period. The pads were constructed of eight inches of compacted clay material sourced from a local supplier overlying a two inch sand blanket. One pad was amended by the addition of three percent sodium bentonite (by dry weight) to increase the expansive behavior of the material. Radar scans were conducted on a weekly basis or after significant precipitation events. Additionally in Phase I-B, an additional three percent bentonite was added to the expansive pad and both pads were reconstructed. Results generated by this research project indicate that the LIDAR was able to detect the presence of ground movement due to expansive material. However, processing limitations severely curtailed the accuracy of this method. There were several issues encountered with the installation of the in-situ monitoring equipment in the compacted clay. Further research is required to determine the optimum method of installing TDR probes in compacted clay. TDR probes and tensiometers were used to develop the soil water characteristic curve. However, the pads did not experience a large enough change in volumetric water content to develop a large portion of the curve.

17. Key Words	18. Distribution Statement
Swelling soil, remote sensing, weather conditions	No restrictions. This document is available from the National Technical Information Service, Springfield, VA 22161

19. Security Classif. (of this report)	20. Security Cassif. (of this page)	21. No. of Pages	22. Price
unclassified	unclassified	168	N/A

Abstract

Researchers at the University of Arkansas have conducted research on the suitability of using remote sensing techniques (radar and LIDAR) to monitor the shrink-swell behavior of an expansive clay material in a field test site as part of the Mack Blackwell Rural Transportation Center Project 3031. The field test site consisted of two 5,000 square foot compacted clay pads installed at the University of Arkansas' Cato Springs Research Center (CSRC). In Phase I-A of the project four LIDAR scans and 335 radar scans were captured over an eight month period. The pads were constructed of eight inches of compacted clay material sourced from a local supplier overlying a two inch sand blanket. One pad was amended by the addition of three percent sodium bentonite (by dry weight) to increase the expansive behavior of the material. Radar scans were conducted on a weekly basis or after significant precipitation events. Additionally in Phase I-B, an additional three percent bentonite was added to the expansive pad and both pads were reconstructed. Results generated by this research project indicate that the LIDAR was able to detect the presence of ground movement due to expansive material. However, processing limitations severely curtailed the accuracy of this method. There were several issues encountered with the installation of the in-situ monitoring equipment in the compacted clay. Further research is required to determine the optimum method of installing TDR probes in compacted clay. TDR probes and tensiometers were used to develop the soil water characteristic curve. However, the pads did not experience a large enough change in volumetric water content to develop a large portion of the curve.

Table of Contents

List of Figures

List of Tables

List of Equations

Chapter 1. Introduction

1.1. Introduction

The purpose of this report is to describe the progress on the Mack Blackwell Rural Transportation Center (MBTC) project number 3031. The purpose of this project is to identify the behavior of expansive clay materials under the influence of changing environmental conditions at a test location at the University of Arkansas. Both Laser and Radio Detection and Ranging (LIDAR and RADAR) equipment have been used to remotely monitor the pad both during and after construction. Additionally traditional surveying techniques were used to determine the layout of the test pads and the inclusion of various test configurations (gravel pad, amended/non-amended clay, and geosynthetic membrane). Two separate test phases have been implemented as part of this project. The first test phase (Phase I-A) utilized the remote sensing technologies described in this report. The second test phase (Phase I-B) incorporated in-situ measurement techniques such as tensiometers and time domain reflectrometry probe to measure the effects of soil-moisture interactions.

1.2. Background

Expansive clay materials are responsible, nationwide, for more than a billion dollars (US) in annual damage (Gourley et al., 1993). As a result the identification and characterization of expansive soils have historicaly and remain an area of active research. The MBTC-3031 project used advanced remote sensing technologies to determine the suitability of these new technologies for the research/monitoring of expansive clay deposits in the field. Most of the research to date has involved laboratory testing or has required extensive field instrumentation.

1.3. Objectives

The objectives of this project were to evaluate the effeciacy of remote sensing techniques and in-situ testing equipment to characterize the behavior of the expansive clay. Specifically, the remote sensing equipment was evaluated on its ability to accurately detect, characterize, and quantify the deformation of the ground surface in response to the shrink-swell cycle of the expansive clay material. The in-situ equipment (TDR and tensiometers) were evaluated on their ability to accurately monitor the conditions and response of the clay body as a function of changing environmental conditions (temperature, precipitations, freeze-thaw etc.). Additional objectives of the research project included the evaluation and investigation of installation techniques for the in-situ instrumentation and different methods to collect, analysize, and reduce the remote sensing data.

1.4. Summary

Identified in this chapter are a brief description of the project background, purpose, and objectives of the MBTC-3031project. Specifically, this project was developed and implemented to increase the understanding of the field behavior of expansive clay materials and to evaluate the efficacy of different measuring techniques in identifiying and monitoring expansive clay behavior

Chapter 2. Literature Review

2.1. Introduction

Contained in this section is a description of the current state of knowledge in expansive soils as it applies to the MBTC-3031 project. The fiscal impacts of damage due to expansive soil behavior has been estimated to run in excess of one billion U.S. dollars per annum (Gourley et al., 1993) and to exceed the damage caused by earthquakes, fires, floods, and tornadoes combined (Chen, 1988). As a result a significant body of research has been developed regarding the behavior of expansive soils (e.g. Nelson and Miller, 1992; Fredlund and Raharjdo, 1993; and Mitchell and Soga, 2005). To date the majority of research in this field has involved laboratory investigation on small scale samples. Academic research has historically investigated the small scale behavior of expansive soils under simulated environmental conditions (e.g. clay mineralogy, shear strength, cation exchange capacity, etc.). Converesly, most of the geotechnical design practice for foundations or structures underlain by expansive soils has incorporated the concept of "swelling potential" to evaluate and characterize the risk and design considerations at an expansive site (USACE, 2004). Typically the "swelling potential" of an expansive clay is evaluated using a correlation to commonly tested soil parameters such as plasticity index (e.g. Seed et al., 1962 and Nayak and Christensen, 1971).

2.2 Mechanism of Expansion

The volume change experienced by soils under the influence of changing environmental conditions has been attributed to the action of crystalline swelling and osmotic swelling (Norrish, 1954). Crystalline swelling occurs at lower water contents and is responsible for up to 13 percent

of the total swelling experienced by an expansive material upon hydration (Villar, 2004). The remainder of the swelling can be attributed to the osmotic swelling.

Crystalline swelling occurs when water enters into the bound cation layer between the negatively charged clay particles. As water molecules associate with the adsorbed cations the effective radius of the ionic particle increases causing the adsorbed cation layer to increase in length. As the clay particles move apart the material expands. An visual representation of crystalline swelling is presented in Figure 2.1.

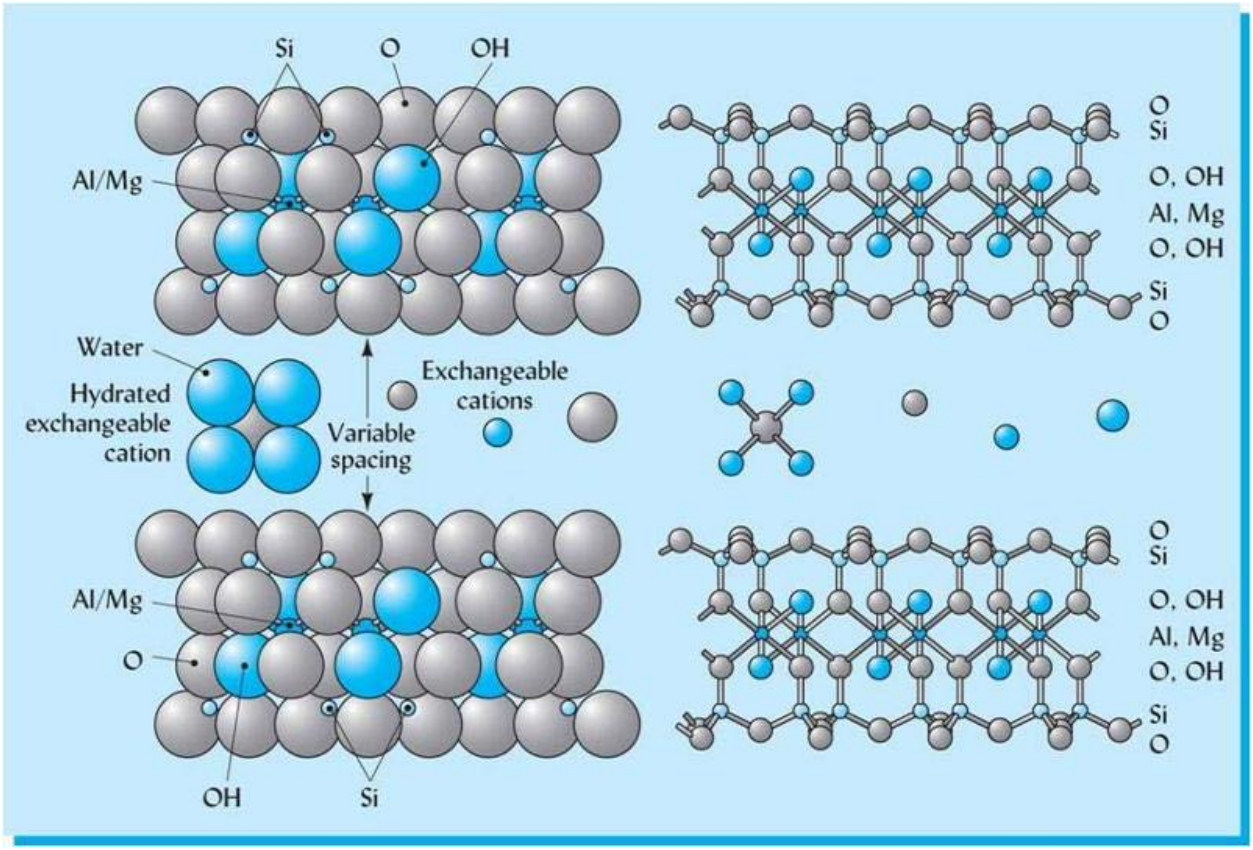

Figure 2.1. Schematic of clay particles showing crystalline expansion (Yavapi College, 2012).

Osmotic swelling occurs when the clay particles have separated far enough (with sufficient hydration of the entrained cation layer) to allow entry of bulk (non-bonded water) that the electro-static force changes from net attraction between clay particles into a net repulsive

force (Norrish, 1954). The repulsive electrostatic force results in a dramatic expansion of the clay material. Osmotic swelling typically occurs at gravimetric water contents in excess of 30 percent. A schematic of osmotic expansion of clay particles is presented in Figure 2.2

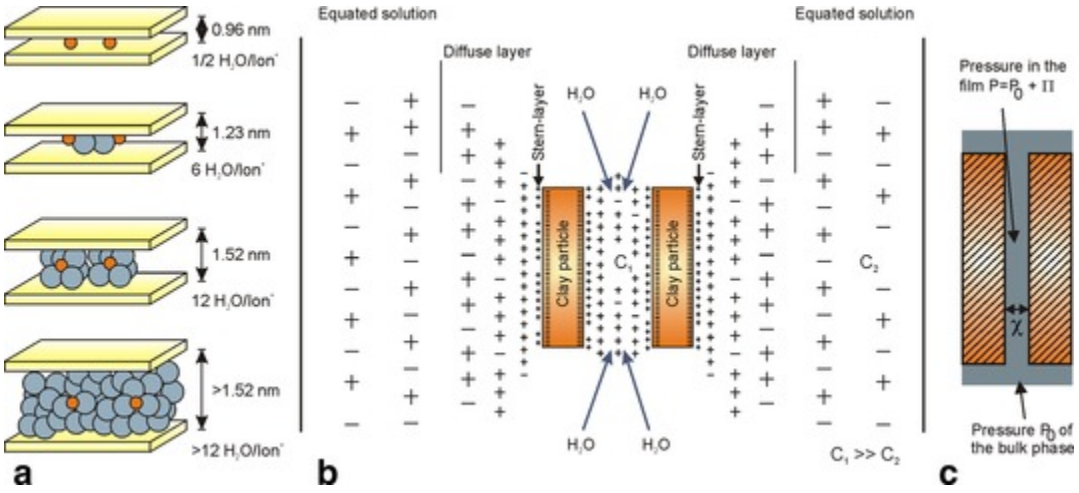

Figure 2.2. Schematic of clay particles showing osmotic expansion (after Madesn and Muller, 1988; Heim, 1990, and Butt et al., 2003 as cited by Ruedrich et al., 2011).

2.3. Laboratory Investigation

In geotechnical practice expansive soil behavior is typically measured using laboratory testing. Indirect testing methods include the Texas Department of Highways and Public Transportation Method (TDHPT), the Van Der Merwe method, Vijayvergia and Ghazzaly, Schneider and Poor, McKeen-Lytton by McKeen, and Johnson methods (USACE, 2004). Other testing includes the physiochemical tests which use Cation Exchange Capacity (CEC) to determine swelling index. Direct measurement of soil expansion in the laboratory include the consolidometer and soil suction testing (USACE, 2004).

The indirect methods use empirical or semi-empirical correlations to commonly measured soil parameters including the clay fraction of the sample and the plasticity index. For example the Van Der Merwe method is presented in . Here the expansion potential is indexed versus the clay fraction (percent passing the 0.0075 mm sieve) and the plasticity index. The

relationship proposed between plasticity index, clay fraction and expansive potential is presented in Figure 2.3.

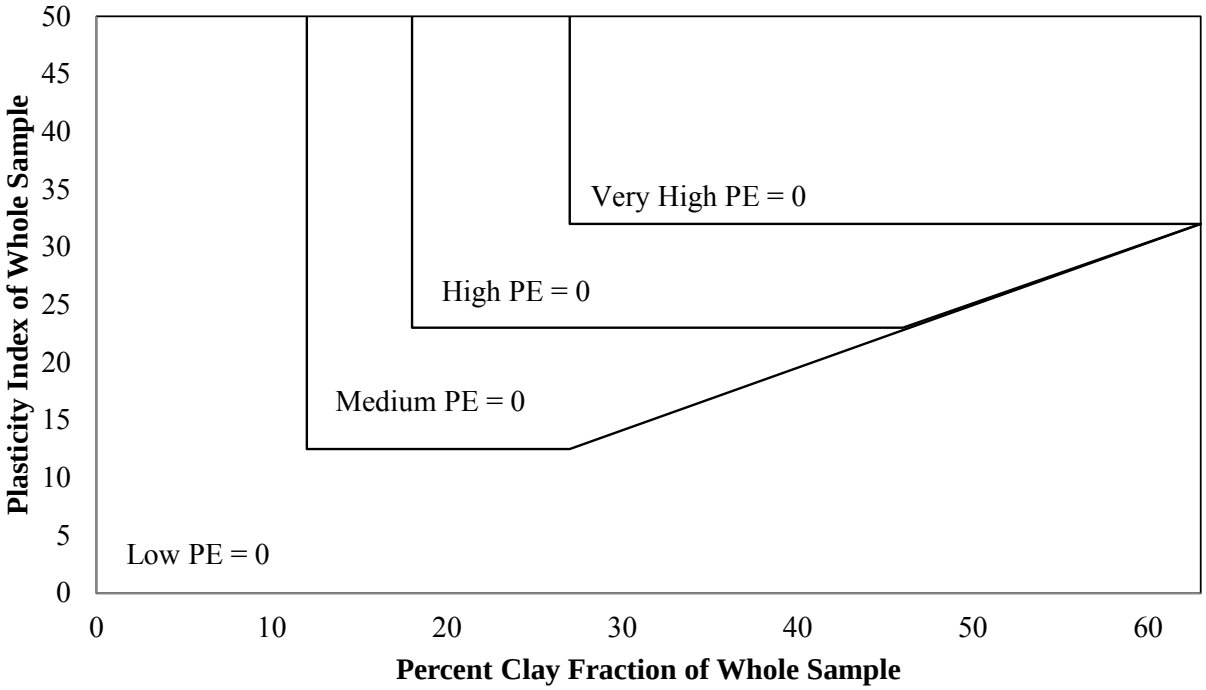

Figure 2.3. Expansive potential as a function of plasticity index, clay fraction, and expansive potential in the Van Der Merwe method (USACE, 2004).

2.4. Direct testing methods

As previously described, typical laboratory testing for expansive soil behavior which directly the volume change in a soil sample include consolidometer testing and soil suction testing. A consolidometer testing involves placing a trimmed soil sample in a one dimensional consolidometer. The vertical design pressure (overburden and structural load) is applied to the sample (USACE, 1986). The sample is inundated using a water bath and the resulting swell behavior is recorded. An image of a typical consolidometer testing apparatus is presented in Figure 2.4 and a graph of an example output is presented in Figure 2.5.

Figure 2.4. One dimensional consolidometer for use in swell testing (image from Humbold Manufacturing, 2012).

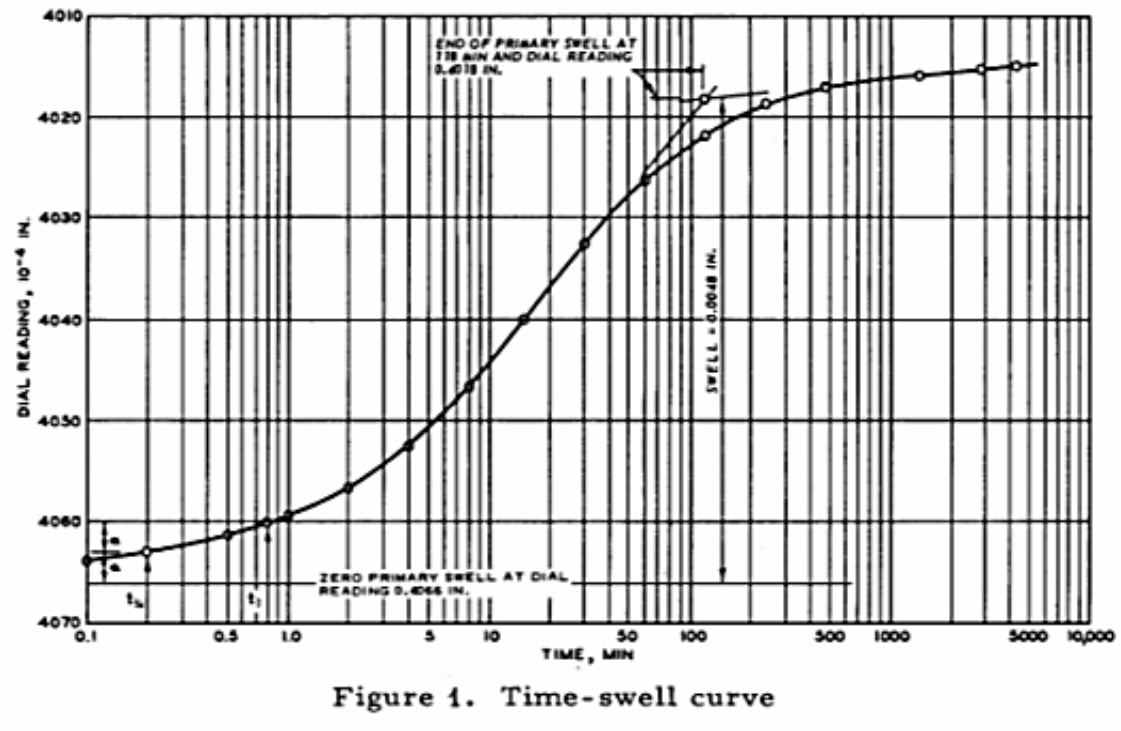

Figure 2.5. Example output of consolidometer used in swell testing on an expansive clay sample (USACE, 2004).

Another typical soil swelling laboratory is the measurement of soil suction. Typical measurement techniques for soil suction include thermocouple psychrometers and the filter paper method.

Thermocouple psychrometers measure relative humidity via Peltier cooling (USACE, 2004). By applying a current to a thermocouple junction a temperature drop is induced at across the junction. As the junction temperature approaches the dewpoint of the air condensation occurs on the thermocouple surface. The presence of condensed water stabilizes the temperature at the junction preventing further cooling. As the current is removed evaporation of the condensed layer maintains the temperature of the thermocouple. The difference in temperature between the junction and a reference circuit induces a voltage which can be recorded to determine the dewpoint of air. The relative humidity (from the dewpoint) is then used to calculate the suction in the soil samples. Advantages of the thermocouple psychrometers is the rapid data acquisition (semi-real time) and the relative accuracy (versus some other laboratory methods) when properly calibrated (USACE, 2004). Disadvantages include the requirement for specialized equipment, calibration required, and the limited range of measurement.

The filter paper method also measures relative humidity but instead uses filter paper to absorb the moisture from air. A dry piece of filter paper is placed in contact with an unsaturated soil sample. The absorbed moisture is detected by weighing the humid paper to determine the absorbed water. A critical advantage of the filter paper method is the low equipment requirements meaning many geotechnical testing labs already have the requisite equipment to perform this testing. Another advantage is the range of suction values the test can accommodate. The disadvantages include lack of accuracy compared to more advanced methods and the relatively slow data acquisition. The equation used to relate soil suction to expected vertical

displacement is presented as Equation 2.1. An example of the relationship between soil suction and gravimetric water content is presented as Figure 2.6.

$$\frac{\Delta H}{H} = \frac{e_1 - e_0}{1 + e_0} = \frac{\alpha G_s}{100B(1 + e_0)} \log\left(\frac{\tau^o_{m0}}{t^o_{mf}}\right)(B - 6) \quad \text{(Modified from USACE, 2004)} \qquad \text{Equation 2.1}$$

Where ΔH is the vertical heave (ft), H is the thickness of the soil layer, e_1 is the final void ratio, e_0 is the initial void ratio, α is the compressibility factor, G_s is the specific gravity, B is the slope soil suction parameter, τ^o_{ma} initial matric suction prior to surcharge pressure (tsf), and τ^o_{ma} is the final matrix suction without surcharge pressure (tsf).

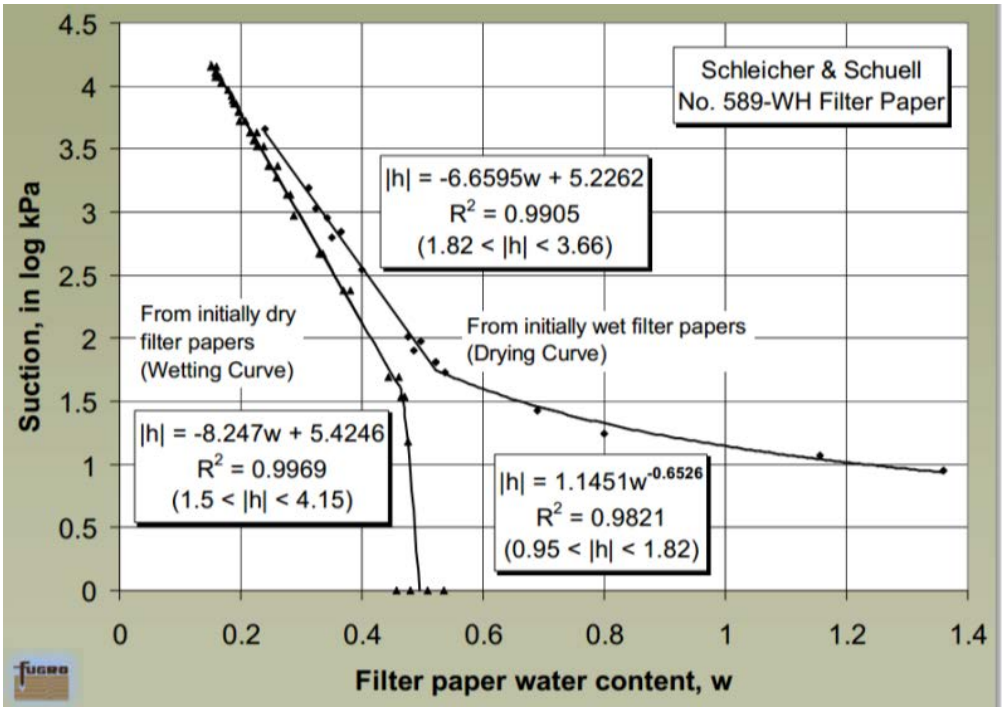

Figure 2.6. Soil suction vs. gravitmetric water content (Bulut, 2012).

2.5 Field testing methods

Techniques to measure expansive soils in the field can be broken largely in two different methods. These methods are field measurement of soil characterization using soil mineralogy or using the suction swell calculations. The soil characterization can be done using laboratory techniques such as X-ray diffraction. For use in the field it is possible to use remote sensing

technology (Infared Spectrometery) to detect the mineralogy of a clay sample at the surface (Chabrillat et al., 2002 and Goetz et al., 2006). Advantages of infared spectrometery include good spectral and spatial resolution and no need for installed infrastructure. Disadvantages include measurement of surface deposits only and the need for expensive, specialized instrumentation and data reduction. A plot of reflectance versus wavelength for clay minerals is presented in Figure 2.7.

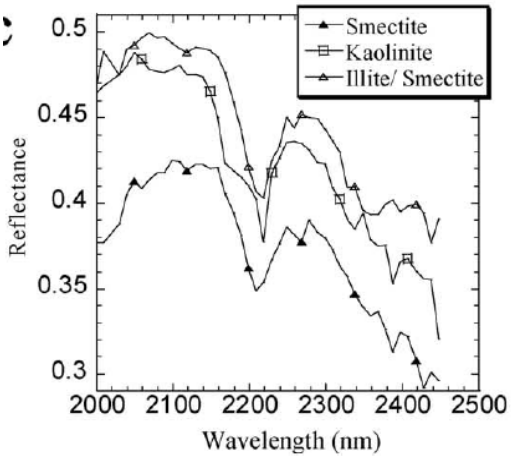

Figure 2.7. Reflectance spectra of clay mineralogy of interest in expansive soils (Chabrillat et al., 2002).

Field measurements of suction include tensiometers and gypsium block suction gauges. The tensiometers and suction gauges directly measure soil suction in an expansive soil deposit. Both techniques have been widely used in both research and industry in both engineering and agricultural applications (Rowe et al., 2007; Irrometer, 2012; and IAEA, 2008). Advantages include the ability to continuously monitor a deposit at depth. Additionally, there is a large body of literature describing the use of these techniques. Some of the disadvantages include the need for extensive installation for both sensors and supporting equipment and a limited spatial range (e.g. only the immediate area of the sensor is monitored).

2.6 Remote Sensing

Remote sensing techniques have been widely used to detect movement of the ground surface (Coffman, 2009 and Conte, 2012). While many of these applications have been used to detect the movements identified with slope failures the concept is also applicable to tracking movements caused by the shrink swell cycles of expansive soils in the field. In the context of the MBTC-3031 project two advanced remote sensing technologies were employed (radar and LIDAR). Radar (or RADAR – RAdio Detection And Ranging) and LIDAR (LIght Detection And Ranging) are active remote sensing technologies which "illuminate" a target of interest with electromagnetic radiation (either microwave or visible light) and then record the backscattered energy. An idealized graphic of an active remote sensor is presented in Figure 2.8.

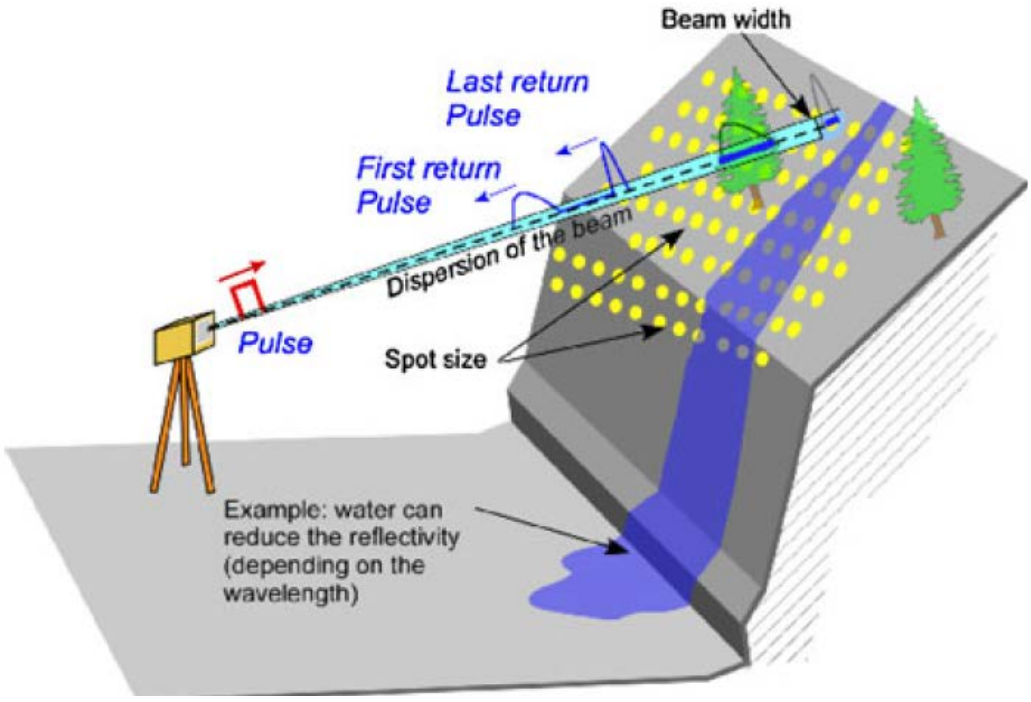

Figure 2.8. Idealized schematic of terrestrial active remote sensor principles showing multiple return geometries (from Jaboyedoff, 2010).

Some of the advantages of using remote sensing for detection and quantification of expansive soil movements is that the two techniques discussed here provide a direct

measurement of ground surface movement. This direct measurement is opposed to the suction based methods which must rely on a correlation to the measured suction. Remote sensing techniques also can provide superior spatial and temporal resolution to in-situ sensor systems. A remote sensing system may be employed to cover an area where the extents make it uneconomical to instrument. Additionly, the system can be deployed rapidly in response to environmental condtions. However, remote sensing systems can be effected by site conditions like vegetation, standing water, line of sight, equipment siting for repeated visits, etc. The remote sensing equipment also significantly more complicated

The radar system employed for this project was a Gamma Remote Sensing Portable Radar Interferometer (Generation 2) or GPRI-2. The radar system consists of a three, two meter antennas (one transmitting, two receiving) mounted to a tower assembly. The assembly is pivoted on a servo controlled bracket (tri-brach) which allows for a 360 degree scan angle at up to 10 degrees per second. The radar transmits at 1.74 cm wavelength (17.2 GHz). The nominal range of the system is 10 kilometers. The system has the advantage of being highly portable and high ease of deployment. For the MBTC-3031 project measurements on the roof were typically performed by two researchers. The UA personel were able to transport the radar system onto the roof (using a rope), set-up the system, acquire images, tear down the instrument, and clear the roof in approximately two hours. An image of the GPRI-II radar system is presented as Figure 2.9.

Figure 2.9. GPRI-II acquiring images of a mountain near Gumligen, Switzerland on October 31, 2010 (from GAMMA Remote Sensing AG, 2011 as cited by Conte, 2012).

The LIDAR system employed in this research project was a Leica Geosystems C-10 Laser Scanner. The C-10 uses a green visible laser (532 nm) and has a scan angle of 360 degrees (horizontal) and 270 degrees (vertical) (Leica, 2012). The maximum range of the system is 300 meters. Data is acquired at a maximum rate of 50,000 points per second.

2.7. Time Domain Reflectrometry

Time domain reflectrometry (TDR) has been extensively employed in geotechnical research over the past two decades. In general time domain reflectrometry allows for real-time monitoring of the volumetric water content of a soil body. The theory of operation for TDR testing in geotechnical engineering relies on changes in the bulk capacitance of the soils as a function of the water content. As water content increases the soil becomes more conductive and therefor resists the passage of a current down the unshielded portion of the TDR probes (Lorentz effect). The measured travel time is converted to an apparent probe length (using the speed of the electrical pulse in the rod in a nonconductive media like air). By comparing the apparent length

of the probe to the actual (measured) length of the probe the apparent dielectric constant of the soil body can be determined. Work by Topp et al., (1980) has provided a method to correlate the volumetric water content of a soil body to the apparent dielectric constant measured using the TDR equipment. The relationship proposed by Topp et al., (1980) is presented here as Equation 2.2.

$$\theta = 4.3\times10^{-6}\varepsilon_m^3 - 5.5\times10^{-4}\varepsilon_m^2 + 2.92\times10^{-2}\varepsilon_m - 5.3\times10^{-2}$$ (Topp et al., 1980) **Equation 2.2**

While the Topp et al., (1980) equation is widely used in geotechnical practice (e.g. Nemmers, 1994; Rowe et al., 2007; and Campbell Scientific, 2012) it is conterindicated in several cases. For the specific purpose of this project it has been suggested that in the case of soils with high organic and/or clay content that a soil specific calibration be performed. For the MBTC-3031 project the calibration procedure was conducted as documented by Rowe et al., 2007. As documented by the authors the calibration was conducted by compacting clay samples at various moisture contents (similar to the method employed for the proctor test). After the samples had been compacted a TDR prove was installed in the sample and the apparent dielectric constant measured. The gravimetric water content of the sample was then determined by oven drying. A phase diagram was then employed to determine the volumetric water content. Therefore, the authors were able to correlate the measured dieletric constant to the actual volumetric water content and fit a soil specific polynomial function to the data.

2.8. Summary

There has been a large body of research regarding the prediction and measurement of expansive soils in both field and laboratory enviroments. With the exception of the consolidometer testing many of the established techniques discussed in this section do not directly measure soil expansion. The consolidometer testing is limited by the effects of sample

disturbance and the simulated laboratory enivorment. The use of remote sensing technologies provides a means to directly measure the expansive behavior. However, the use of remote sensing in this application has not yet been proven.

Chapter 3. Project Site and Project Materials and Testing Protocols

3.1. Introduction

This chapter describes the MBTC-3031 project site, construction materials, construction schedule, as well as an overview of the testing protocols employed in this research project. The description of the project site include the topography, location, and pre-construction appearance and conditions. The construction materials section provides a discussion of the various soil materials that were installed in the test pads. The construction scheduling provides an overview of each day of construction process describing the equipment and scheduling used by the researchers. Additionaly, described in this chapter are the testing protocols used for the remote sensing techniques employed in this project.

3.2. MBTC-3031 Project Site

The project site for MBTC-3031 is located at the University of Arkansas's Cato Springs Research Center (CSRC) at 1475 Cato Springs Road in Fayetteville, Arkansas. The test site

consists of two compacted clay pads laid out in a field located to the southeast of the CSRC building. The building provides an overlook from the southeast corner of the building for both the radar and LIDAR observations. The location of the test set-up is presented in Figure 3.1. The layout of the test site is presented in Figure 3.2 (before construction) and Figure 3.3 (after construction).

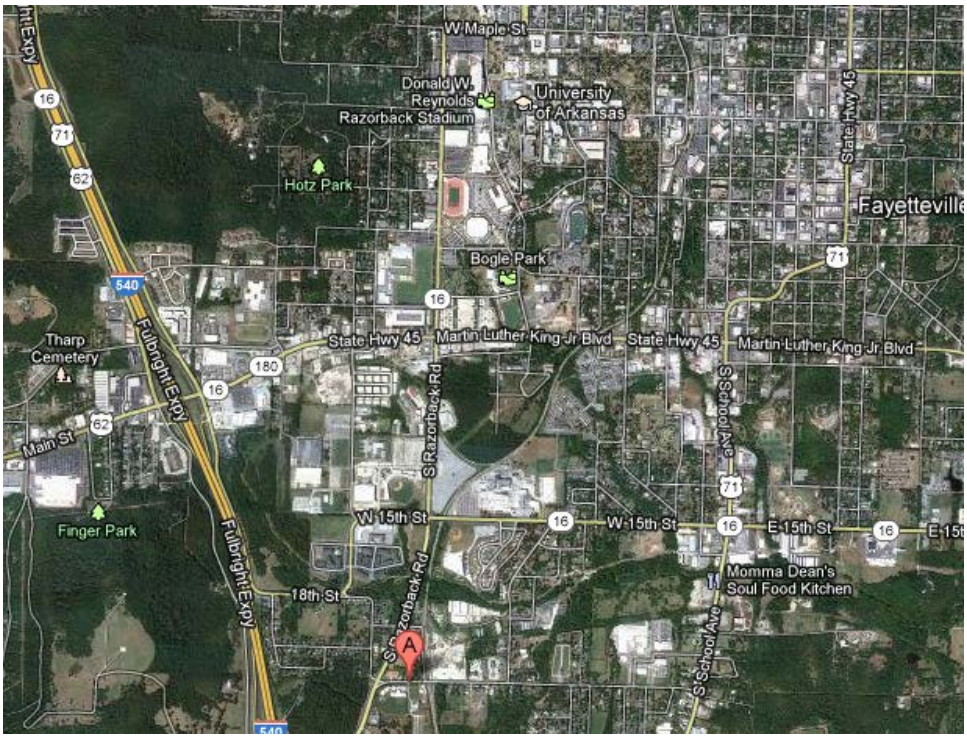

Figure 3.1. Location of the MBTC-3031 project site (marked with red "A") relative the University of Arkansas in Fayetteville, AR (Google Maps, 2012).

Figure 3.2. Layout of MBTC-3031 project site showing the two (2) working pads (top and bottom large red rectangle) and the overlook point (small red square) [modified from Google Earth, 2012].

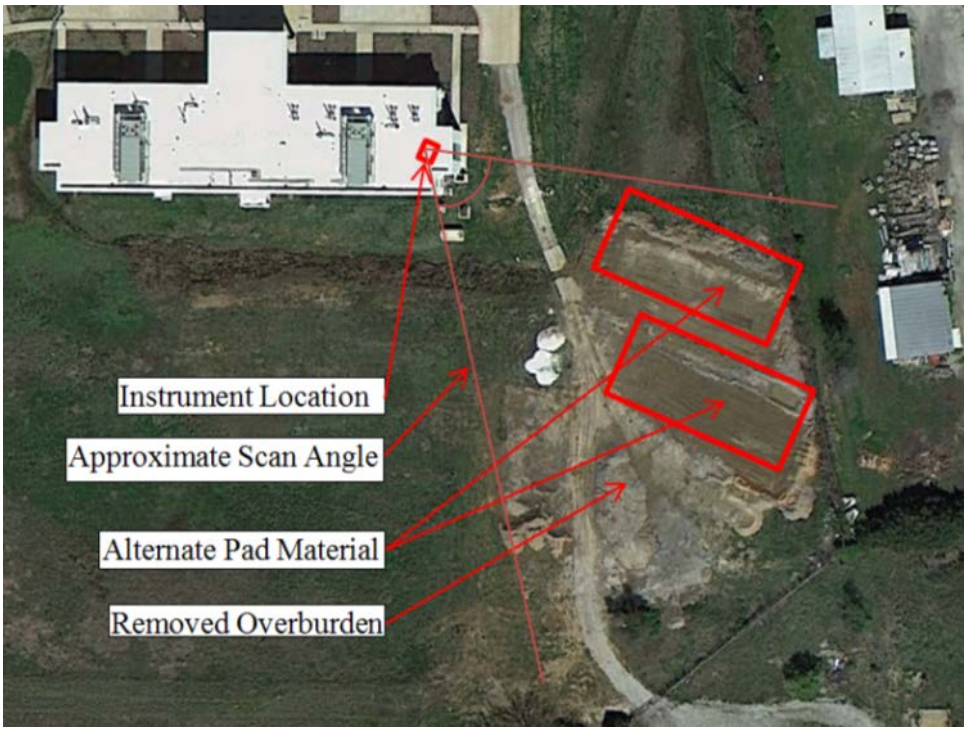

Figure 3.3. Post construction layout of MBTC-3031 project site (modified from Google Earth 2012).

The two working pads are the top and middle large red rectangles and are hereinafter referred to as Pads 1 and 2. The third pad is the proposed location of a third pad if future

expansion is undertaken. The overlook point is indicated as the small rectangle on the Southeast corner of the building roof. Pad 1 consists of a two inch sand drainage blanket overlain by an eight inch compacted clay layer amended with three percent (by dry weight) sodium bentonite. Pad 2 consists of a two inch sand blanket overlain by an eight inch thick compacted clay layer. Prior to project construction the site location was a previously developed area with scattered vegetation. The soil conditions at the site consisted of compacted road base overlain by approximately two inches of variably weathered asphalt. At the North end of the site this constructed layer was overlain by several inches of vegetated clayey topsoil material. Exposed sections of asphalt were typically highly weathered and buried sections were typically intact. The road base depth was variable between approximately 6 and 12 inches. The constructed layer was underlain by several layers of soft, saturated clay to an undetermined depth. The site typically drains South to North ultimately draining into the retention pond abutting Cato Spring Roads at the North East corner of the site.

3.3. Project Materials

The following materials were selected for project construction. Material purchased off site and imported included the clay fill, sand fill, and bentonite for amendment. The sand material was used as a drainage blanket to provide a known boundary condition between the bottom of the compacted clay layer and the underlying subgrade. The clay material was used for the construction of the compacted clay layer. The clay was placed in a single eight inch thick compacted layer. The bentonite material provides a highly expansive material in order to increase the shrink swell potential of the clay material.

3.3.1. Sand

The sand used in this project was sourced from a local supplier, Les Rodgers, Inc. The sand was classified as a fill sand. No specific gradation or permeability testing was conducted on

this material but it is anticipated that the permeability would fall between $4x10^{-2}$ and $6x10^{-2}$ cm/sec based on the values obtained from testing similar material from another vendor.

3.3.2. Clay

The clay material for this project was obtained from a local source pit located to the west of Fayetteville off of Broyles Road. Material was mechanically sifted in order to remove particles greater than ½ inch in diameter. Testing conducted on this material including grain size distribution and proctor curve analysis in order to determine both the suitability of this material for the project as well as to provide a window for field placement. The material gradation is presented as

Figure 3.4. Two separate gradations are shown the left gradation was performed on an oven dried sample.

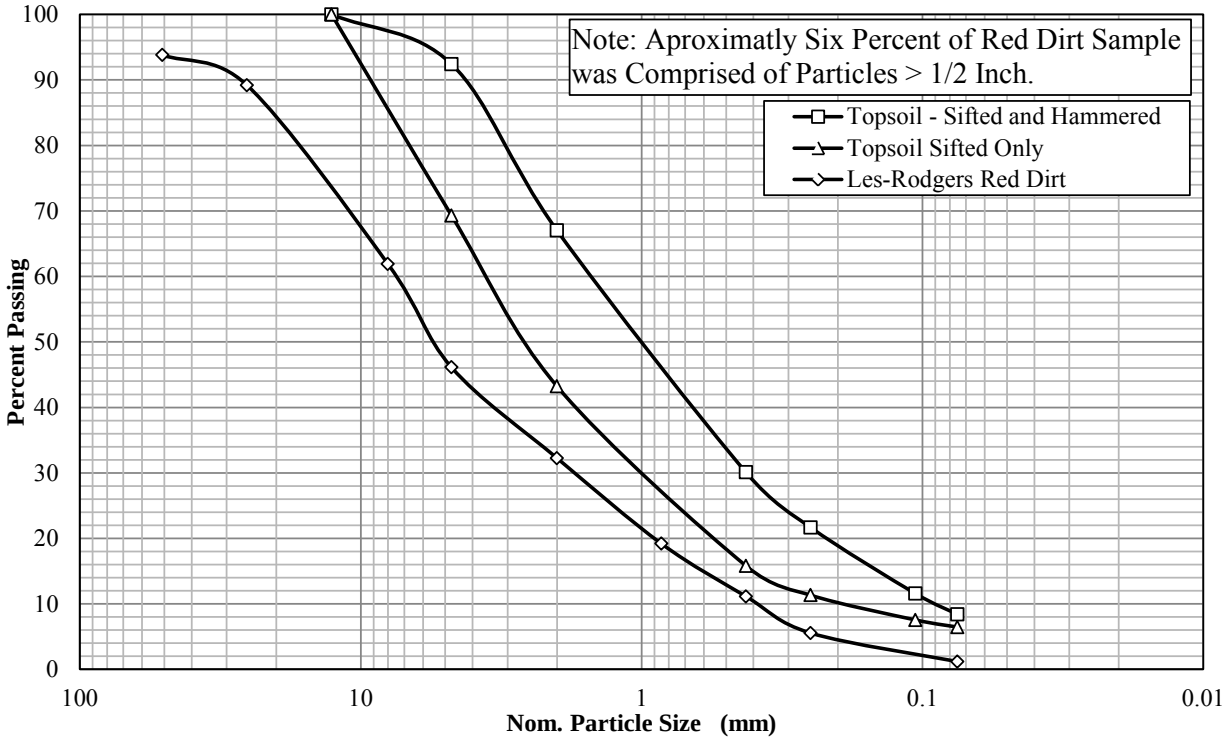

Figure 3.4. Percent passing vs. nominal particle size (mm) for MBTC-3031 clay samples.

The right gradation curve was determined after breaking up large clumps of clay material using a rubber mallet. The mallet was utilized in an attempt to simulate the mechanical energy imparted by the on-site sifting screen at the source pit. The data generated by the proctor testing for both the amended and unamended samples is presented in Table 3.1.

The zone of acceptance for both the amended and unamended material is presented in Figure 3.5 and Figure 3.6, respectively (also showing the field compaction data). In order to generate the zone of acceptance three proctor testing series were conducted on both the. A 75% reduced standard energy compaction testing (9,222 ft*lb/ft^3) curve was conducted using at least five different moisture contents (stepping in 2% increments as required). A standard proctor energy compaction testing (12,350 ft*lb/ft^3) was conducted using at least five moisture contents. Finally, a modified proctor energy compaction testing (56,138 ft*lb/ft^3) was conducted using at least five moisture contents.

Table 3.1. Maximum dry density and optimum water content for amended and unamended clay samples.

Unamended Clay Samples			
Comp. Energy	$w_{optimum}$ (%)	γ_{dmax} kN/m^3	γ_{dmax} lbs/ft^3
Modified	12.48	18.42	117.23
Standard	14.20	17.42	110.91
75% Standard	15.55	17.24	109.76
Amended Clay Samples with 2 Percent Sodium Bentonite			
Comp. Energy	$w_{optimum}$ (%)	γ_{dmax} kN/m^3	γ_{dmax} lbs/ft^3
Modified	9.29	19.09	121.49
Standard	13.74	17.39	110.71
75% Standard	14.23	17.11	108.89

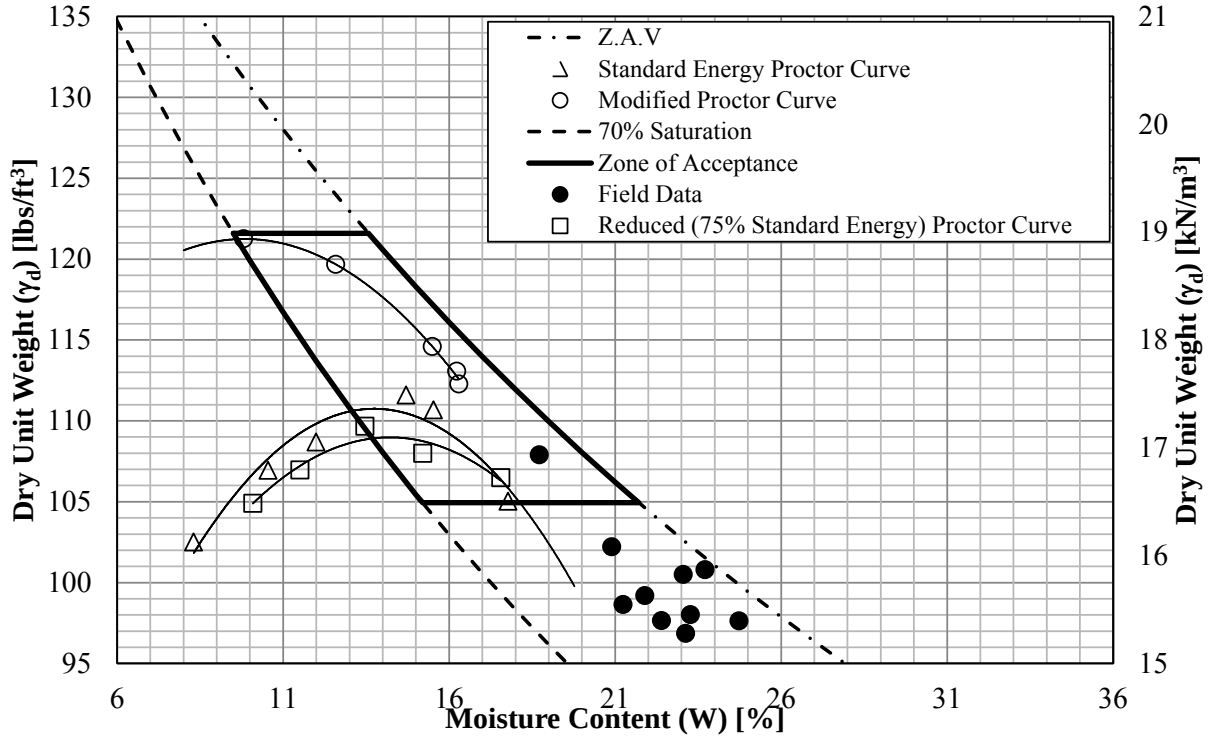

Figure 3.5. Zone of acceptance and field compaction data for ammended clay material (two percent sodium bentonite by weight added).

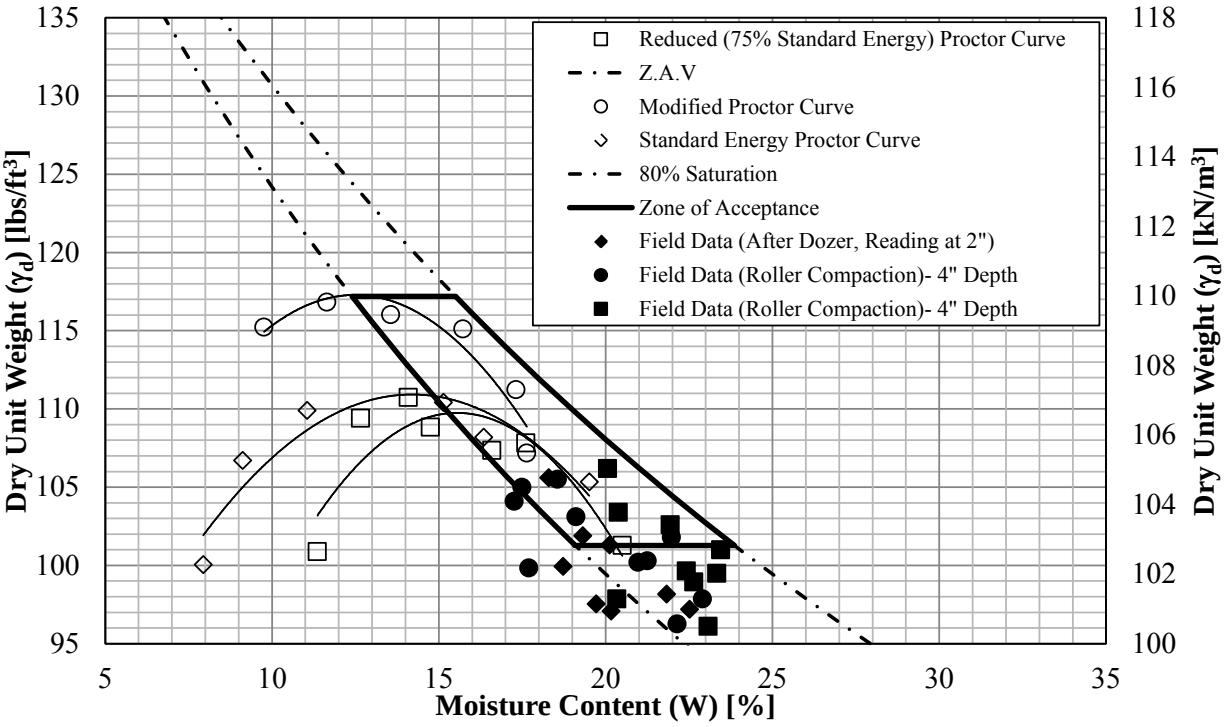

Figure 3.6. Zone of acceptance and field compaction data for unammended clay.

3.3.3. Bentonite

The bentonite for this project was sourced from a commercial supplier in Wyoming (Wyo-Ben). The product name is Enviro-Plug No. 8 which the manufacturer describes as, "a high-swelling Wyoming Bentonite in granular form" with 98 percent passing the number 4 mesh (Wyoben, 2012). The bentonite was transported to the site in palletized 50 pound bags sealed with shrink wrapping.

3.4. Pad Construction Activities (Phase I-A)

Pad construction proceeded in two (2) phases designated as the pre-construction and construction phases. The preconstruction phase consisted of activities performed before the mobilization of construction equipment to the site. In order to minimize construction costs as much work as was possible was performed prior to equipment delivery. The construction phase began with the delivery of the first piece of equipment to the project site. Construction equipment utilized for this project included a Case 850M backhoe loader, a Case 530H tracked tractor, a Case SV210 padfoot roller, and a Kioti DK40 utility tractor. Images of the rental equipment on site is presented as Figure 3.7, Figure 3.8, and Figure 3.9.

Figure 3.7. Project equipment on site.

Figure 3.8. Case 560H tracked tractor use on the MBTC-3031 project.

Figure 3.9. Case 580M backhoe loader used on MBTC-3031 project (Kioti utility tractor in background).

3.4.1. Pre-Construction

Pre-construction began with a site survey to determine the topography and provide an estimate of the amount of material to be removed in order to construct a level subgrade for the test pads. It was determined that the pads would be leveled by material removal only with no off or onsite material placed on the pads. The decision to not employ fill material was done to avoid any influence from consolidation in the fill material. The survey was performed using a total station. Points were taken in approximate ten by ten foot spacings as determined by inspection. The surveyed area was bound by the retention pond to North, the perimeter fence to the East and South, and the access road to the West. The project area is presented as the shaded area in Figure 3.10.

Figure 3.10. MBTC-3031 disturbed project area (modified from Google Earth) [in color].

The total disturbed area of the site was approximately 0.80 acres (35,000 ft^2) excluding the lay down area to the West of the access road. Additional points were taken in the each of the

three proposed pads (the two project pads and the proposed future pad) at the visually determined maximum and minimum elevations in each pad. The surveyed site topography is presented in Figure 3.11.

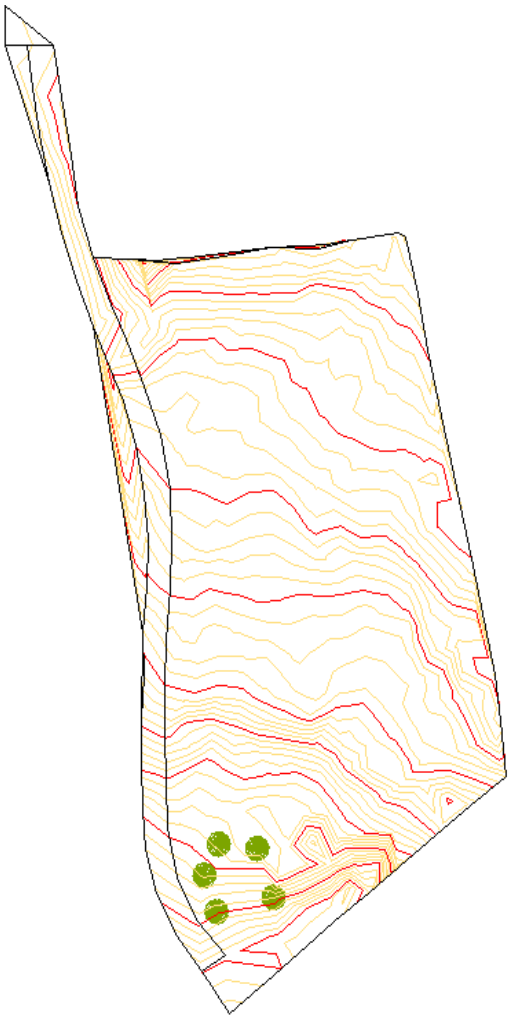

Figure 3.11. Topography of the MBTC-3031 project site.

After the completion of the initial surveys the pads were laid out and an initial stripping and grubbing operation was performed utilizing the University of Arkansas' Kioti DK40 utility tractor. A pile of road base already onsite was relocated from Pad 1 to the West side of the access road. Exposed areas of asphalt were removed using the loader bucket. However, it was found

that the tractor was not suitable for the removal of the compacted road base and further grading required the use of the rented equipment.

Project material was stockpiled on site during this phase. Approximately 750 tons of clay material was stockpiled to the west of the road and approximately 180 tons of fill sand were stockpiled along the south edge of Pad 2. An image showing the locations of the clay stockpile, sand stockpile, and spoil heaps is presented in Figure 3.12.

Figure 3.12. Project under construction showing stockpile locations, spoil heaps, and rough grading underway.

3.4.2. Construction (Phase I-A)

Construction activities proper began on the 9th of January, 2012 and continued for 10 days until the 18th of January. The project work flow began with stripping and grubbing on Pad 1 (Pad 2 being cleared during preconstruction), followed by rough grading on Pads 1 and 2. Rough leveling was performed using a transit and dumping level (as shown in Figure 3.13).

Figure 3.13. Transit and dumping level used for rough grading.

After the pads were roughly graded, final grading was performed utilizing outside personnel and a laser level to ensure that the final subgrade was within +/- one tenth of a foot. Placement of the two inch thick sand drainage blanket began on Pad 2 and then continued on to Pad 1. Following placement of the sand layer, the gravel pads and geosynthetic membrane were installed in both pads (Figure 3.14).

(a) (b)

Figure 3.14. (a) Geosynthetic membrane in place on sand blanket of Pad 1. (b) Excavating the sand blanket prior to placement of gravel pad in Pad 1.

The clay material was then placed and compacted on Pad 2. For Pad 1 (the amended pad) the clay was placed (but not compacted) and then the bentonite was placed manually in 50 lb bags which were then opened and spread manually. The loose bentonite powder was then mixed into the clay layer using a rotary tiller and the Kioti utility tractor. The mixed clay bentonite material was then compacted using the pad foot roller. Each compaction series consisted of two (2) passes of the pad foot roller. Since the clay material had an excessively high moisture content (the gravimetric water content was greater than 20 percent prior to initial placement), in order to facilitate drying the placed material was disked up with the roto-tiller and then recompacted. A brief description of construction activities by day is described in further detail in the following sections.

3.4.2.1. Monday 9th-January-2012 (Day 1)

Construction began at approximately 1300 hours after delivery of equipment (bulldozer and backhoe) and continued until 1715 hours (equipment previously presented in Section 3.4).

Construction activities consisted of grubbing and leveling Pads 1 and 2. Four University of Arkansas personnel were on site this day.

3.4.2.2. Tuesday 10th-January-2012 (Day 2)

Construction began at approximately 0800 hours and continued until approximately 1700. The Pad foot roller was delivered to the site at approximately 0900 hours. Significant precipitation on site slowed work. Pad 1 (lower pad) was substantially leveled by the end of the day. Leveling work continued on Pad 2. Of special note significant construction debris (concrete, rebar) were encountered near the center of Pad 1 and required over excavation to clear the material. Four University of Arkansas personnel were on site this day.

Preliminary LIDAR and RADAR images of site were obtained. LIDAR and RADAR equipment pads were set up for subsequent imaging on roof of CSRC. One LIDAR image (interrupted) and seven RADAR images were taken. The LIDAR scan was performed by Malcolm Williamson with the University of Arkansas's Center for Advanced Spatial Technology (CAST). Five University of Arkansas personnel were on site this day.

3.4.2.3. Wednesday 11th-January-2012 (Day 3)

Construction began at approximately 0800 hours and continued until 1700 hours. The site was very wet from overnight precipitation. Limited construction activities including moving and stockpiling of spoils and minor work on leveling Pad 2 were performed. A survey of Pad 1 and Pad 2 extents was performed. One LIDAR scan was performed by Malcolm Williamson with CAST. Fourteen RADAR images were taken in the afternoon. The weather was generally cool and partly cloudy in the morning but cleared in the afternoon. Five University of Arkansas personnel were on site this day.

3.4.2.4. Thursday 12th-January-2012 (Day 4)

Construction began at approximately 0800 hours and continued until 1800 hours. The day was cold (below freezing), windy and partly cloudy. Significant ponded water was present on pads 1 and 2. Construction activities continued on Pad 2, including leveling and rudimentary dewatering (via mechanical removal using the backhoe loader). Pad 2 was substantially level by end of day (+/- 0.2 feet) except for areas around the perimeter and where water ponding made work difficult. No RADAR or LIDAR surveys were performed on this day. Four University of Arkansas personnel were on site this day.

3.4.2.5. Friday 13th-January-2012 (Day 5)

Construction began at approximately 0800 hours and continued until 1800 hours. This day was also cold (below freezing), windy and partly cloudy. Construction activities continued on Pad 1 and 2 consisting of leveling and grading. Pad 1 was leveled to with-in +/- 2 tenths with several low spots were water removal had occurred previously. RADAR images were taken this day. Four University of Arkansas personnel were on site this day.

3.4.2.6. Saturday 14th-January-2012 (Day 6)

Construction began at approximately 0730 hours and continued until 1800 hours. Day was cool and sunny. Construction activities occurred on both pads 1 and 2. Pad 1 was leveled to within +/- 0.1 feet and sand and clay were spread on Pad 2. Additionally, the gravel and membrane sections were placed in Pad 2. Pad 2 was compacted using the bulldozer after the in-situ water content was too high for compaction via the padfoot roller. Sand was placed on Pad 1. The rotary tiller was brought to site this day. Seven University of Arkansas personnel were on site this day.

3.4.2.7. Sunday 15th-January-2012 (Day 7)

Construction began at approximately 0800 hours and continued until 1800 hours. The day was cool and windy. Limited construction activities occurred on both pads 1 and 2. Surveys for elevation were taken on the placed sand layer for Pad 1 and on the placed clay layer for Pad 2. Additional surveys were performed to determine extents of various pad feature (gravel area, non-amended area, membrane). Multiple RADAR images were taken this day. Three University of Arkansas personnel were on site this day.

3.4.2.8. Monday 16th-January-2012 (Day 8)

Construction began at approximately 0730 hours and continued until 1800 hours. Day was warm and windy. Construction activities occurred on both pads 1 and 2. Clay was placed on Pad 1 and leveled. Bentonite was added to Pad 1 (~150-160 bags) and mixed using the rotary tiller, Pad 1 was subsequently beaten down with the dozer and then rolled with the pad foot roller. Pad 2 was tilled and recompacted. Nuclear density gauge testing was performed on Pad 2. Additional surveys were performed to determine extents of various pad features (gravel area, non-amended area, membrane) and elevations. Multiple radar images were taken this day. Seven University of Arkansas personnel were on site this day.

3.4.2.9. Tuesday 17th-January-2012 (Day 9)

Construction began at approximately 0730 hours and continued until 1800 hours. Day was mild and windy. Pads 1 and 2 were tilled to try to dry the soil. Two University of Arkansas personnel were on site this day.

3.4.2.10. Wednesday 18th-January-2012 (Day 10)

Construction began at approximately 0800 hours and continued until 2000 hours. Day was cold and windy in the morning but warmed considerably towards the afternoon. Construction activities occurred on both pads 1 and 2. Pad 2 was re-compacted using the padfoot

roller. Pad 1 was tilled, beaten down with bulldozer and recompacted with the roller. Nuclear density gauge readings were taken on Pad 1 and Pad 2. Equipment was cleaned prior to pick-up by rental company. Surveys were conducted to record locations of nuclear density tests. Four University of Arkansas personnel were on site this day.

3.4.3. Construction QA/QC (Phase I-A)

During construction the site elevation was initially controlled using a transit and dumping level. Fine grading was performed using a laser level. Placement density was measured using a nuclear density gauge. After each series of compaction ten points were taken in each pad. The location of each test was hand leveled using a shovel and all voids were filled in to provide a level surface. Test locations were chosen semi-randomly (ensuring sufficient coverage of the entire pad). The locations were marked and then surveyed using a total station to record the distribution of the test locations. The results of the nuclear density gauge testing were previously presented in Figure 3.5 (Pad 1) and Figure 3.6 (Pad 2).

3.5. Remote Sensing Technology

Two advanced remote sensing technologies were implemented during this project (LIDAR and radar). Both technologies utilized active electromagnetic sensors (i.e. used emitted energy to "illuminate" the area of interest). The radar system employed was the Ground based Portable Radar Interferometer (GPRI-II) developed by Gamma Remote Sensing. The GPRI-II system consists of two receiving antennas, one transmitting antenna, a radio frequency assembly, a field computer, and a computer controlled rotating assembly mounted to a fixed tripod.

3.5.1. Radar Observations

A series of radar observations were taken both during construction and post construction. The GPRI-2 scans were performed from the rooftop overlook on the CSRC building. All radar observations were captured using an antenna angle of -5 degrees (downwards) and scanning

from 5 degrees (relative to the home position) to 80 degrees. Additional project scans were conducted later with wide angle sweeps (-20 to 80 degrees). Alignment between scans was verified by aligning the scope (at zero degrees elevation and 37 degrees from the home position) with the left side of a white pole a distance from the site. During construction, radar images were taken on days two, three, five, seven, and eight. Post construction scans were captured once a week (typically 7 images captured) or after significant weather events. Each radar observations was conducted by first setting up the equipment over the refrence mark (a surveying stake set into a concrete block on the roof of the CSRC building). The tripod legs were maintained at constant settings on each scan to minimize the displacement of the radar equipment between scans. The leg lengths used for each scan are presented in Table 3.2. Each leg was anchored to a concrete block with the use of sleeved anchor. To further prevent movement the blocks and legs were weighted down using commercial sandbags. Care was taken to ensure that the blocks were not moved or impacted during the assembally and dissambally of the radar. A list of all the radar scans conducted for the MBTC-3031 project are presented in Table 3.3 (for the -5 to 80 degres scans) and Table 3.4 (for the wide angle scans and Phase I-B scans).

Table 3.2. GPRI-2 leg lengths for MBTC-3031 project.

Leg	Direction	Length
1	South	40.2
2	East	38.8
3	North	44.1

Table 3.3. Normal scan angle scans conducted on the MBTC-3031 project.

Scan No.	Date	Images Acquired	Notes
1	1/10/2012	7	Site Construction
2	1/11/2012	9	Site Construction
3	1/13/2012	9	Site Construction
4	1/14/2012	9	Site Construction
5	1/15/2012	9	Site Construction
6	1/16/2012	9	Site Construction
7	1/18/2012	7	Site Construction
8	1/19/2012	7	
9	1/30/2012	37	Images taken over 8 hour period
10	2/6/2012	7	
11	2/13/2012	7	
12	2/20/2012	7	
13	2/28/2012	7	
14	3/5/2012	7	
15	3/12/2012	7	
16	3/22/2012	7	
17	4/6/2012	7	
18	4/26/2012	7	
19	5/16/2012	7	
20	5/16/2012	7	Images taken after field was mowed
21	5/24/2012	7	
22	6/8/2012	8	One image not captured
23	6/26/2012	7	

Table 3.4. Wide angle scans conducted on MBTC-3031 project.

Scan No.	Date	7	Notes
14	3/5/2012	7	
15	3/5/2012	7	
16	3/12/2012	7	
17	3/22/2012	7	
18	4/6/2012	13	
19	4/26/2012	7	
20	5/16/2012	7	Images taken after field was mowed
21	5/16/2012	7	
22	5/24/2012	7	
23	6/8/2012	7	
24	6/26/2012	7	
25	7/7/2012	10	
26	7/10/2012	7	
27	8/9/2012	7	
28	8/10/2012	10	
29	8/17/2012	9	

3.5.2. LIDAR Observations

LIDAR scans were performed using CAST's Leica C10 LIDAR system. To date three scans have been performed. One was performed during construction (day 3) and two subsequent scans were performed after the completion of construction. The scans were conducted using the settings provided in Table 3.5. Similarly to the radar, the LIDAR was installed over a fixed refrence point (surveying nail in a concrete block) and the legs were anchored to three concrete blocks. Again care was taken not to disturb the blocks during the deployement and subsequent mobilization of the laser scanner. An example LIDAR image of Pad 1 is presented as Figure 3.15.

Table 3.5. LIDAR scan parameters.

Parameter	Setting
Instrument Height	1.661 m
Leg 1 (South)	38 cm
Leg 2 (North)	34.6 cm
Leg 3 (East)	41.6 cm
Distance to Pad 2	82 m
Resolution	1 cm @ 85 m
Scan Window (Degrees)	
Left	73.8
Right	130.3
Bottom	25.3
Top	-4.8
Camera Resolution	1920x1920 pixels

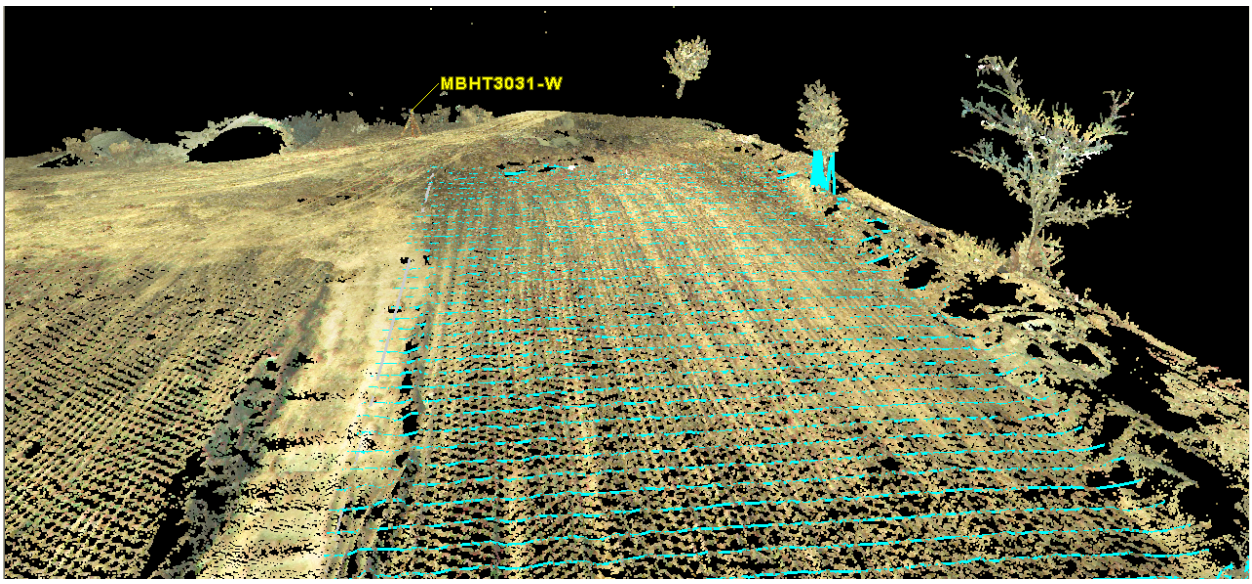

Figure 3.15. Sample LIDAR image showing Pad 1 as viewed in Cyclone.

The processing of LIDAR data was performed in several different software environments. A more complete description of the LIDAR data collection, data processing, and data reduction process can be found in Conte (2012). The LIDAR point cloud was first

visualized and rectified using the Leica Geosystem's Cyclone software suite. The point cloud was then exported as a .pts ASCII file containing the x,y, and z coordinates of each returned echo. Processing was performed using the LAStools suite developed by Martin Isenburg. The processing consisted of removal of points classified as vegetation (using the built in software algorithm in LASground) and thinning of the point cloud to a maximum size of ~ 60,000 points in order to not exceed the capabilities of the AutoCAD software. The AutoCAD software was used to compare "master" and "follower" surfaces created from the LIDAR point clouds.

3.6. Site Construction (Phase I-B)

Beginning on Monday June 25th construction activities began for Phase I-B of the MBTC-3031 project. Specifically, pads 1 and 2 were cleared of vegetation using a combination of a commercial lawn mower, a gas powered string trimmer, and hand tools. Once the vegetation had been removed then the pads were mechanical tilled using a rotary tiller (same unit employed in the Phase I-A construction). Each pad was tilled to a depth of six inches below the ground surface in three passes of the tiller. Care was taken to separately till the disparate portion of each pad (i.e. the amended portion of the unamended pad and the unamended portion of the amended pad) in order to avoid possible contamination of the control areas. After both pads had been tilled each pad was irrigated to provide proper water content for compaction. Irrigation was accomplished using a combination of commercial lawn sprinklers and manually placed water (with five gallon buckets). Aproximatly 9,000 gallons of water were added to pads 1 and 2. Following irrigation an additional three percent (by dry weight) bentonite was added to Pad 1 and the amended portion of Pad 2 (a total of 8,200 lbs of bentonite). The bentonite was placed and spread using the same techniques employed in Phase I-A. Compaction of both pads was accomplished using a "walk behind" trench compacter. Two passes of the trench compactor were

used to provide a more uniform and complete compaction. Field placement densities were then verified using a nuclear density gauge.

3.6.1. Placement of In-Situ Instrumentation.

Following pad compaction, instrumentation was placed in each pad. Fourteen Irrometer –E model tensiometers and fourteen CS-610 model Time Domain Reflectrometery (TDR) probes were placed in pads 1 and 2 (seven probes in each pad). The tensiometers and TDR probes were installed in pairs (separated by approximately two feet) at various locations throughout the pads. The tensiometers were installed at the existing penetrations from nuclear density gauge guide rod which was widened by driving a 0.75 inch outside diameter pipe to a depth of six inches below ground surface. The tensiometers were then installed through the widened penetration using hand pressure to avoid damaging the instrumentation but still providing intimate contact with the surrounding material.

The TDR probes were installed by first excavating a trench approximately 18 inches long, six inches wide, and six inches deep with the long axis of the trench transverse to the long axis of the test pad. Excavation was conducted using hand tools (sharpshooter shovel and hand awl) to minimize disturbance to the surrounding pad. A custom made jig was fabricated to allow the TDR probes to be pushed horizontally using a hydraulic ram. The jig was manufactured using 0.5 inch thick plate steel. One end of the jig was bored out to allow the RG-8 coaxial cable for each probe to be passed through prior to and after the probe had been pushed into place. An image of the probe, jig, and ram assembly is presented as Figure 3.16.

Figure 3.16. Installation of TDR probe in Pad 1.

Once the trench had been excavated and hand grubbed the probe in the jig was placed into the trench horizontally at a depth of three inches. The probe tips were slightly spread (to avoid the probe tips crossing during driving) and then manually pushed firmly into the soil at the end of the trench. A 12-ton hydraulic jack was then used to smoothly insert the probe into the compacted soil. A series of concrete and wooden blocks were used to provide a reaction surface and spacers. The reaction mass was provided by the Kioti Utility tractor. Due to the limited stroke of the hydraulic ram the use of concrete spacers was necessary to provide the required twelve inches of drive to completely seat the probe. After the probes were placed the jig was then removed and the trench recompacted. Care was taken to fill the void left by the jig underneath the epoxy body of the TDR probe head. Water was added to the excavated soil which was then manually mixed to ensure a uniform consistency prior to placement in the excavation. The trench was compacted through multiple lifts using both body weight and an 8x8 inch square hand tamper.

3.6.2. Connection / Wiring of In-Situ Instrumentation.

The connection between the in-situ instrumentation and the data collection system was accomplished using RG-8 cables (for the TDR probes) and shielded three-pair 22 AWG (American Wire Guage) braided wire cabling. Where possible all cables were connected using

soldered connections (for the tensiometers). For the coaxial cable, where extensions were necessary the connection was formed using a combination of N-type connectors and BNC connectors. In all cases wiring was left exposed on the ground surface.

3.6.3. Location of Instrumentation at MBTC-3031 Project Site.

The TDR and Irrometer probes were placed in the two pads in 14 locations. Where possible the TDR and Irrometer probes were paired in order to provide combined moisture content and soil suction measurements at proximal points in the pad. The locations of the probes in each pad are presented in Figure 3.17.

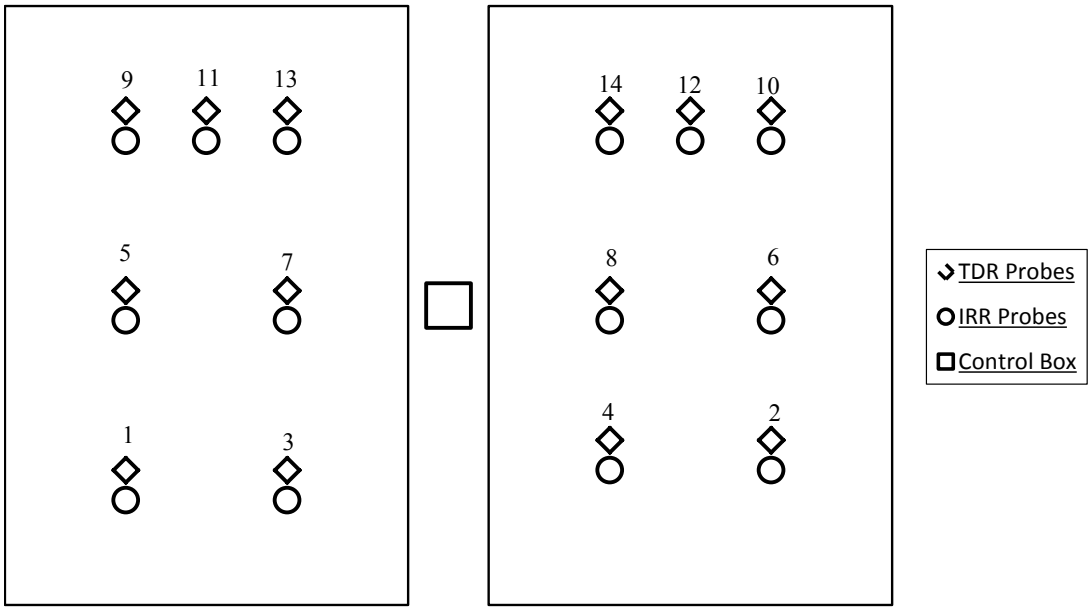

Figure 3.17. Instrument positions at the MBTC-3031 project site.

3.7. Summary

The construction, remote sensing data acquisition and in-situ instrumentation of the MBTC-3031 project site is documented in this chapter. The construction sequencing is discussed to describe how the University of Arkansas research team constructed the pads and identifies the

challenges encountered during this phase of the project. Specifically, the construction period coincided with adverse weather conditions which made soil placement and compaction problematic. Also described was the techniques employed to monitor the site from the overlook on the roof of the CSRC building. Specfic issues encountered where the placement of the instrumentation and alignment of subsequent images. For the in-situ instrumentation, important points discussed in this chapter include the installation of the TDR and irrometer probes into the compacted clay layer and the techniques required to accomplish this action.

Chapter 4. In-Situ Instrumentation

4.1. Introduction

Contained in this section of the document is a description of the in-situ instrumentation used for the Mack-Blackwell rural Transportation Center (MBTC) project 3031. The purpose of this instrumentation was to collect in-situ, real-time data on the behavior of expansive clays in a full scale field experiment. Specifically, the instrumentation package contained Time Domain Reflectrometery (TDR) probes (moisture content), Irrometer-E soil suction gauges (soil suction), thermocouples (soil temperature), tipping bucket (precipitation), and photo-voltaic cells (proxy measurement of solar intensity). The data was collected through the use of Campbell Scientific CR-10x datalogger to enable continuous data collection even when researchers where not on site. Specifically, this section is divided into subsections which describe the laboratory calibration/validation between the apparent soil dielectric constant and the measured volumetric water content of compacted samples; the set-up and calibration procedures for the Irrometer soil suction gauges; the configuration, wiring, and programing used to automate data collection using the datalogger; and the layout of instrumentation in the MBTC-3031 test pads.

4.2. Time Domain Reflectrometry Probe Calibration

The volumetric water content obtained via TDR instrumentation was derived from a third order polynomial function of the ratio of apparent probe length versus the actual probe length (L_a/L) as proposed by Topp et al., (1980) modified as described later in this section. All of the probes used for the MBTC-3031 project were manufactured by Campbell scientific (model CS610) with an probe length of 0.30 m and an probe offset value of 0.085 m. Each probe consists of three (3) 0.30 meter, 48 mm diameter stainless steel rods, with a 22 mm center to

center spacing (Campbell Scientific, 2012a). The probe was connected to the datalogger using an RG-8 50-ohm coaxial cable. An image of a CS610 probe is presented in Figure 4.1

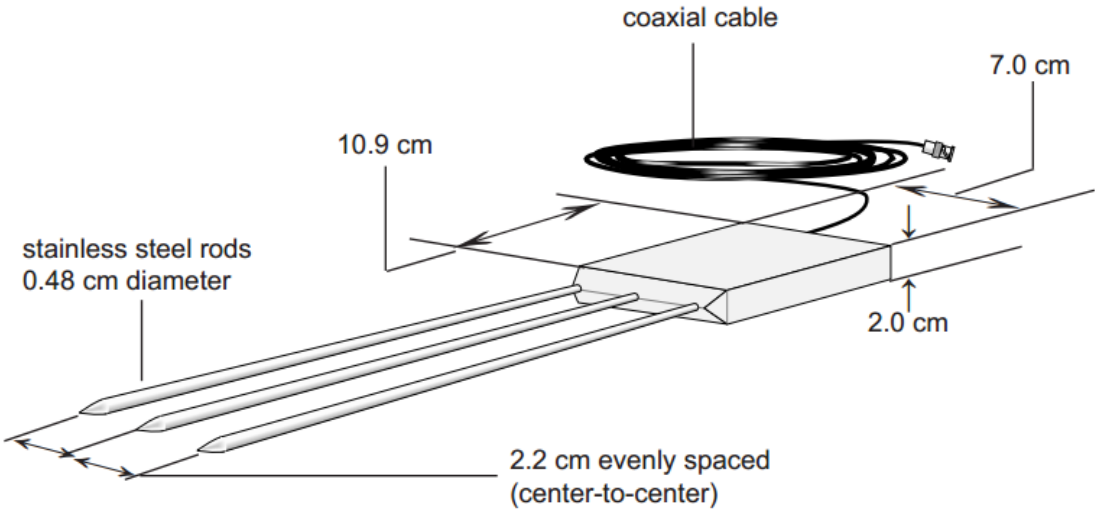

Figure 4.1. Isometric view of CS610 TDR probe (from Campbell Scientific, 2012a).

Five (5) calibration tests (C1, C2, C3, C4, and C5) were conducted using one (1) CS610 probe with a 30 meter (100 ft) RG-8 cable. Three (3) additional calibration tests were conducted using three (3) additional CS610 probes with a 15 meter (50 ft) RG-8 cable (U1, U2, and U3). Five (5) validation tests were conducted using five (5) different CS610 probes (overlapping probes with the U series tests) also with a 15 meter cable (V1, V2, V3, V4, and V5). Samples were compacted in a 13.5 inch tall, 6.5 inch diameter aluminum split mold secured using wire clamps and a collar. Two images of compacted samples in the mold with the probe installed are presented in Figure 4.2.

a) **b)**

Figure 4.2. a) Prepared sample in split mold. b) Prepared sample with mold partially removed.

4.2.1. Soil Sample Extraction

Samples were prepared at varying water content (between seven and 22 percent gravimetric water content) and were compacted using 75% standard proctor energy using a standard proctor hammer. The selection of the reduced (75%) proctor energy was chosen to most closely resemble the in-situ field compaction densities achieved during MBTC-3031 Phase 1 construction. Samples were compacted in nine, 1.5 inch thick (compacted) lifts. Compaction was conducted using 42 blows for each of the first five (5) lifts and 43 blows for the last four (4) lifts. Total compactive energy was 9, 422 ft-lbs/ft^3 which is 76 percent of standard proctor. The volumetric water content was determined using a phase diagram and the gravimetric water content. The phase diagrams and captured waveforms for all 13 tests are attached to this document as Appendix A. The results of the calibration and validation testing are presented in Table 4.1 and Figure 4.3. While there was noticeable scatter in the data the measured volumetric moisture contents did lie along the function proposed by Topp et al. (1980). There was however a significant departure from the tops equation at $(L_a/L)^2$ ratios less than 12.8. Therefore for this project the calibrated function was used for $(L_a/L)^2$ below 12.8 and the Topps et al., (1980)

equation was used for $(L_a/L)^2$ values exceeding the cut off value. It was intended to develop a site specific function to relate the $(L_a/L)^2$ ratio to volumetric moisture content however more tests are required to develop a credible, comparable polynomial.

Table 4.1. Results of calibration and validation tests.

	Water Content			
Test	Gravimetric (%)	Volumetric (%)	Vw (%) [Topps, 1980]	Error (%)
C1	19.87	33.10	33.34	0.73
C2	7.40	12.20	22.18	81.80
C3	16.62	27.80	25.24	-9.21
C4	16.80	28.40	28.13	-0.95
C5	11.85	19.87	22.81	14.80
U1	18.10	30.72	33.40	8.72
U2	15.29	26.29	29.10	10.69
U3	11.99	19.86	23.50	18.33
V1	16.80	26.70	31.08	16.40
V2	21.86	33.30	32.63	-2.01
V3[1]	20.07	33.10	57.00	72.21
V4	21.39	34.86	36.05	3.41
V5	18.07	30.59	30.12	-1.54

[1]CR-10X/TDR-100 shutdown due to low voltage during this test

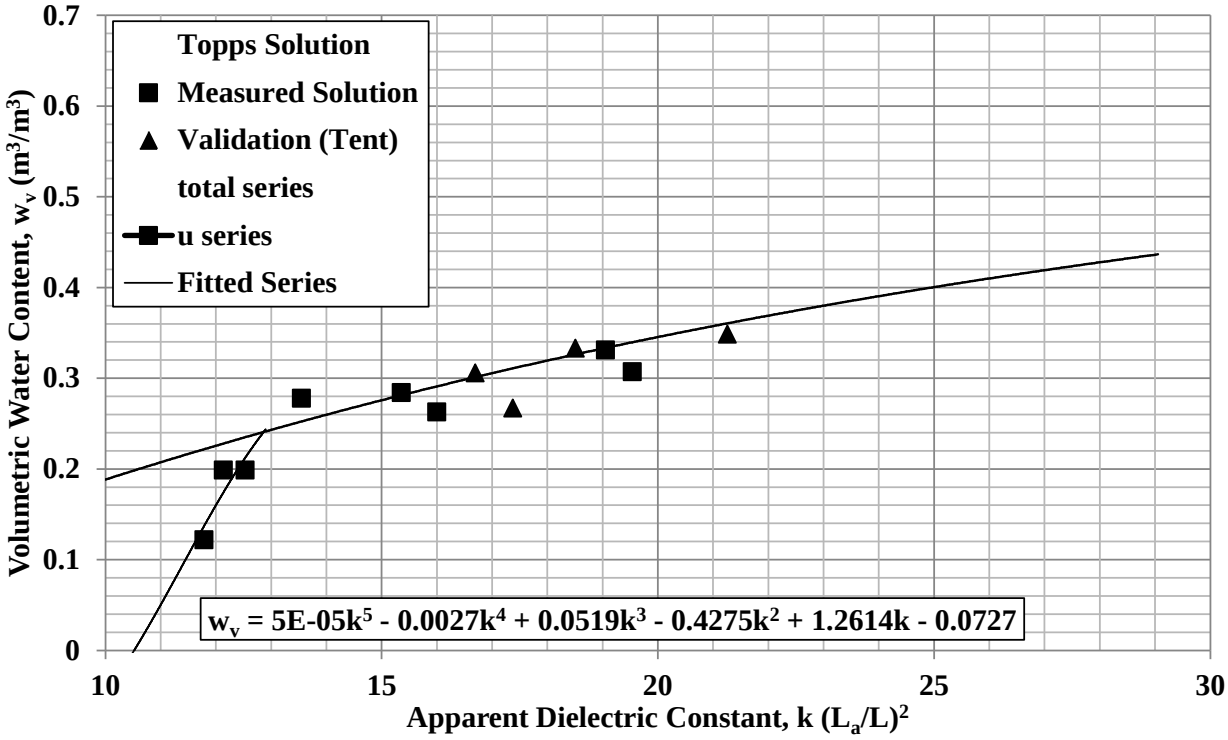

Figure 4.3. Results of thirteen calibration and validation tests.

The apparent probe length (L_a) can be calculated using several different methods as documented by Nemmers (1998). The two methods to extract the apparent probe length from a captured waveform used during this research project were the Campbell Scientific method (Campbell Scientific, 2012b) and the tangent method. An example waveform showing the implementation of the tangent method is presented in Figure 4.4 (manually implemented) and Figure 4.5 (using MATLAB code).

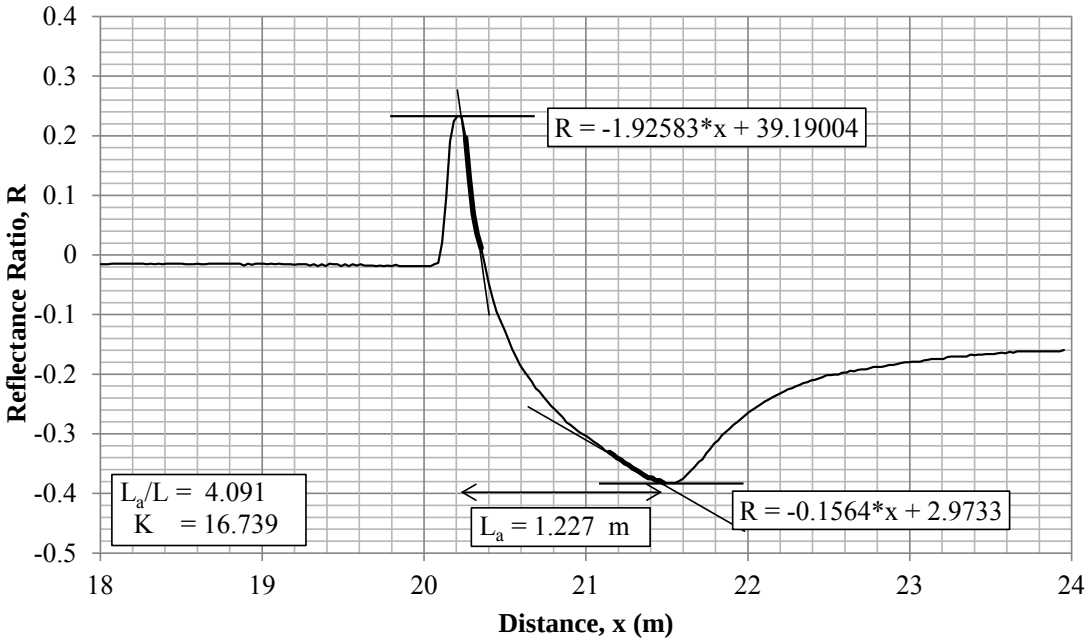

Figure 4.4. Example waveform showing application of the tangent method.

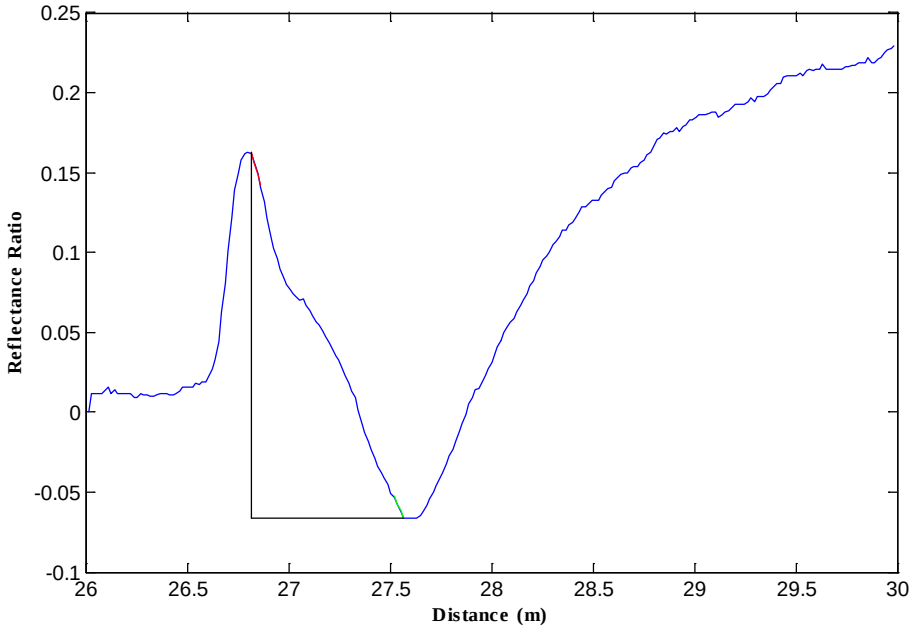

Figure 4.5. Implementation of tangent method in Matlab (in Color).

4.3. Irrometer-E Soil Suction Gauge Calibration and Set-Up Procedure

For the MBTC-3031 project 14 Irrometer – E tensiometer were employed. Each Irrometer probe was equipped with a six inch tip (sampling depth from four to six inches) and an electronic

gauge. The probe consists of a butyrate plastic body and a ceramic filter stone. An image of the probe is presented in Figure 4.6.

Figure 4.6. Irrometer tensiometer (Image from Irommeter, 2012).

Each probe is filled with a de-aired mixture as specified by the irrometer user's manual (Irrometer, 2012). The electric gauge works by using a variable resistor which causes a suction dependent voltage drop relative to the input voltage (5 V DC). As the gauge reading increases (more suction) the resistance of the gauge linearly increases. The resulting voltage drop is then read to remotely determine the suction. The soil suction is then determined using Equation 1. An image of the electronic gauge is presented in Equation 4.1.

$$P_s = \frac{(V_E - V_m)}{265^{\circ} * F_c} \qquad \text{(Irrometer, 2012)} \qquad \textbf{Equation 4.1}$$

Where V_E is the excitation voltage; V_m is the measured (signal) voltage; and F_c is the sensor calibration factor (0.00111 Volts / Degree / Centibar

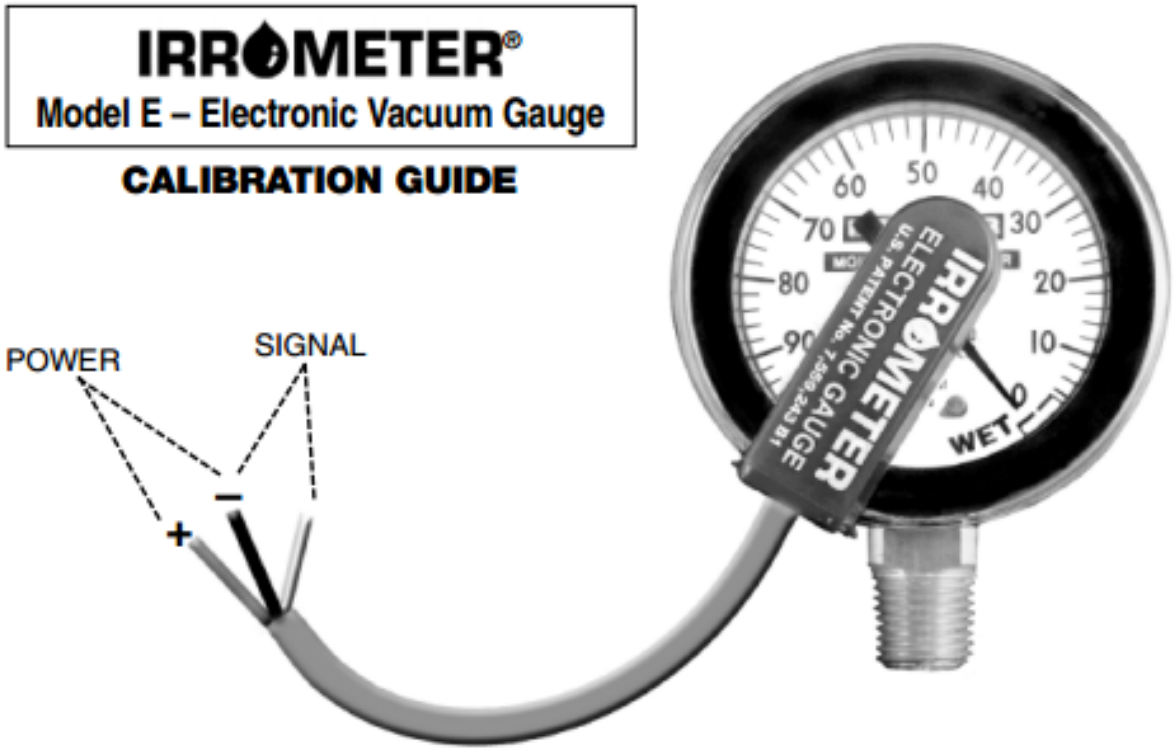

Figure 4.7. Irrometer model "E" electric gauge (Image from Irrometer, 2012).

4.4CR-10X Datalogger Programing and Configuration

The datalogger employed for this project was a Campbell Scientific CR-10X. A program was written in CRBasic (attached as Appendix B) using EDLog (part of the PC400 software suite). The program was written to query each of the 14 TDR probes three (3) times in order to obtain three (3) separate measurements. The first measurement recorded was the volumetric moisture content using the Campbell Scientific method and the Topps et al., (1980) equation (as documented in the Campbell Scientific TDR Manual [Campbell Scientific, 2012b]) which was stored as two input locations in memory (L_a/L ratio and calculated W_v). The second measurement recorded for each probe was the bulk electrical conductivity. The third measurement query captured a 250 point wave form which was then processed using a MATLAB script to determine the volumetric water content using the Tangent Method (Nemmers, 1998). After the TDR probes were queried the next set of measurements was the

fourteen Irrometer suction gauges which were attached to an AM-416 multiplexer. Other measurements taken in each 60 minute interval consisted of monitoring the voltage from both photovoltaic panels, temperature measurements from two thermocouples (referenced to the temperature of the datalogger), and precipitation (by tipping bucket). The program outputs the measurements as an ASCII string that is approximately 4200 comma delineated spaces long. An example output for the program is attached to this document as Appendix C.

The data was downloaded at regular intervals from the CR-10X using PC400 and stored as an ASCII comma-delineated text file. Each line of data (representing one set of measurements), is coded with a time stamp (year, day, hour-minute). The data was extracted using a MATLAB script that imports the data file and then separates each of the requisite variables and performs processing on the TDR waveforms using the tangent method. In order to determine the apparent length of the probe (L_a) the maximum and minimum values of the waveform are identified. A linear trendline is then fitted to a variable number of points (a fraction of the distance between the maximum and minimum values) after the maximum value. The x-location of the calculated maximum value is the intersection between the fitted trendline and the measured maximum value. Similarly, a second linear trendline is fitted to a variable number of points before the waveform's minimum value. The x-location of the calculated minimum value is the intersection between this trendline and the minimum waveform value. The apparent probe length is then taken as the distance between the x-locations of the minimum and maximum waveform values. The MATLAB function used to extract the data is attached as Appendix D.

The data collection package consisted of the CR-10X, three (3) SDM-50 multiplexers, one (1) AM-416 multiplexer, one (1) TDR-100, one (1) 12-V 70 amp-hour power-supply, two

(2) 30 V photovoltaic panels, two (2) solar power controllers, and a relay assembly. The wiring diagram of the data collection package is presented in Appendix E. A tabulation of the equipment used and the purpose of each component are presented in Table 4.2

Table 4.2. Data collection package components.

Item	# Used	Purpose
CR-10X	1	Data collection and data storage
SDM-50	3	8 channel multiplexer for TDR probes
AM-416	1	16 channel multiplexer for Irrometer probes
TDR-100	1	Time domain reflectrometry sensor
Solar Energy Controller	2	Charging and regulating 12 V power supply
Photovoltaic Panel	2	Power supply and proxy for solar intensity measurement
12-V 70 amp-hour power supply	1	Power supply and regulation
Relay Assembly	1	Used to provide switched 5 V power to AM-416 Multiplexer

Not included on the list of components is the four (4) voltage dividers used to reduce incoming voltage at the data logger. The differential measurement ports on the CR-10X have a range of +/- 2500 mV. Several of the measurements (the photovoltaic panel voltage, the irrometer excitation voltage, and the irrometer signal voltage) exceeded the 2500 mV limit. In order to not over range the datalogger voltage dividers were used to reduce the range of the voltage at the measurement ports. The circuit diagrams for the voltage dividers and integrated voltage divider and relay are presented in Figure 4.8.

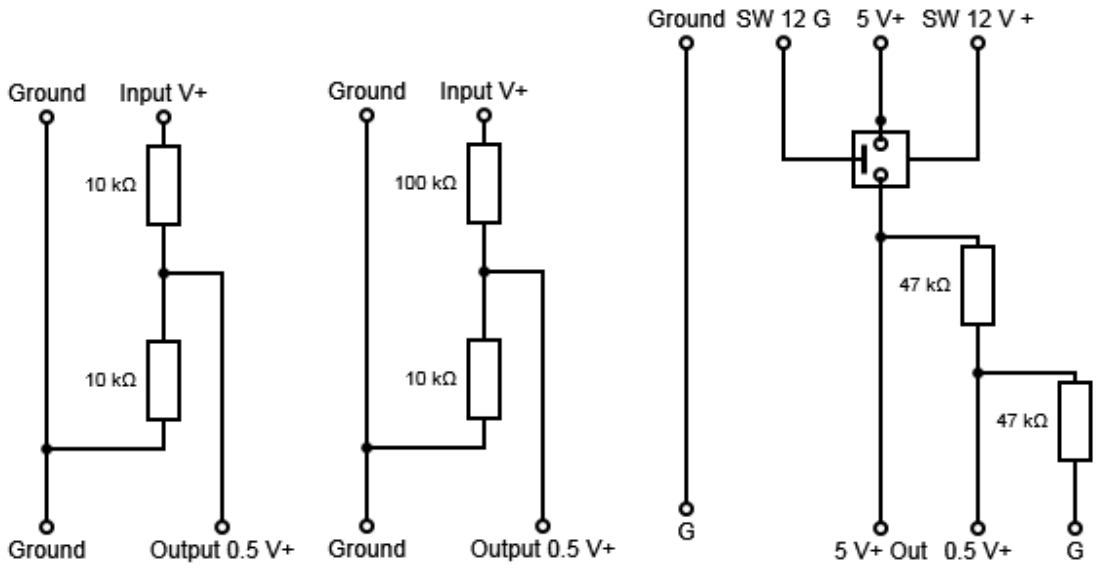

a) b) c)

Figure 4.8. Circuit diagrams for a) 2:1 voltage divider, b) 10:1 voltage divider, and c) integrated 2:1 voltage divider and relay assembly.

4.5. Summary

This chapter is devoted to a discussion of the MBTC-3031 Phase 2 instrumentation and thhe development of the data collection system required to allow for automated monitoring of the in-situ conditions. Some of the important aspects of the Phase 2 instrumentation include the calibration and validation of the site specific relationship between the apparent probe length measured by the TDR system and the volumetric water content of the soil samples. Additionally, the existing Campbell Scientific data collection system (based on the CR-10X data logger) required significant modifications to allow for interoperability with the Irrometer –E suction gauges.

Chapter 5. Results and Discussion

5.1 Introduction

Contained in this section is a discussion of the results generated during the MBTC-3031 project. Specifically, discussed are the results generated via the remote sensing (radar and LIDAR) along with the initial results generated using the Phase II in-situ instrumentation.

5.2. LIDAR Results

The results from three of the scans were compared to determine the effectiveness of the LIDAR scanner to detect movement in the pads. Scan 1 was taken during the site construction and was not used in subsequent comparisons. Scan 2 was used as the master image and Scans 3 and 4 were used as follower images to determine the change in elevation of the ground surface relative to the initial scan. LIDAR images were captured over a three month period (January 19th – March 16th, 2012). The master image (to which all others were compared) was used to generate a digital elevation map of the site. The "master" digital elevation map is presented as Figure 5.1. The relative displacement between the Scans 2 3, and 4 is presented in Figure 5.2.

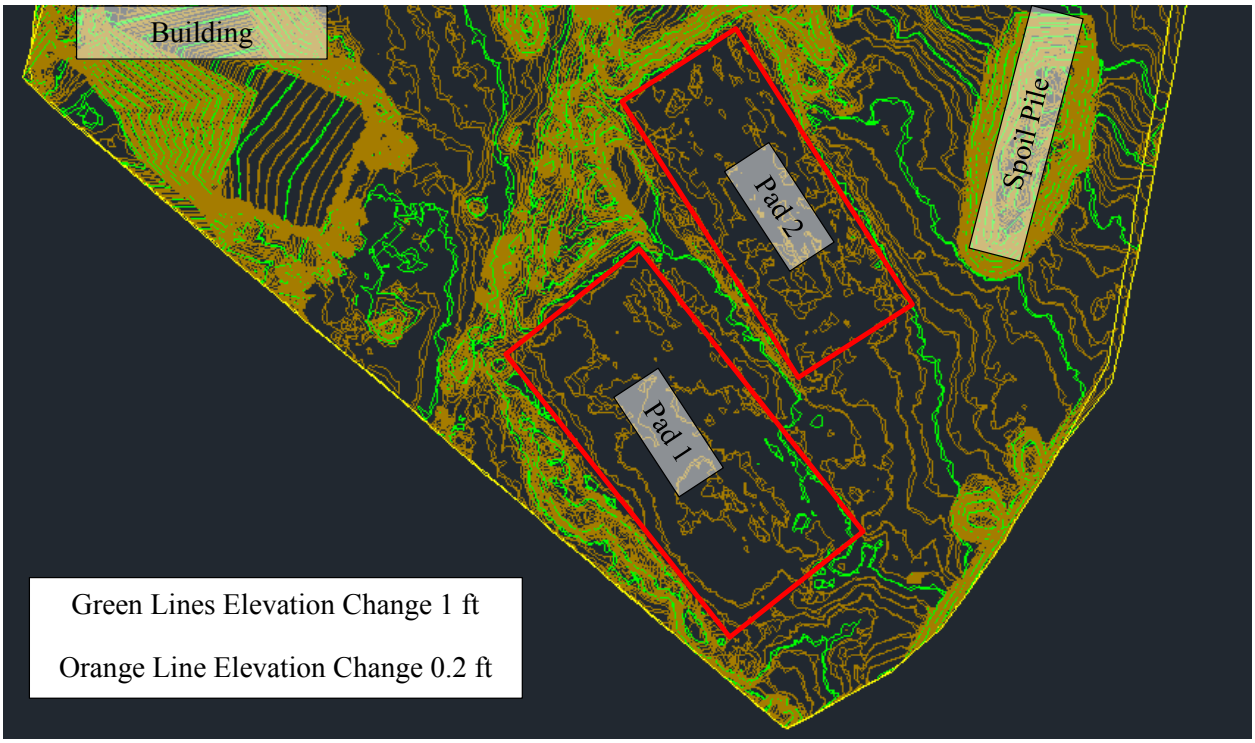

Figure 5.1. Constructed site topography and master digital elevation map with test pads outlined in red [in color].

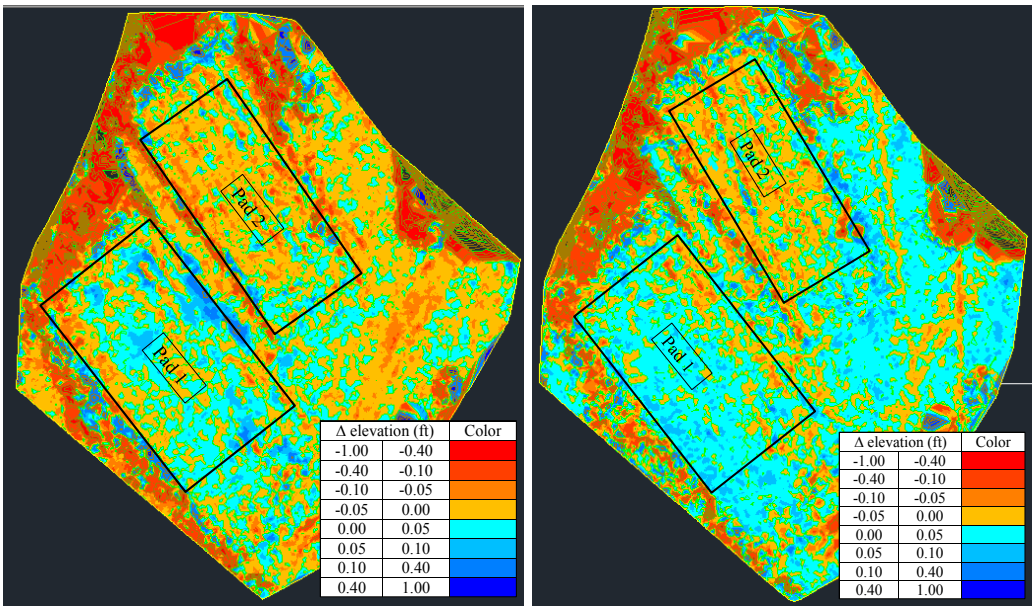

(a) (b)

Figure 5.2. a) Elevation difference between scans 2 and 3 (January – February 2012). B) Elevation difference between scans 2 and 4 (January – March 2012) [in color].

The amended pad (Pad 1) displayed expansive behavior (relative to the initial elevation) in both scans 3 and 4. Conversely, the native soil pad (Pad 2) showed a very slight subsidence in both scans 3 and 4. Significant precipitation and cool/freezing temperatures occurred between scans 2 and 3 with approximately 4.5 inches of rain falling during this period (NOAA, 2012). An image of the site taken on February 6th, 2012 (between scans 2 and 3) is presented as Figure 5.3.

Figure 5.3. Project site image taken February 6th, 2012 after heavy rainfall.

The areas of standing water identifiable in Figure 4 correlate to the areas of expansion observed between scans 2 and 3 (along the upper right boundary of Pad 1 in Figure 3). Precipitation was significantly reduced (less than one inch) between scans 3 and 4 (NOAA, 2012). No discernible difference was detected between the pads overall and the control sections incorporated into each pad. However, it is possible that the movement in the control sections was not accurately captured due to the resolution lost when the point cloud was thinned in order to use in AutoCAD. Improved processing techniques which do not require the large reduction in the point cloud density would improve the spatial resolution of each scan significantly. While these results do indicate that the LIDAR scanner is capable of detecting relatively small changes in elevation further investigation is needed with respect to data processing in order to achieve sufficient spatial resolution.

1.1. Radar Results

Although data was collected using the GPRI-II, the data was not fully processed due to time and budgetary constraints. Specifically, computation time (multiple weeks) and computational resources (multiple terra bytes of storage capacity) prevented processing of the data collected at the site. Additional computational resources have been purchased and the processing will be completed for the site after the date of printing this document. An addendum, including the results of the radar surveys, to this document will be submitted at a future date.

1.2. In-Situ Instrumentation Results

Preliminary data from the in-situ instrumentation (TDR probes, tensiometers, thermocouples, and rain gauge) has been downloaded and analyzed. Measurements taken include soil and air temperature, precipitation, soil suction, and volumetric water content. The recorded soil suction over 352 hours is presented in Figure 5.4 (for Pad 1) and Figure 5.5 (for Pad 2).

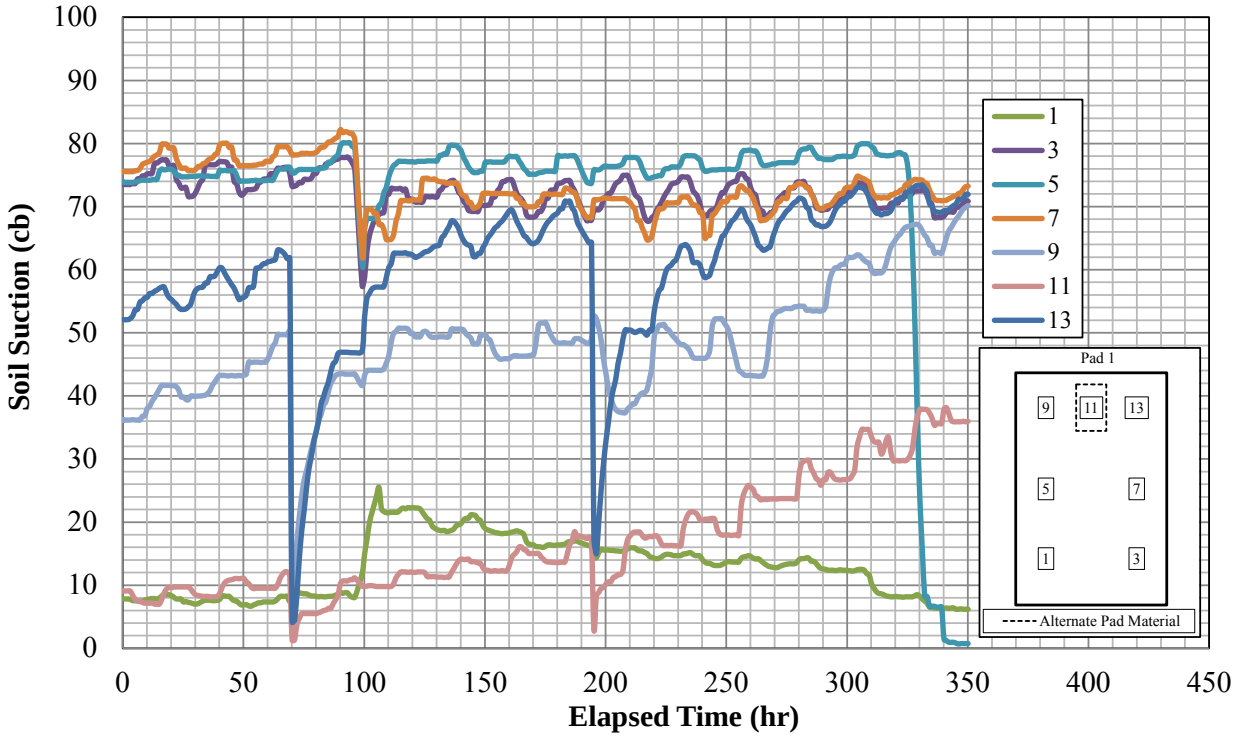

Figure 5.4. Soil suction vs. elapsed time for Pad 1 (in color).

The soil suction readings show a strong reaction accompanying the observed precipitation events at an elapsed time of approximately 70 and 195 hours. The large, sudden decrease in the observed suction recorded at station 13 might be indicative of water migration via a desiccation crack or along the probe body. Additionally, the effects of diurnal cycles can be clearly detected in the observed suction measurements for Pad 1. Measurements of soil suction recorded over a period of aproximatly 2,000 hours (non-continous due to battery failure in the instrument collection package) is presented in Figure 5.6 and Figure 5.7.

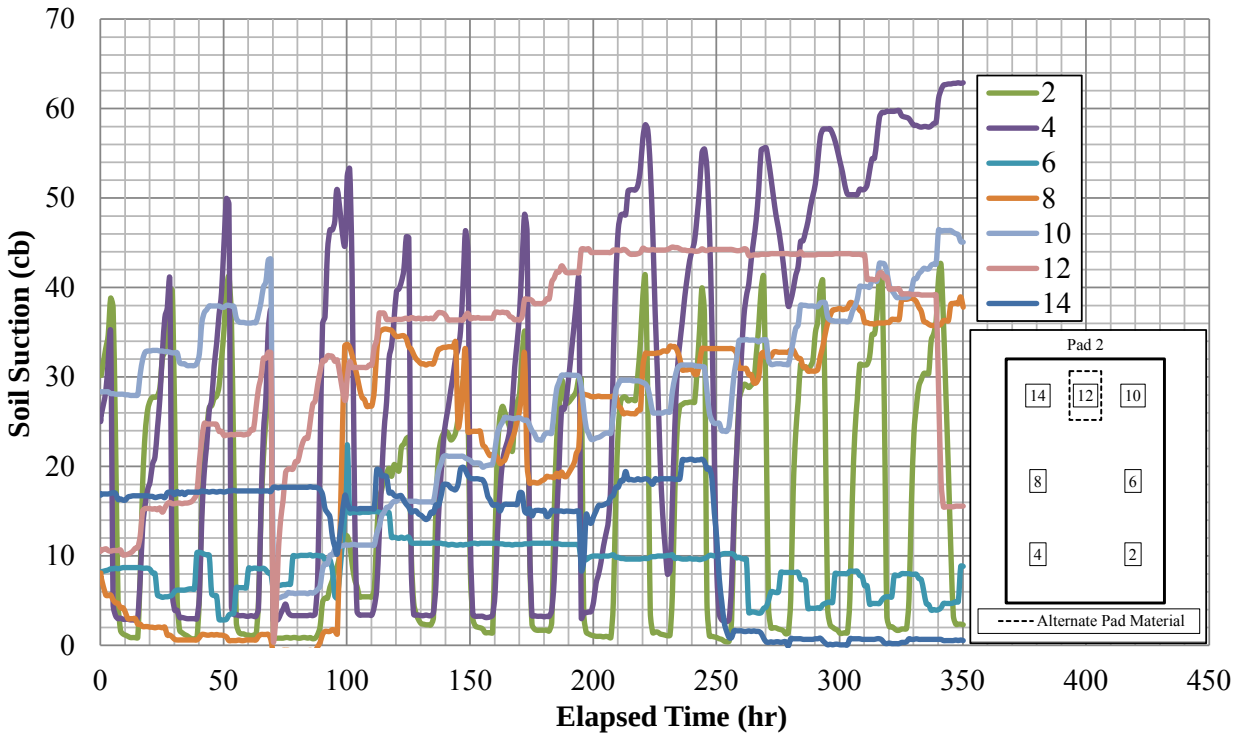

Figure 5.5. Soil suction vs. elapsed time for Pad 2 (in color).

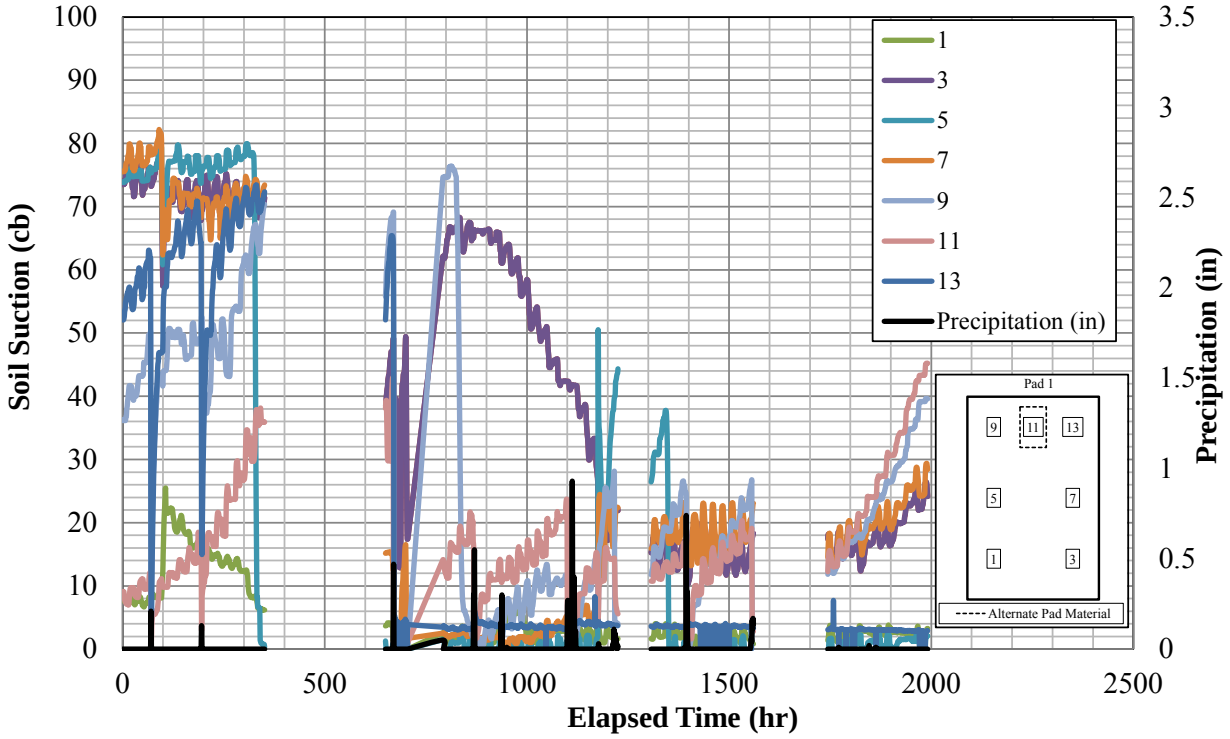

Figure 5.6. Soil suction vs. elapsed time and precipitation for Pad 1 (2000 hours, in color).

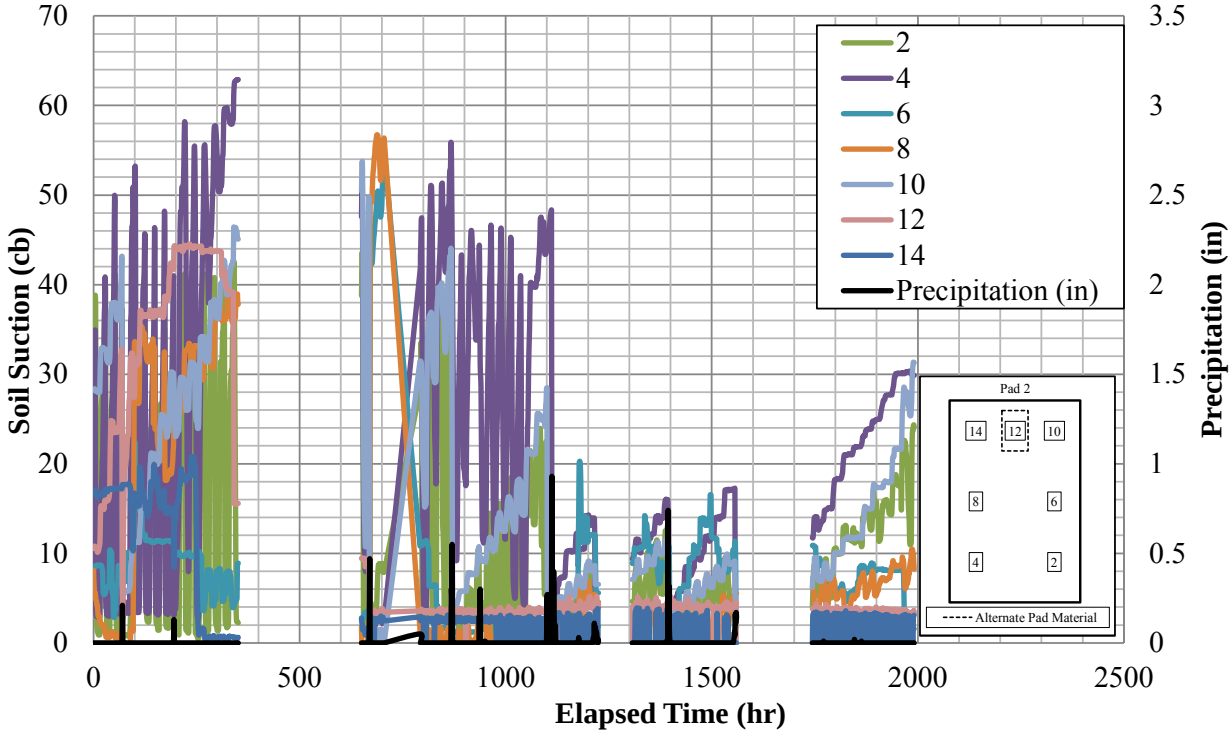

Figure 5.7. Soil Suction vs. elapsed time and precipitation for Pad 2 (2000 hours, in color).

The observed soil suction measurements for Pad 2 showed a significantly greater variation over the entire pad. Stations 2 and 4 showed very large diurnal cycles (~4-50 centibar and 2-40 centibar, respectively). It is hypothesized that this may be attributable to thermal expansion and contraction of the acrylic instrument sealing and unsealing the probe tips. The cyclic behavior is strongly correlated to the temperature (and perhaps especially to the soil temperature. Another potential source of error for the Irrometer tensiometer probes is the growth of algea in the probe reservoir. In order to prevent the growth of algea in the probe bodies a bleach solution was added to the probe fluid. A plot of soil suction at stations 2 and 4 versus temperature is presented in Figure 5.8 and the observed temeperture (soil and air) at the MBTC-3031 site is presented in

Figure 5.9. Due to additional signal losses in the data collection it was necessary to adjust the recorded Irrometer signals by 21 centibar (e.g. a reading of 81 corresponds to a gauge reading of

60).

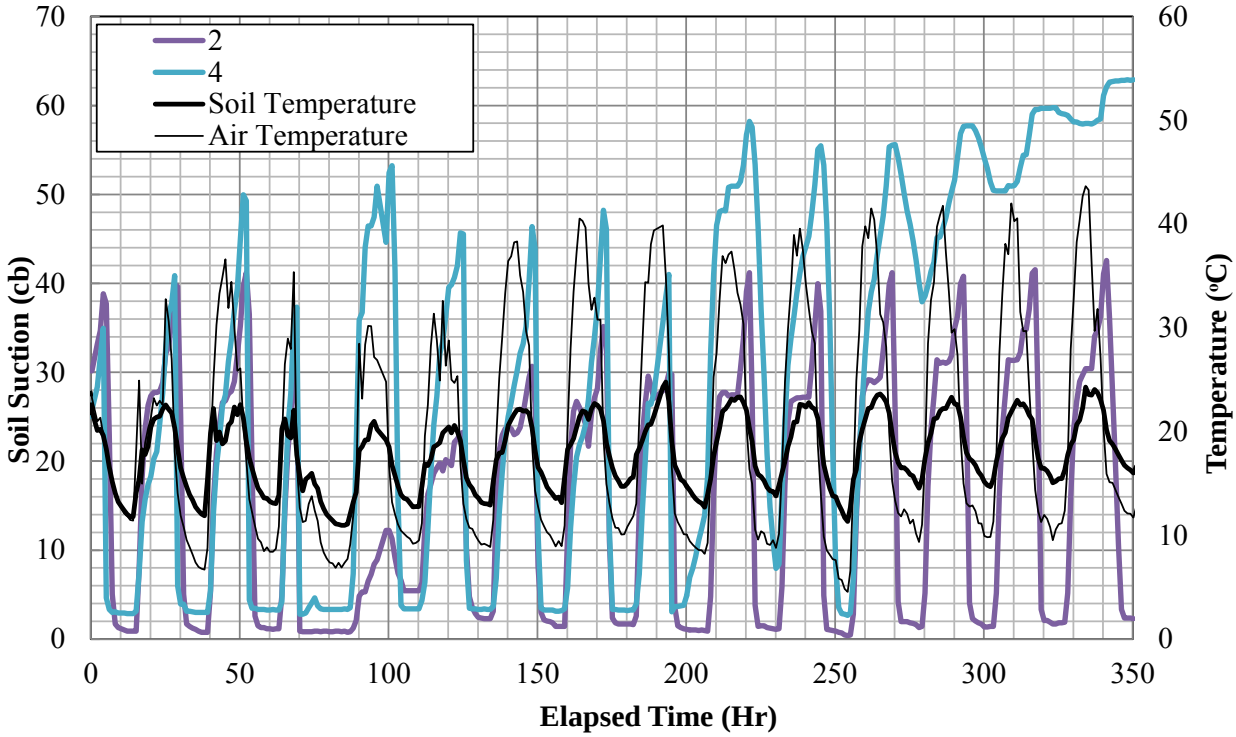

Figure 5.8. Soil suction at stations 2 and 4 and temperature vs. elapsed time (in color).

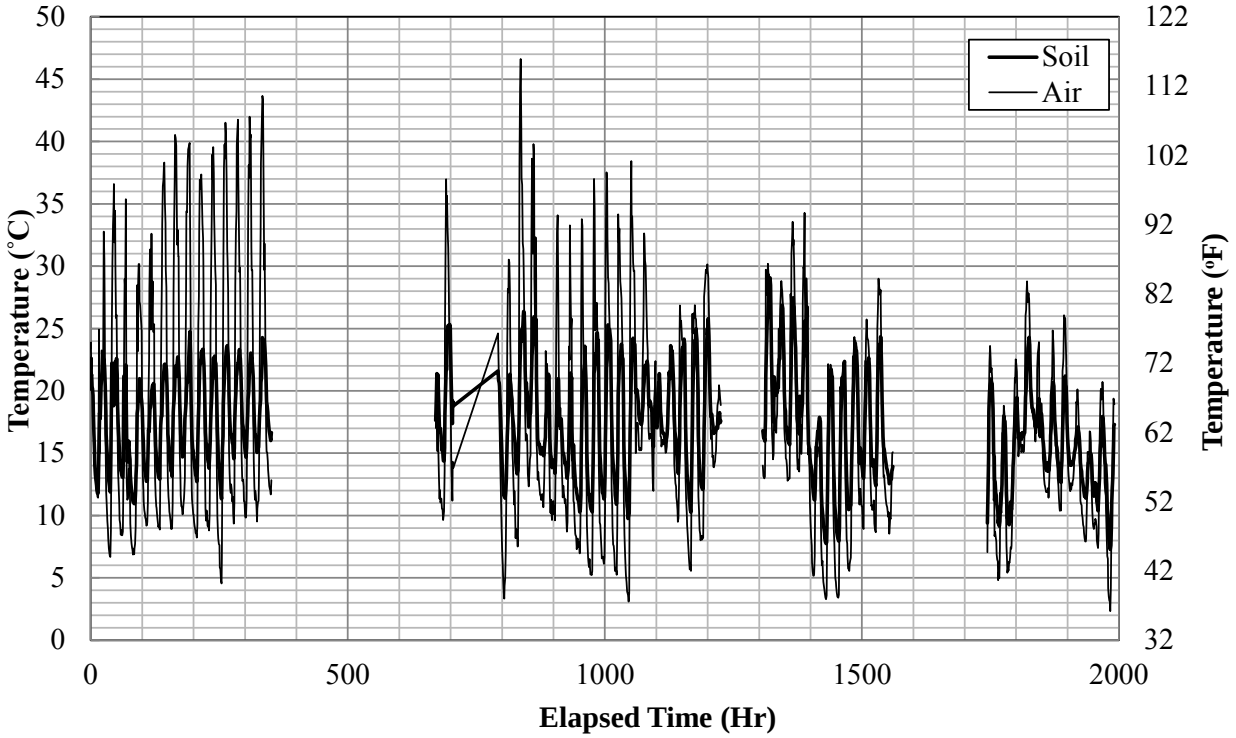

Figure 5.9. Observed soil and air temperatures at MBTC-3031 site.

The volumetric water content was calculated using the TDR probes and the tangent method as previously described in Section 7.1. In conjunction with the matric suction derived from the Irrometer probes the volumetric water content was used to generate a soil-water characteristic curve for the experimental test pads. Due to the limited time span, and particularly the limited precipitation over the observed period, the pad has not experienced the large changes in volumetric water content associated with wetting-drying cycles. Additionaly, three probes (1, 5, and 6) either experienced degrading measurements, no discernible returned, or returned a non-sensical L_a/L value. It is anticipated that these measurement errors can be attributed to installation (improper fill, excessive deformation in the probes on installation) or to the connections used. On some of the probes it was nessecary to splice the RG-8 cable to get enough scope to cover the test pads. As a result a second section of RG-8 cable was spliced on to the probes using a combination of n-type connectors and a BNC/n-type adapters. At some future time the researchers will excavate the probes to determine the cause of these anomoulus results. An example of soil suction versus volumetric water content plot is presented in Figure 5.10 and plots for all stations are contained in Appendix E.

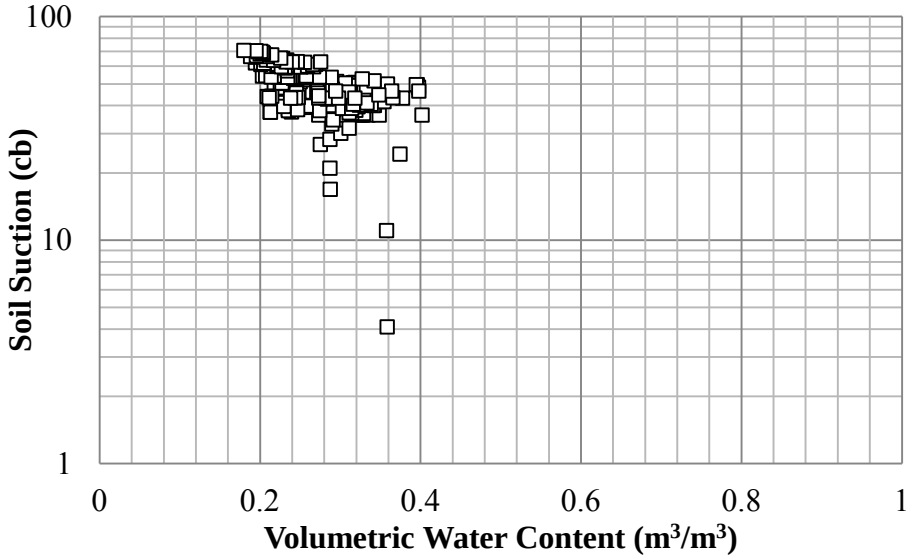

Figure 5.10. Soil suction vs. volumetric water content for station 9.

Additional in-situ measurements taken include the solar panel output which was used as a proxy measurement of solar irradiance. A plot of solar panel output versus elapsed time is attached as Figure 5.11 (for 350 hours) and Figure 5.12 (for 2000 hours). There were two observed rainfall events occurring at the project site in the first 350 hours. Subsequent to the initial monitoring period, an additional seven rainfall events were recorded in aproximatly 2,000 hours (Figure 5.13).

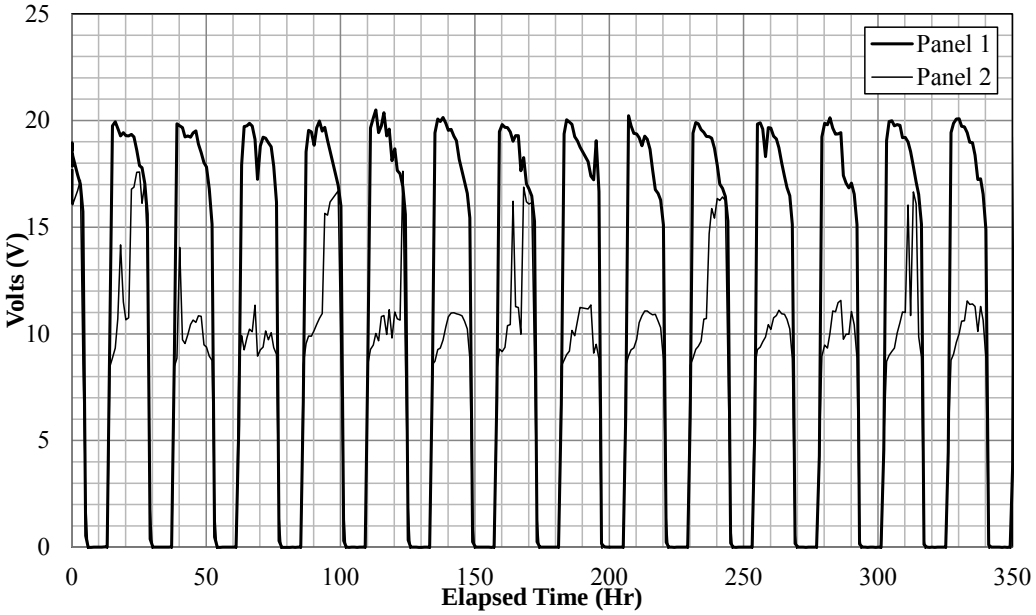

Figure 5.11. Solar panel output vs. elapsed time (350 hours).

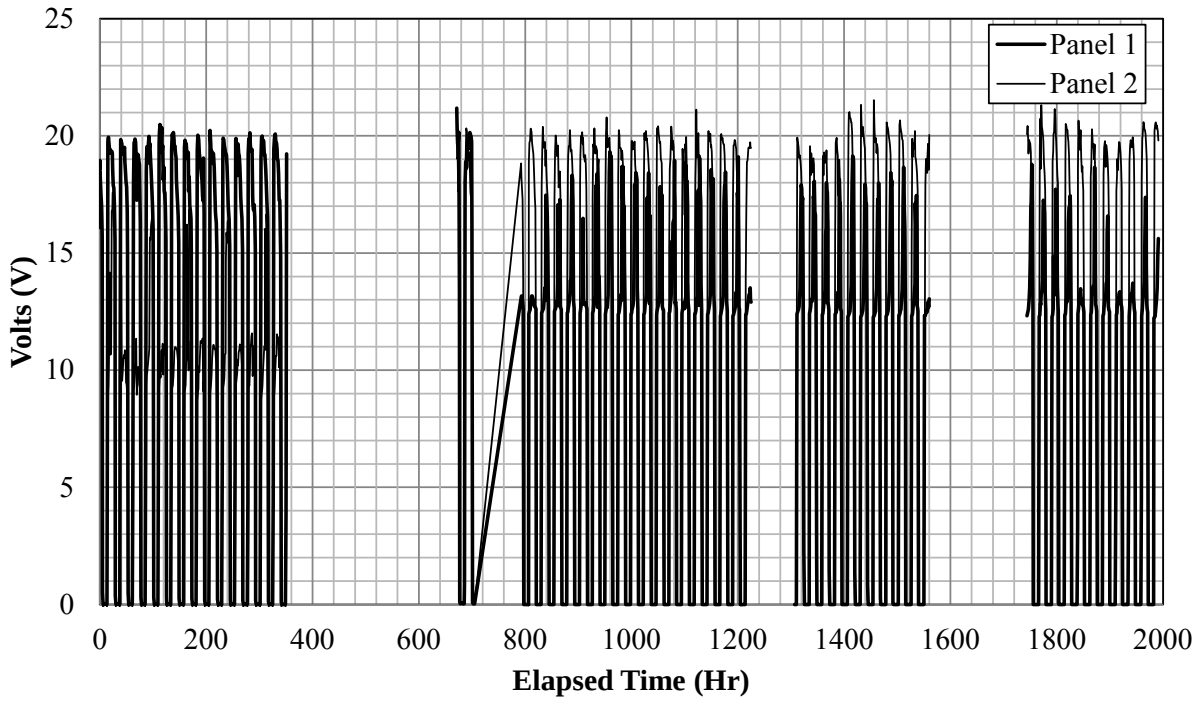

Figure 5.12. Solar panel output vs. elapsed time (2000 hours).

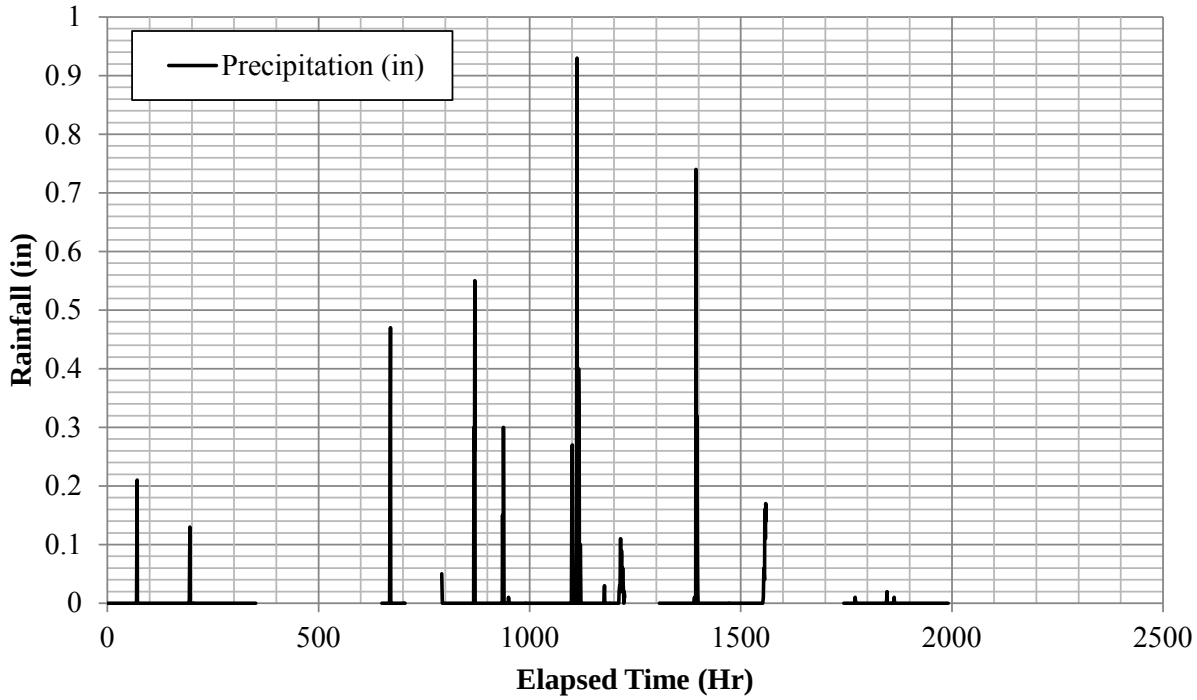

Figure 5.13. Precipitation vs. elapsed time.

5.3. Summary

This chapter contains a description of the results generated during the MBTC-3031 research project. The LIDAR system was capable of detecting ground motions however the limitations in the processing greatly decreased the effectiveness of this system. The in-situ measurement equipment provided real time data regarding the conditions inside the clay layer. However, due to installation and equipment issues there was some loss of resolution. Further investigation is required to determine the most optimum method of installing the probes in a stiff, compacted clay layer.

Chapter 6. Conclusion and Recommendations

6.1. Introduction

The chapter contains the final conclusions and recommendations derived from the MBTC-3031 research project. Some of the conclusions drawn include the effeciacy of the remote sensing in detecting the movement associated with expansive clays. Secondly, the in-situ instrumentation proved capable of monitoring changing conditions.

6.2..Future Work

The following areas have been identified by the authors as requiring further investigation. Firstly, the LIDAR data processing severly reduces the resolution (a loss of ~ 90 percent of the point cloud). The authors are investigating other software platforms to remove the restriction on the size of the point cloud.

With respect to the radar scans the lack of a rigid refrence point may have induced the measurement of "false" displacements. While the roof blocks were not observed to move during the course of the project it is possible that the blocks did experience some movement due to either weather events or inadveradently during routine facility maintance operations. Even if the roof blocks were not directly displaced they were bearing on the roof membrane, insulation, and then the roof structure itself. It is anticipated that the foam insulation may have experienced thermal expansion and contraction over the course of the project which may also be another source of error.

Another area of investigation involves the installation of the in-situ instrumentation. The authors encountered significant difficulties installing both the TDR probes and the tensiometers. For the TDR probes the compacted clay liner caused deformation in the probes. Addtionally, in some cases there is the potential for a void to exist underneath the expoxy head of the probe. In

several cases the installation jig encountered the bottom and or sides of the trench potentially preventing the full installation of the TDR probes. After probe installation, the authors attempted to backfill and hand compact the excavated trench. However, it was difficult to compact the area immediately around and under the probe body without damaging the probe itself. The presence of these voids may be one source of error on the TDR measurements

6.3. Conclusion

The conclusions drawn over the course of this research project include the validation of LIDAR remote sensing to identify and characterize the presence of expansive clay induced ground movement. However, improved processing techniques are required to fully utilize the potential of this technology. With respect to the tensiometers it was difficult to install the probes with an adequate seal and to prevent the growth of algea in the fluid resevior. Additioanly the suction measurements were found to be highly influenced by diurnal cycles. It is unsure if the suction variation between day and night represent accuracte or false results. Despite the difficulties encountered with the installation of the TDR probes it appears that the TDR system is capable of providing real time measurement of the volumetric water content.

References

ASTM D 698. 2005. Standard test methods for laboratory compaction characteristics of soil using standard effort (12400 ft-lbf/ft3 (600 kN-m/m3)), Annual Book of ASTM Standards, 04.08, ASTM, West Conshohocken, PA, USA: 80-90.

ASTM D 422. 2005. Standard test method for particle size analysis of soils, Annual Book of ASTM Standards, 04.08, ASTM, West Conshohocken, PA, USA: 10-17

.

Bulut, Rifat. nd. Total and Matric Suction Measurements with the Filter Paper Method. Presentation by Rifat Bulut, Fugro South Inc. http://www.foundationperformance.org/pastpresentations/FilterPapSuctMeasDemonstrtn.pdf. Retrieved September, 2012.

Campbell Scientific, (2012a). TDR100-based System (Time Domain Reflectometry) brochure. http://www.campbellsci.ca/Catalogue/TDR100_Br.pdf. Retrieved June, 2012.

Campbell Scientific, (2012b). TDR100 Manual http://s.campbellsci.com/documents/us/manuals/tdr100.pdf. Retrieved June 2012.

Chabrillat, S., Goetz, A.F.H, Krosley, L., Olsen, H., (2002), "Use of Hyperspectral Images in the Identification and Mapping of Expansive Clay Soils and the Role of Spatial Resolution," *Remote Sensing of Environment*, vol. 82, 431-445.

Chen, F. H., 1988. Foundations on expansive soils. Elsevier Science LTD. Amsterdam, NL

Conte, Omar A. R. (2012). Slope Stability Monitoring Using Remote Sensing Techniques. Master Thesis. University of Arkansas – Fayetteville. May 2012.

Coffman, Richard A. (2009), "Processing of Synthetic Aperture Radar Data as Applied to the Characterization of Localized Deformation Features," Ph.D. Dissertation, University of Missouri, Columbia, August.

Conte, Omar (2011). MBTC-3031 site survey. Personnel communication to Dr. Richard A. Coffman. Dated August 31, 2011.

Fredlund, D.G., and Rahardjo, H., 1993. *Soil Mechanics for Unsaturated Soils*, Wiley, New York.

Goetz, A.F.H., Olsen, H.W., Noe, D.C., Koehler, J.R., Humble, J.P., Fuschino, J., Johnson, E.L., Johnson, B.J. (2006). "Spectral reflectance as a rapid technique for field determination of soil engineering properties," Proceedings Geo-volution 2006, pp. 33-61.

Gourley, C., Newill, D., and Schreiner, H., 1993. Expansive Soils: TRL's research strategy. First Int. Symposium on Engineering Characteristics of Arid Soils. London, UK

Google Earth, (2012). The Google Earth software suite. The Google Corporation. Imagery retrieved February, 2012.

Google Maps, (2012). Google Maps website. The Google Corporation. http://maps.google.com. Last accessed February, 2012.

Humbold Manufacturing, 2012. Humbolt Manufacturing Website. http:/www.humboldtmfg.com/shc-2.html. Retrieved September, 2012.

IAEA, 2008. Field Estimation of Soil Water Content. International Atomic Energy Agency. Training Course Series 30. Vienna, Austria.

Irrometer, (2012). Irrometer-E gauge and probe documentation. Irrometer website. http://www.irrometer.com/pdf/instruction%20manuals/IRROMETERs/755%20E%20GaugeVACUUM%20hi%20Web4.pdf. Retrieved June, 2012.

Mitchell, J.K, and Soga, K., 2005. *Fundamentals of Soil Behavior*. 3rd. Ed. Wiley, Hoboken, New Jersey.

Nayak, N. and Christensen, R., 1971. Swelling Characteristics of Compacted, Expansive Soils. Clays and Clay Minerals. Vol. 19. P 251-261

Nelson, J.D., and Miller, D.J., 1992. *Expansive Soils Problems and Practice in Foundation and Pavement Engineering*, John Wiley & Sons Inc, New York.

Norish, K. 1954. The Swelling of Montmorillonite. Discussions of the Faraday Society. Vol. 18 p. 120-134

Nemmers, Charles (1998). Volumetric Moisture Content Using Time Domain Reflectometry. FHWA publication number: FHWA-RD-97-139

Ruedrich, J., Bartelsen, T., Dohrmann, R., Siegesmund, S., 2011. Moisture Expansion as a Deterioration Factor for Sandstone Used in Buildings. Environmental Earth Science. Vol 63. P. 1545-1564.

Seed, H. B., Woodard, R. J., Jr., and Lundgren, R., (1962), "Prediction of swelling potential for compacted clays," Journal of American Society of Civil Engineers, Soil Mechanics and Foundations Division, Vol. 88, No. SM3, pp. 53-87.

Take, W., Arnepalli, D., Brachman, R., and Rowe., R. 2007. Laboratory and Field Calibration of TDR Probes for Water Content Measurement. Ottawa Geo 2007. Ottawa, CN.

Topp, GC, Davis, JL, Annan, AP, 1980. Electromagnetic Determination of Soil Water Content: Measurements in Coaxial Transmission Lines. WATER RESOURCES RESEARCH, 16(3), 574-582.

USACE, 1986. EM 1110-2-1906 Laboratory Soils Testing. United States Army Corp of Engineers.

USACE, 2004. Foundations in Expansive Soils. Unified Facilities Criteria Document UFC 3-220-07. United States Army Corp of Engineers, Preparing Authority.

Villar, M., 2004. Influence of temperature on the hydro-mechanical behavior of a compacted bentonite. Applied Clay Science. Vol 26. Issue 1-4. P. 337-350

Wyoben, (2012). Wyo-Ben Enviroplug product information sheet. http://www.wyoben.com/WBAssets/z-downloads/product_sheets/enviroplug16.pdf. Last accessed February, 2012.

Yavapi College, 2012. Website for AGS-105 Soil Colloids. http://faculty.yc.edu/ycfaculty/ags105/week08/soil_colloids/soil_colloids_print.html. Retrieved September, 2012.

Appendix A

A.1. . TDR calibration and captured waveforms

This appendix contains the phase diagrams and captured waveforms utilized in the calibration of the TDR probes for the MBTC-3031 project. Each of the tests was conducted in the same mold using 75 percent reduced proctor compaction energy. This level of compaction was selected based off the nuclear density gauge testing results after the completion of Phase 1 construction. It should be noted that the final compacted samples were significantly less compacted then the field placement (Phase 2).

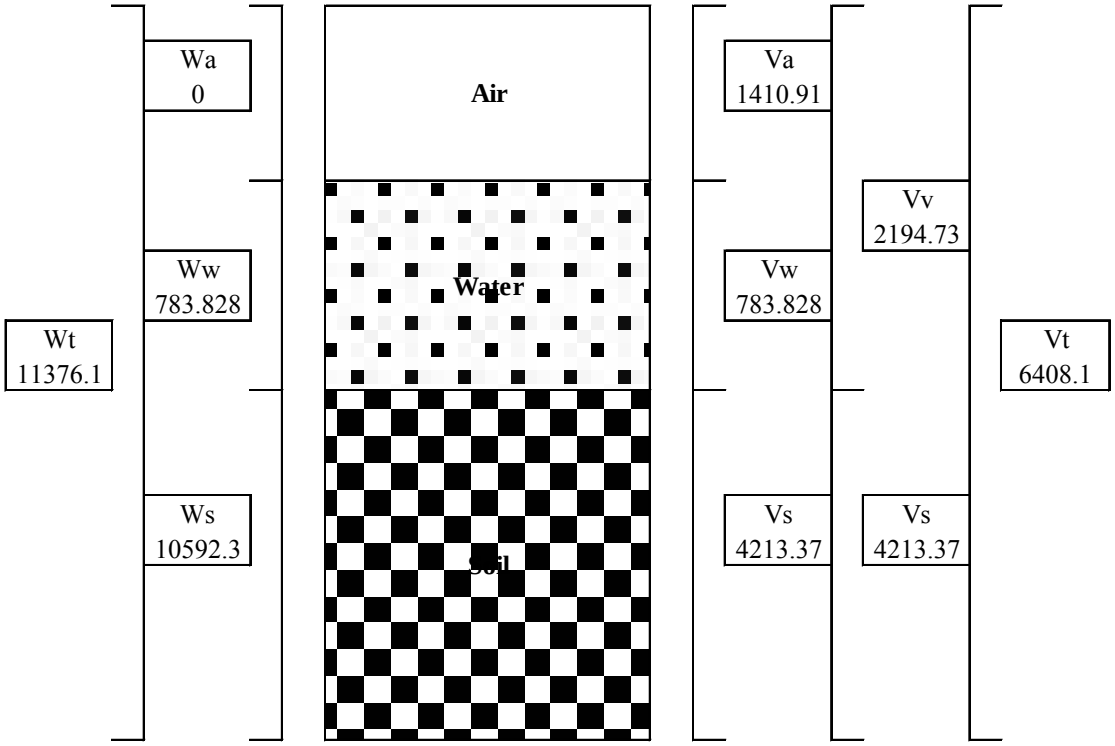

Figure A.1. Phase diagram for test C1 (weights in grams and volumes in cm).

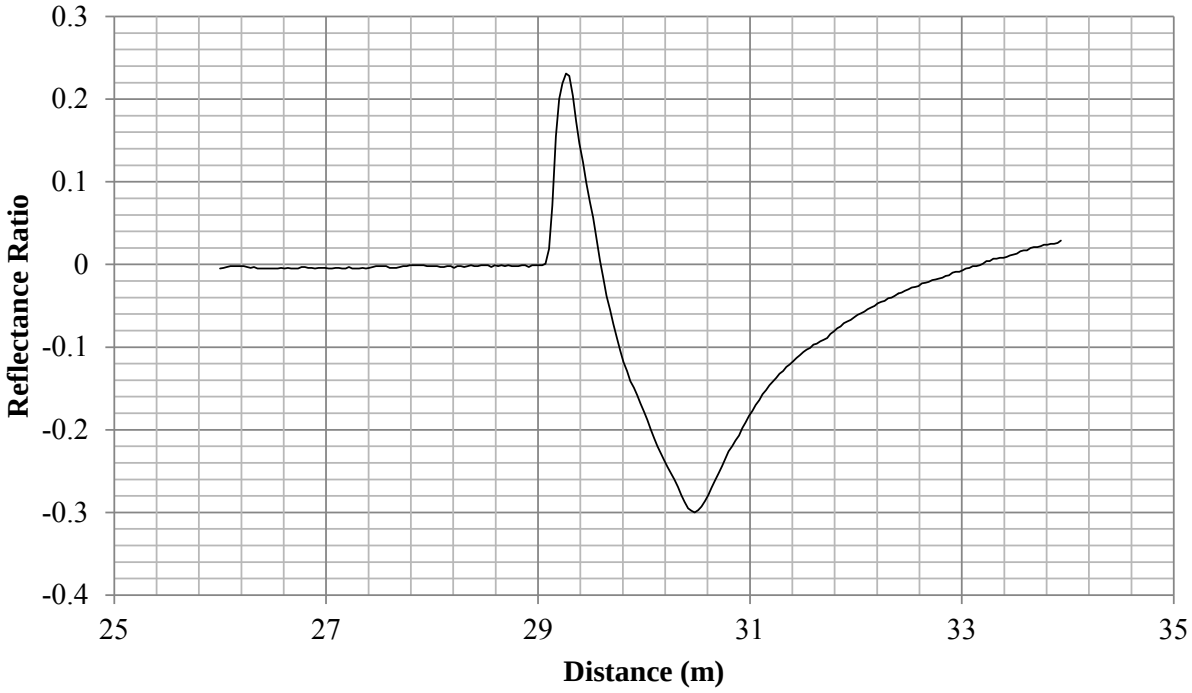

Figure A.2. Captured waveform for test C1.

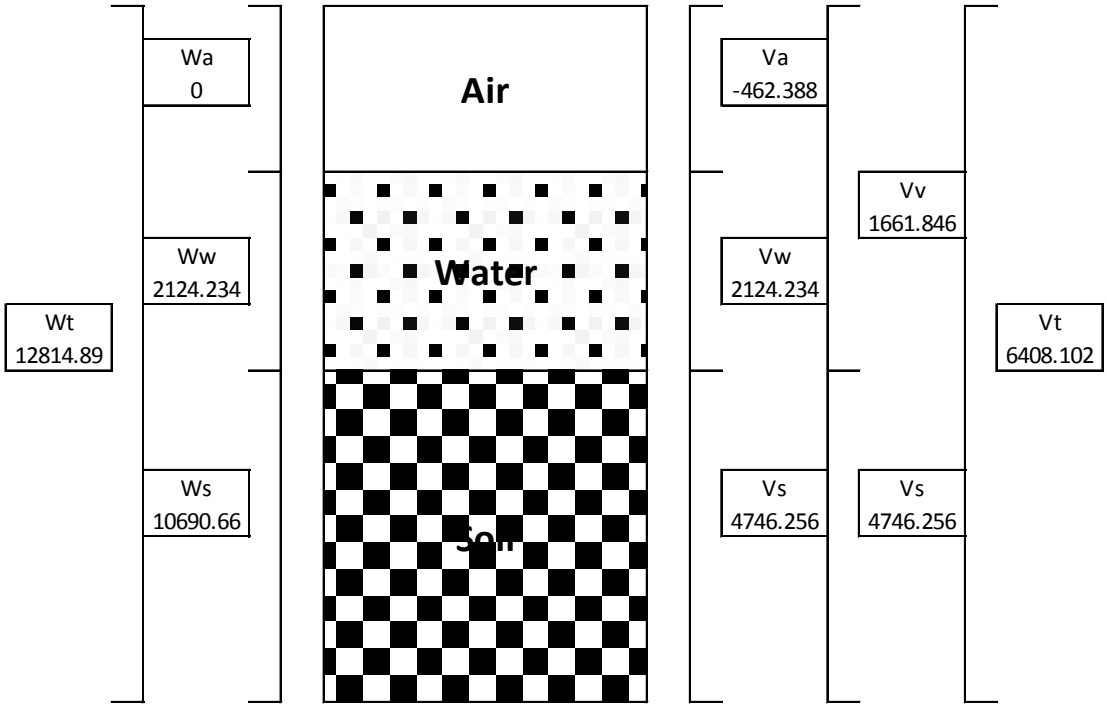

Figure A.3. Phase diagram for test C2 (weights in grams and volumes in cm).

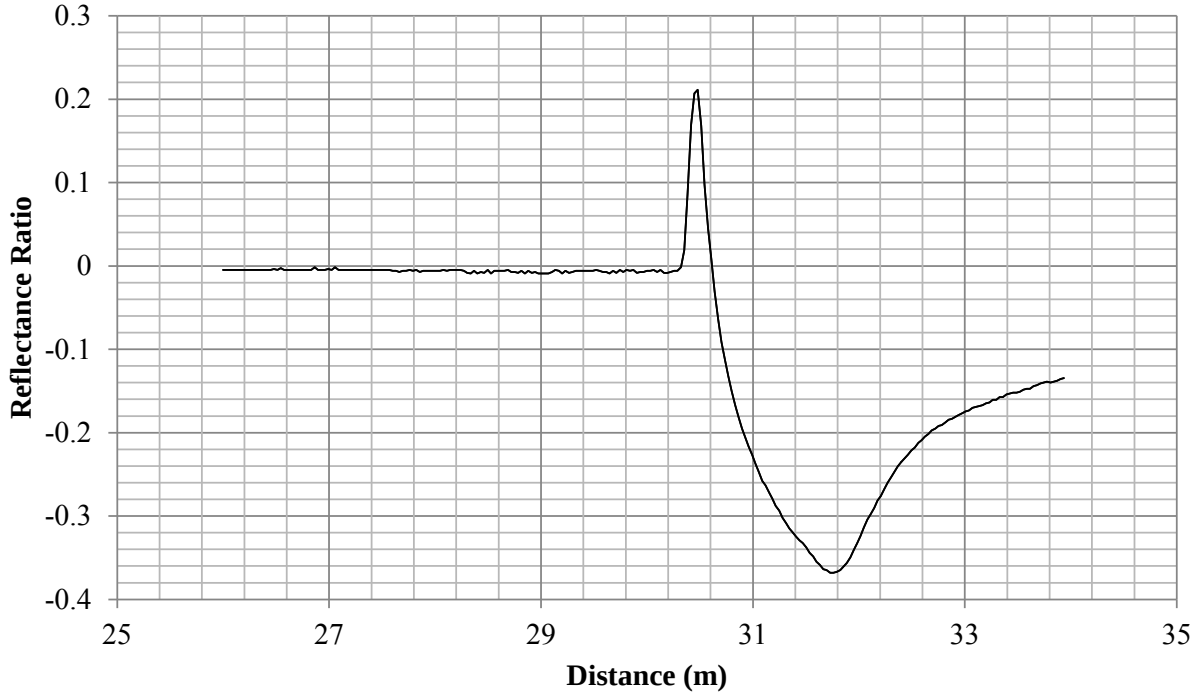

Figure A.4. Captured waveform for test C2.

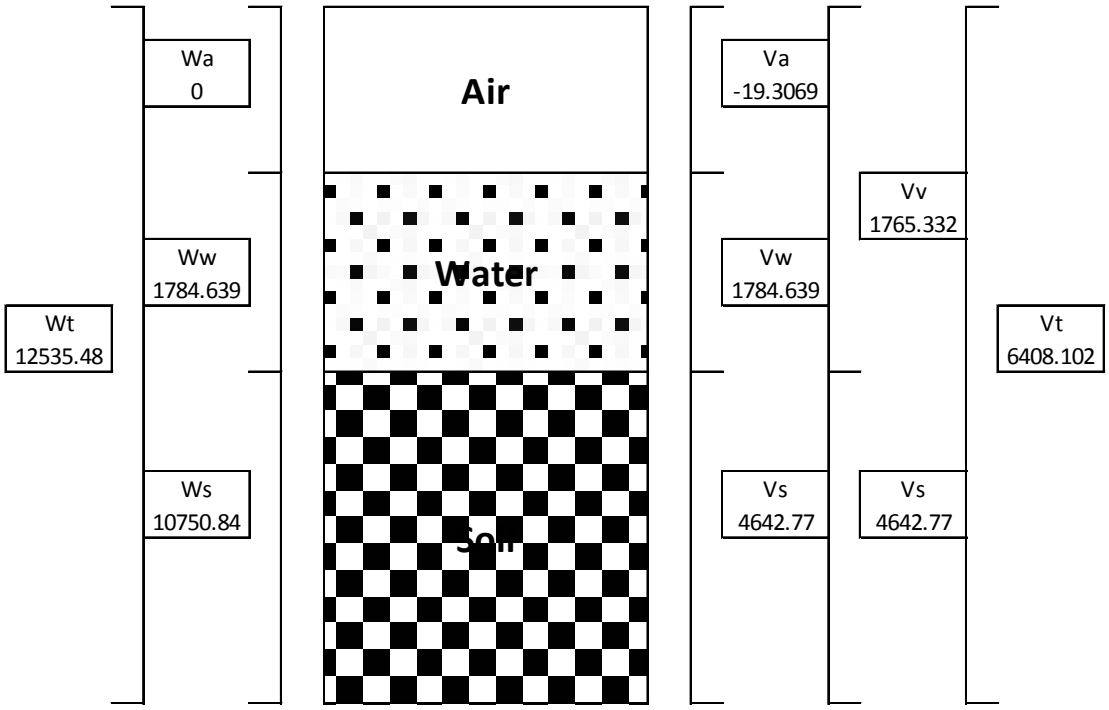

Figure A.5. Phase diagram for test C3 (weights in grams and volumes in cm).

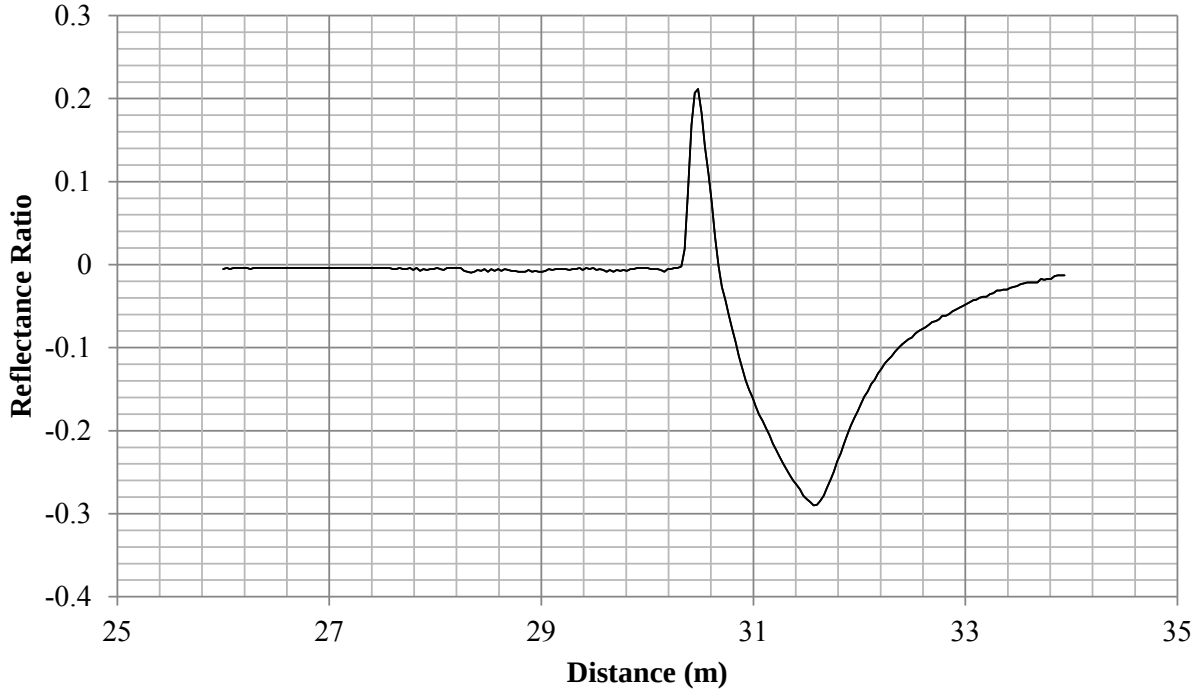

Figure A.6. Captured waveform for test C3.

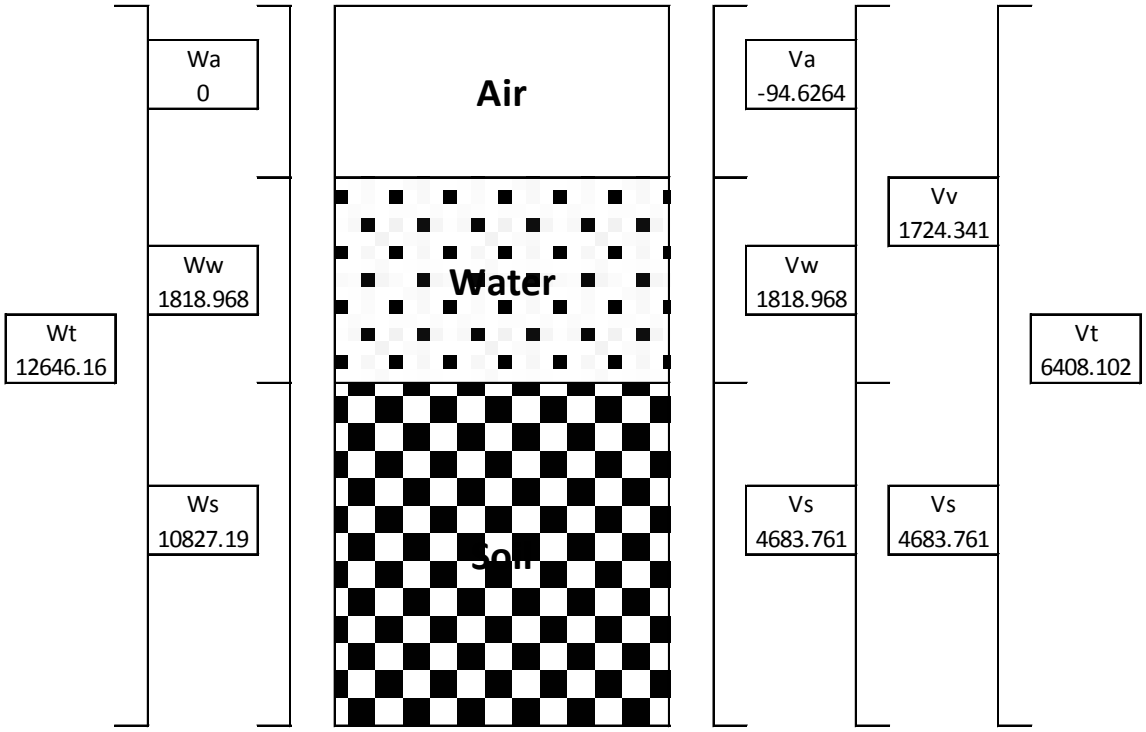

Figure A.7. Phase diagram for test C4 (weights in grams and volumes in cm).

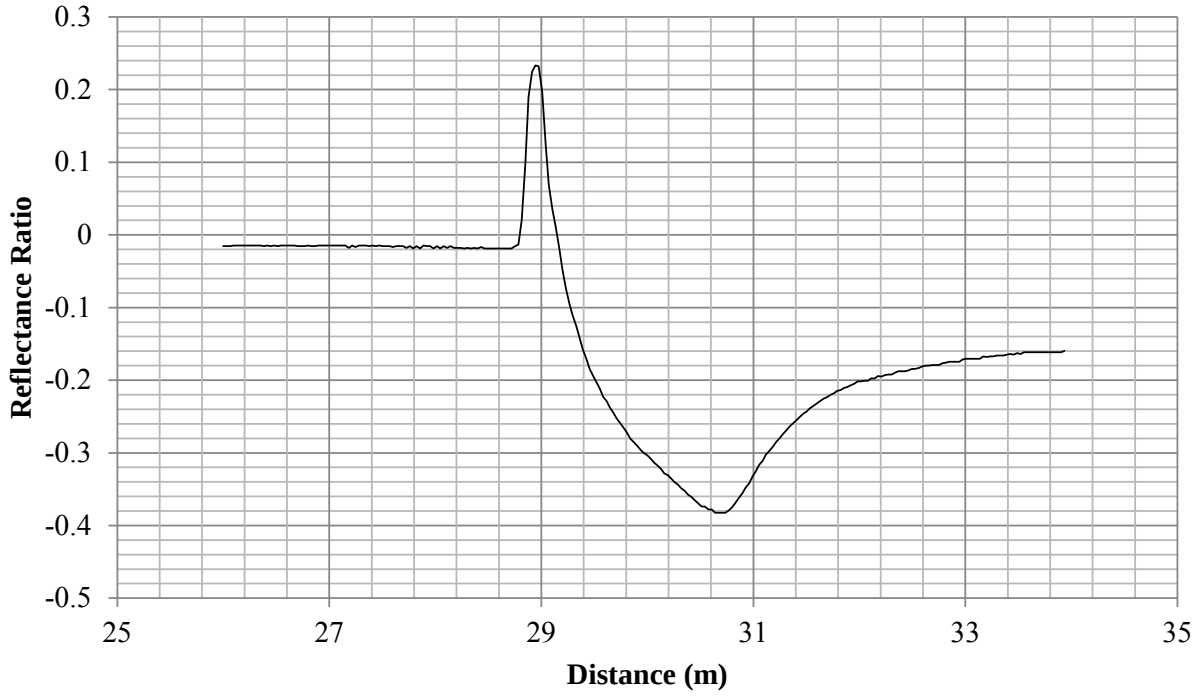

Figure A.8. Captured waveform for test C4.

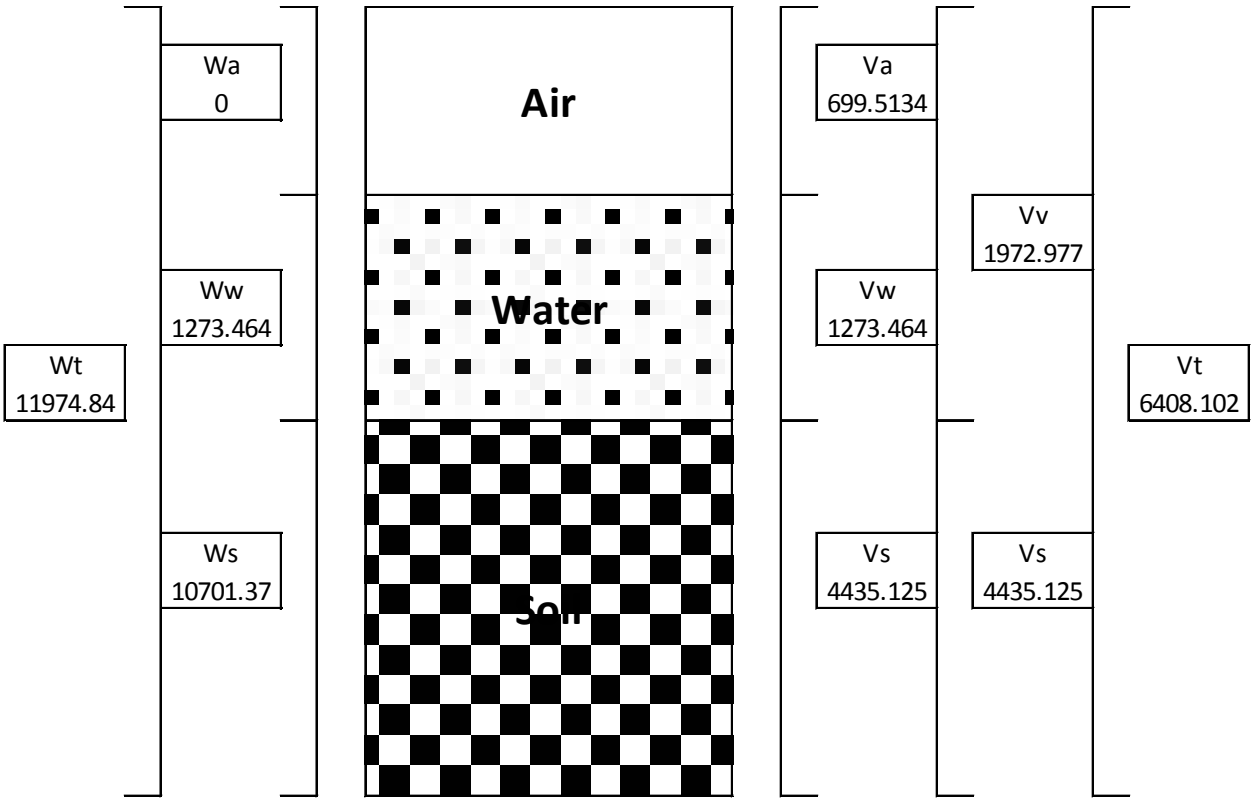

Figure A.9. Phase diagram for test C5 (weights in grams and volumes in cm).

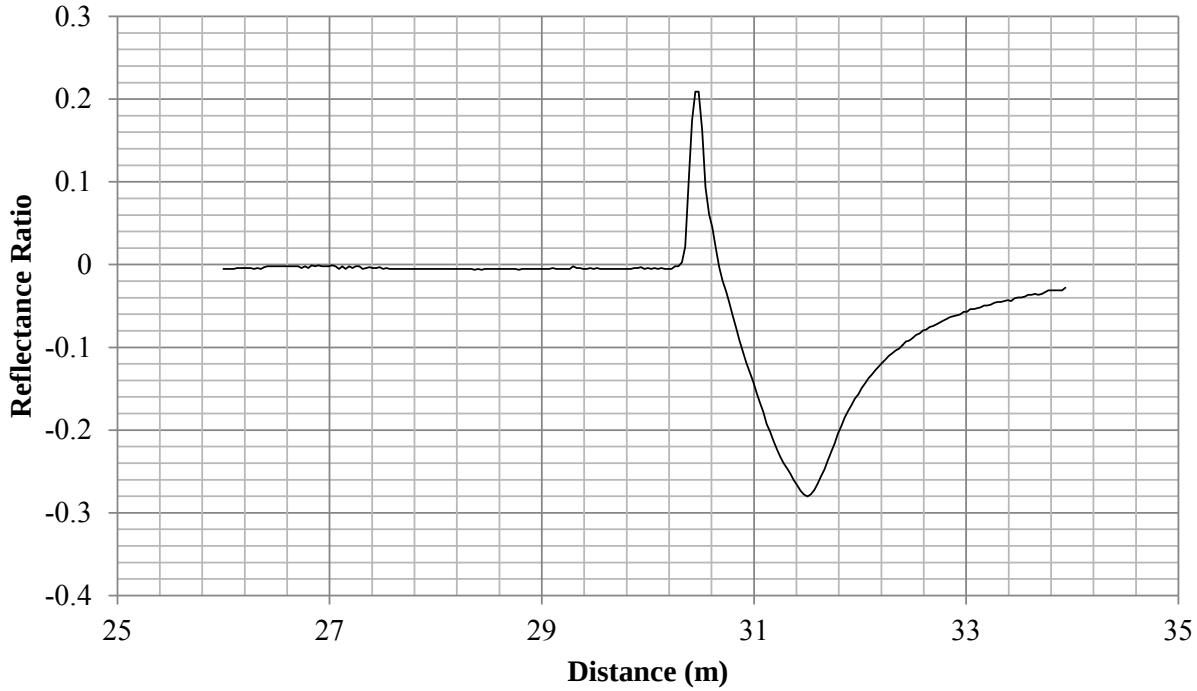

Figure A.10. Captured waveform for test C5.

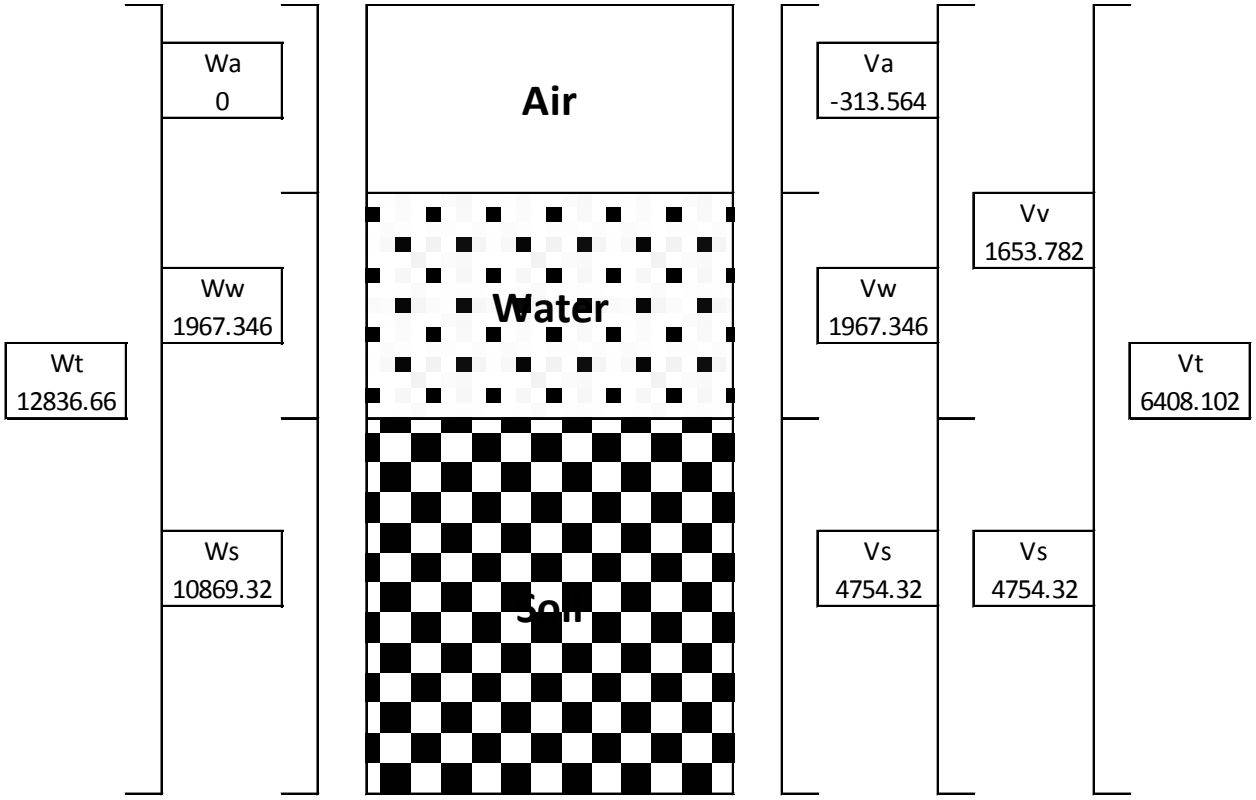

Figure A.11. Phase diagram for test U1 (weights in grams and volumes in cm).

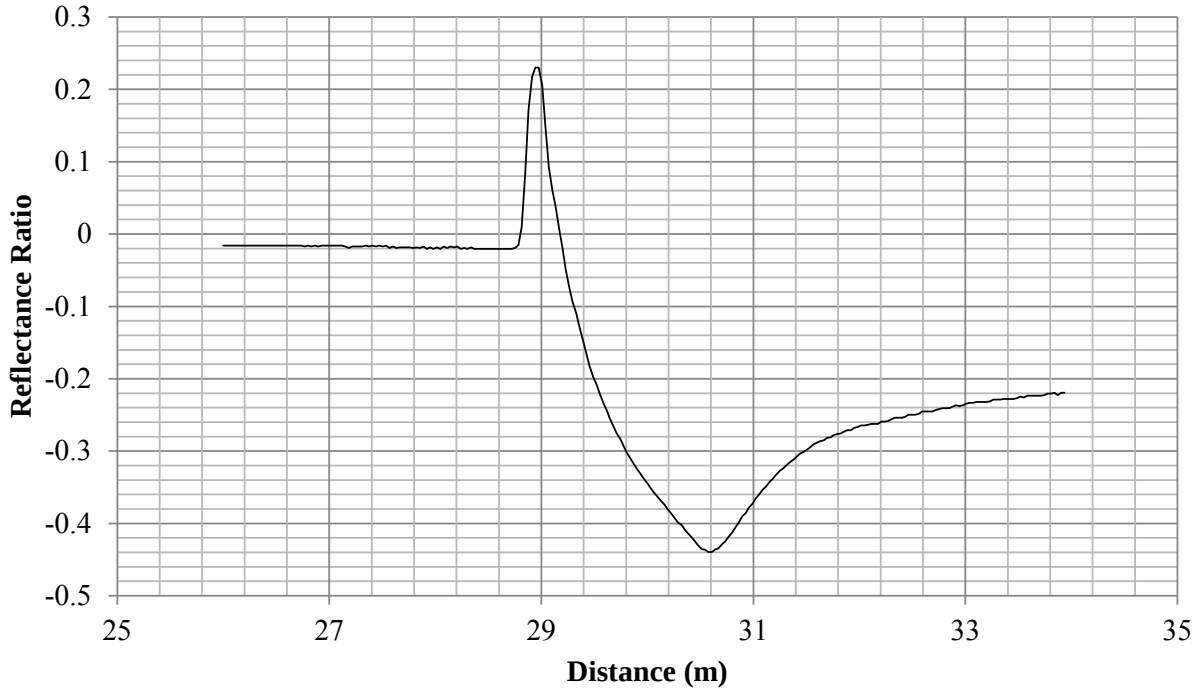

Figure A.12. Captured waveform for test U1.

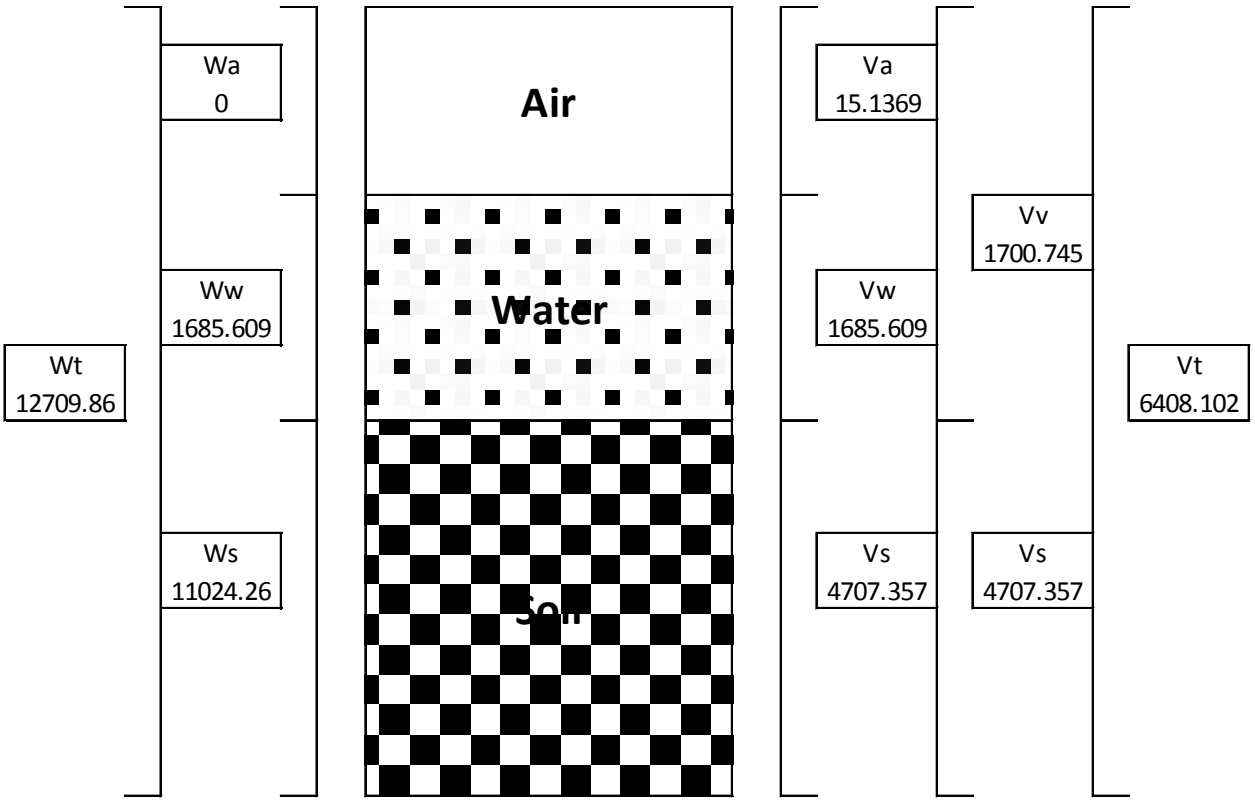

Figure A.13. Phase diagram for test U2 (weights in grams and volumes in cm).

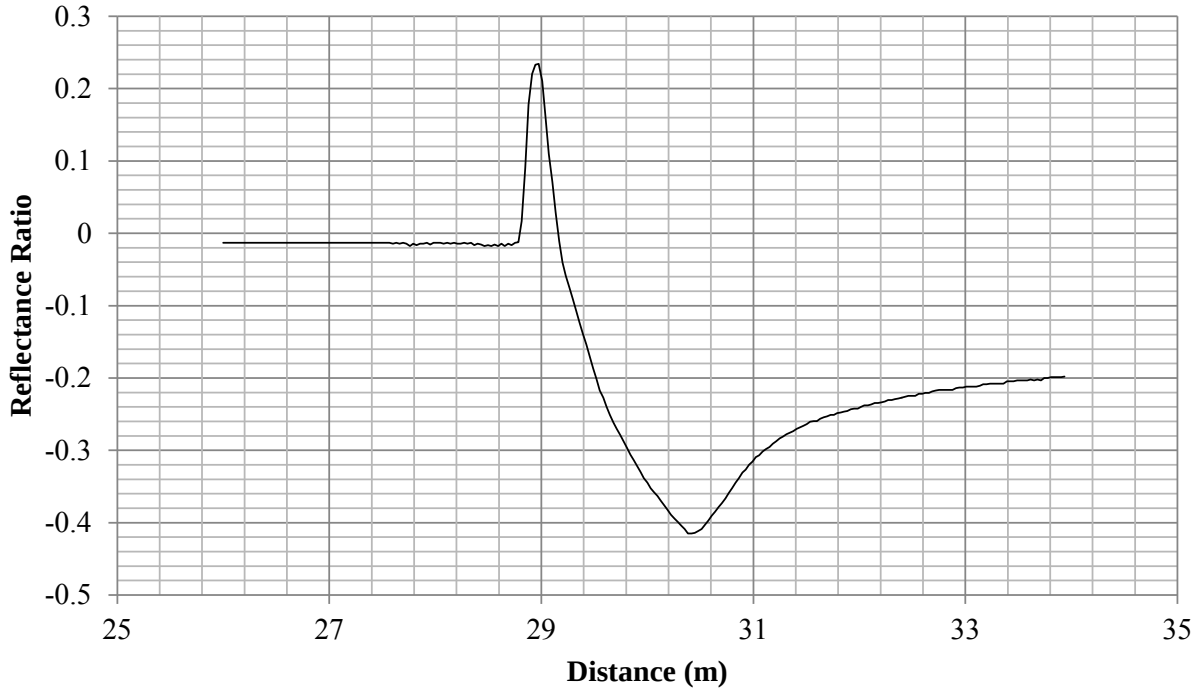

Figure A.14. Captured waveform for test U2.

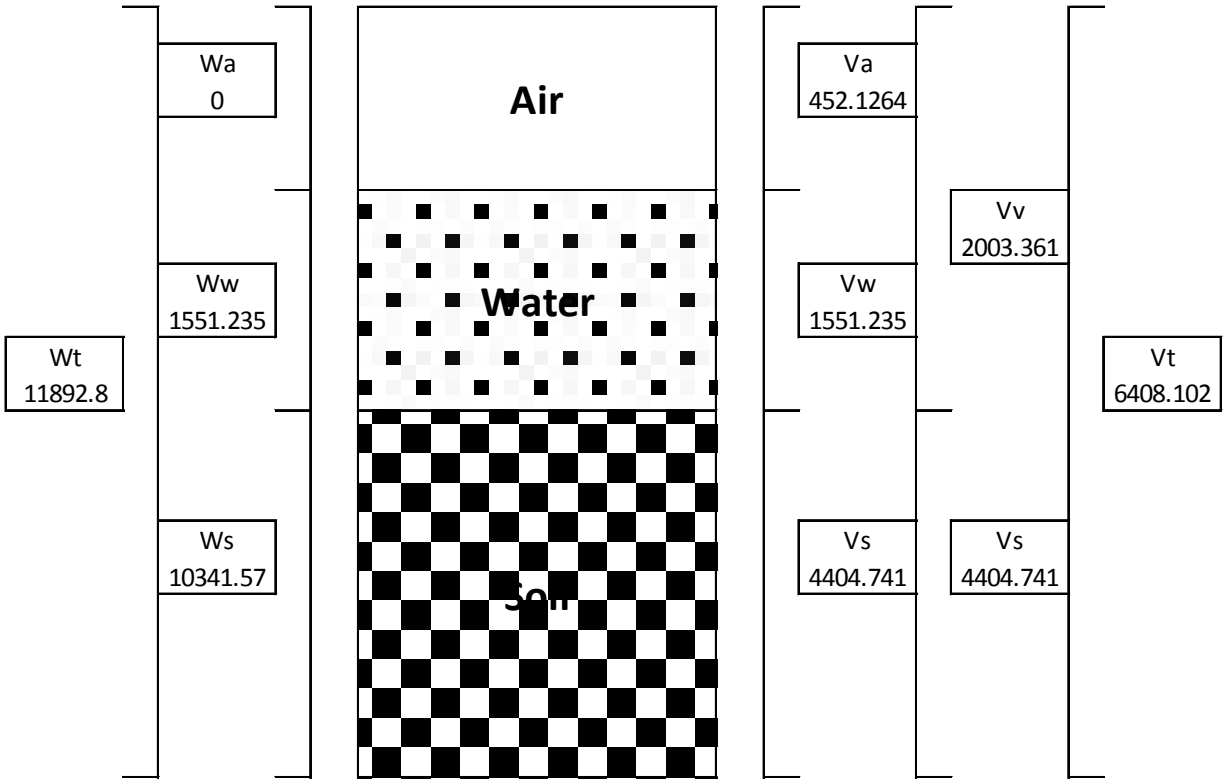

Figure A.15. Phase diagram for test U3 (weights in grams and volumes in cm).

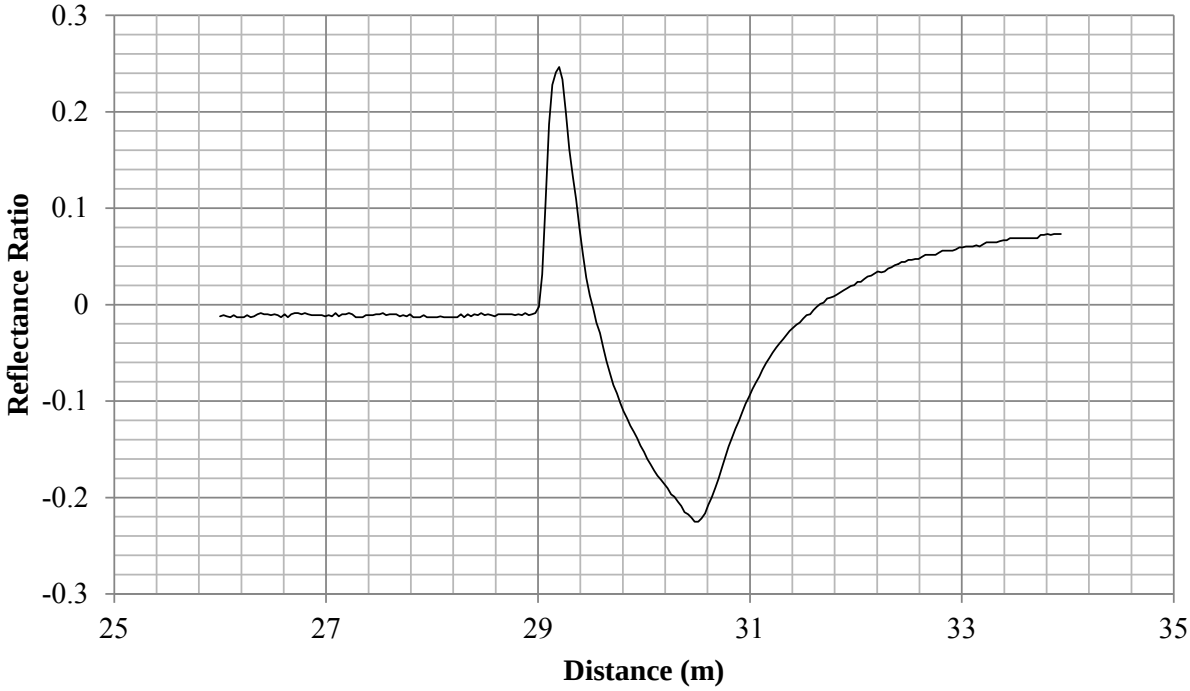

Figure A.16. Captured waveform for test U3.

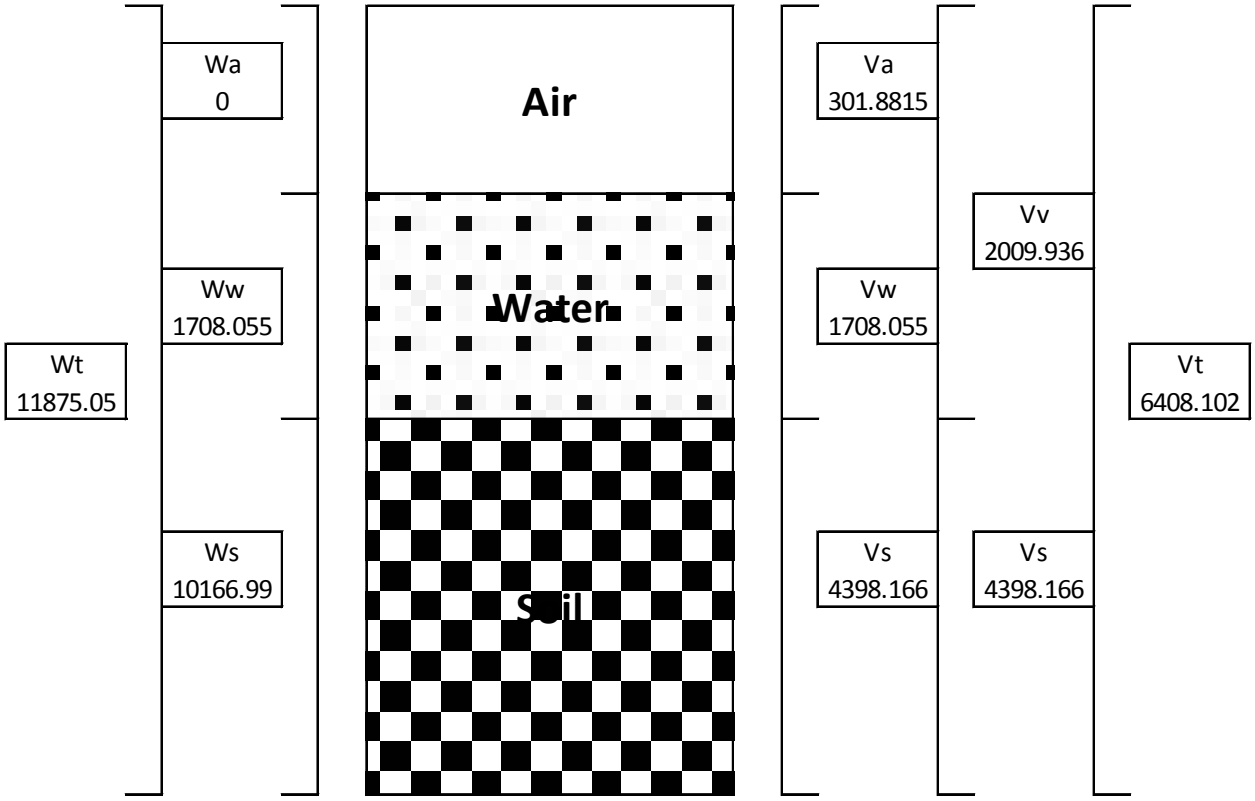

Figure A.17. Phase diagram for test U4 (weights in grams and volumes in cm).

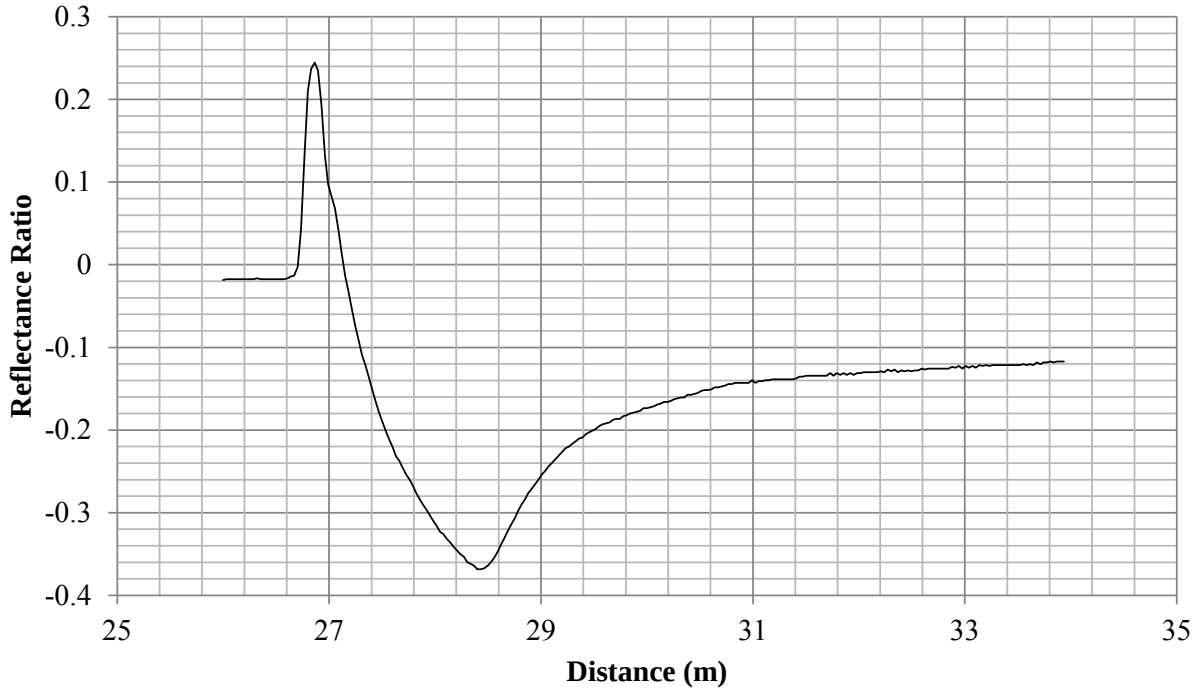

Figure A.18. Captured waveform for test U4.

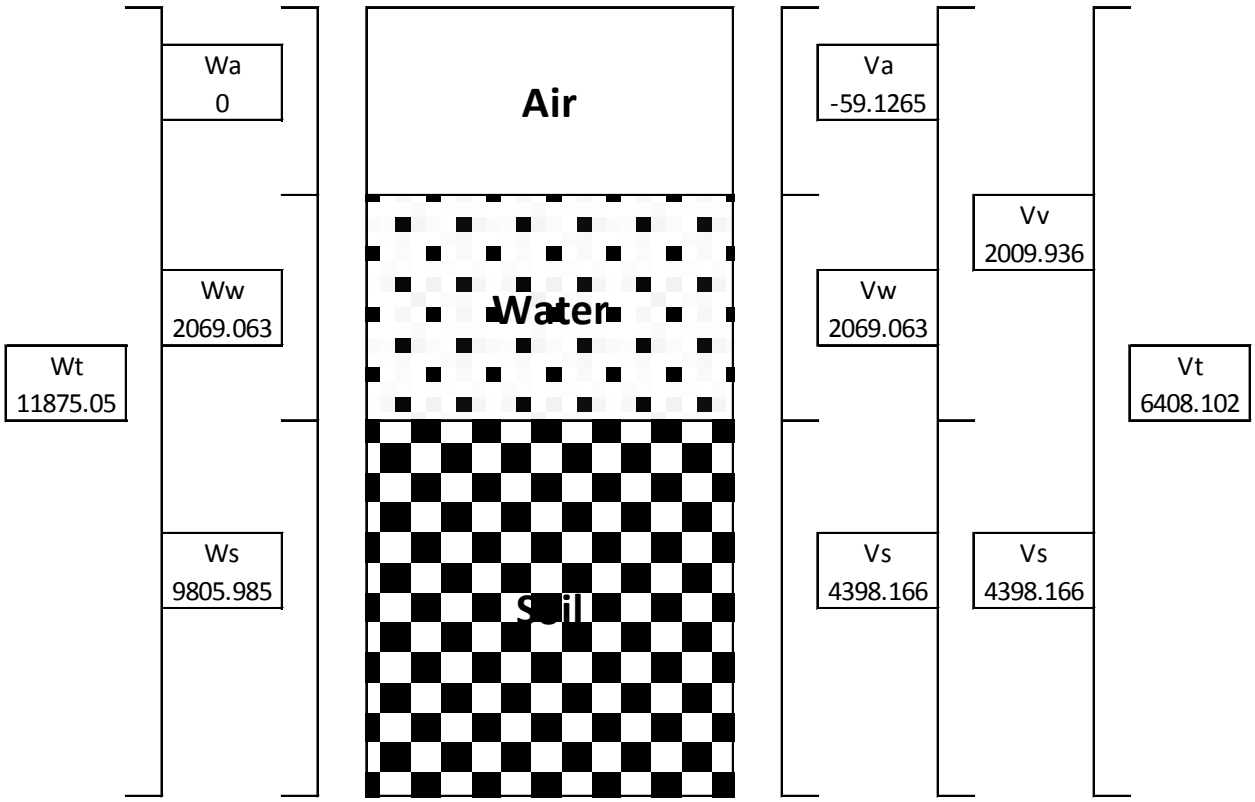

Figure A.19. Phase diagram for test V1 (weights in grams and volumes in cm).

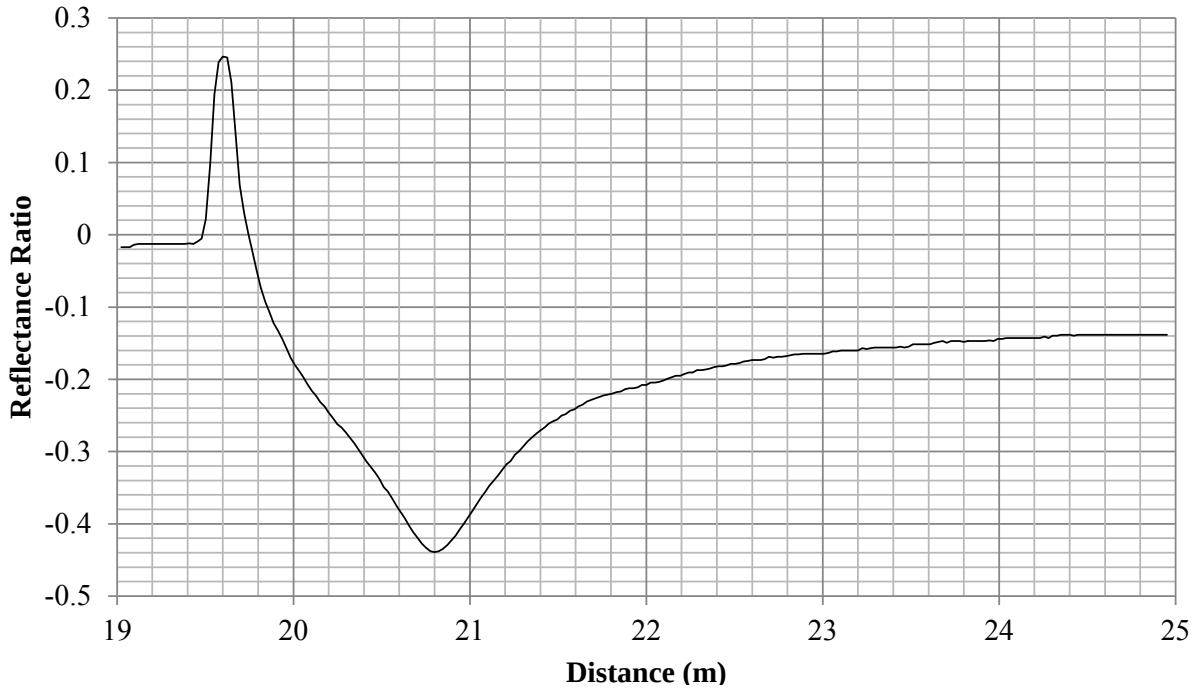

Figure A.20. Captured waveform for test V1.

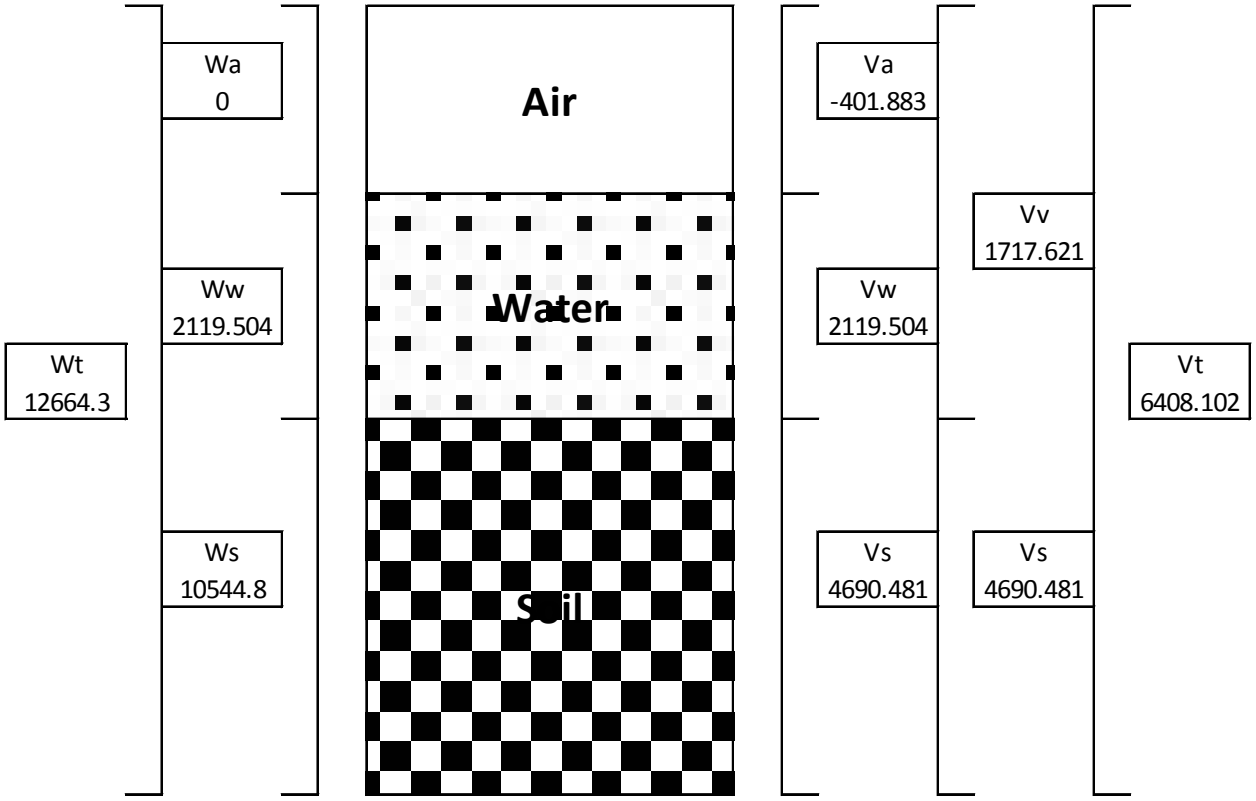

Figure A.21. Phase diagram for test V2 (weights in grams and volumes in cm).

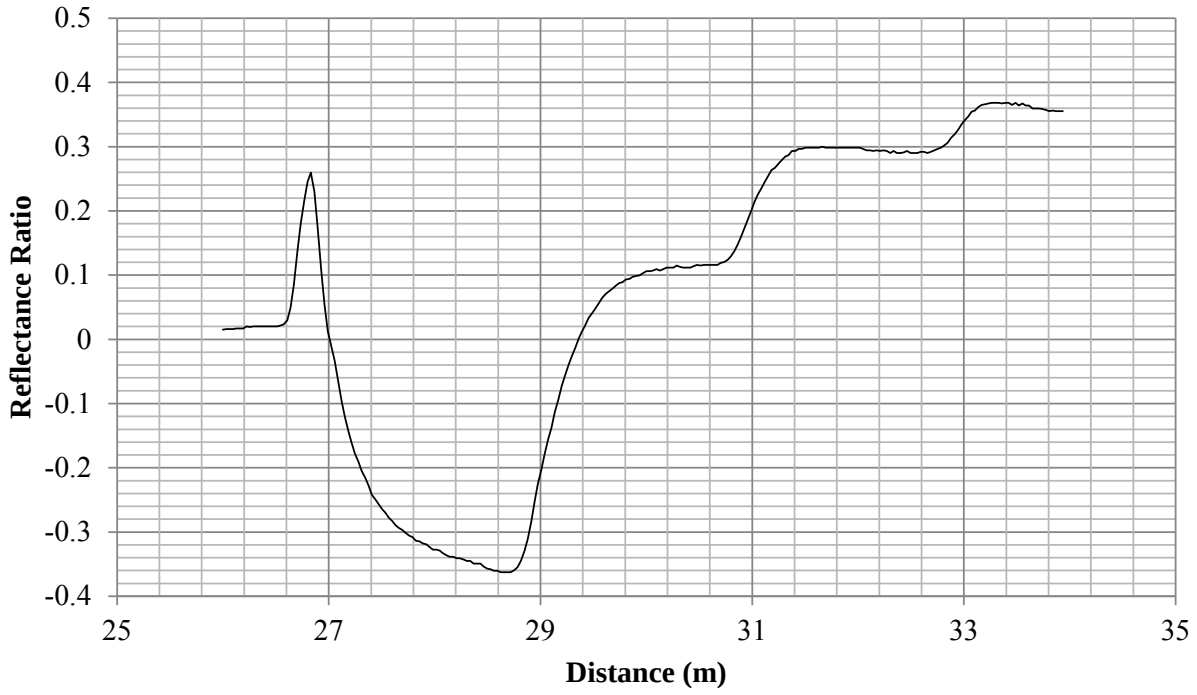

Figure A.22. Captured waveform for test V2 .

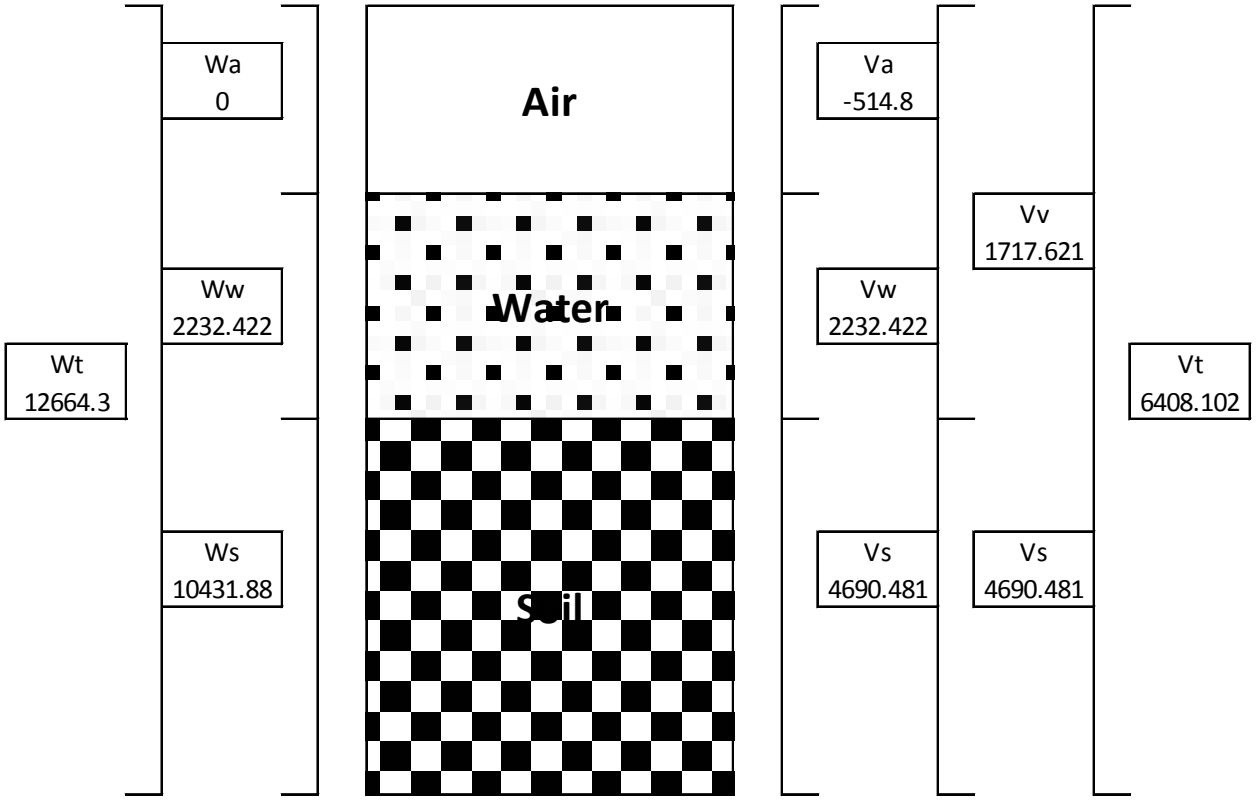

Figure A.23. Phase diagram for test V4 (weights in grams and volumes in cm).

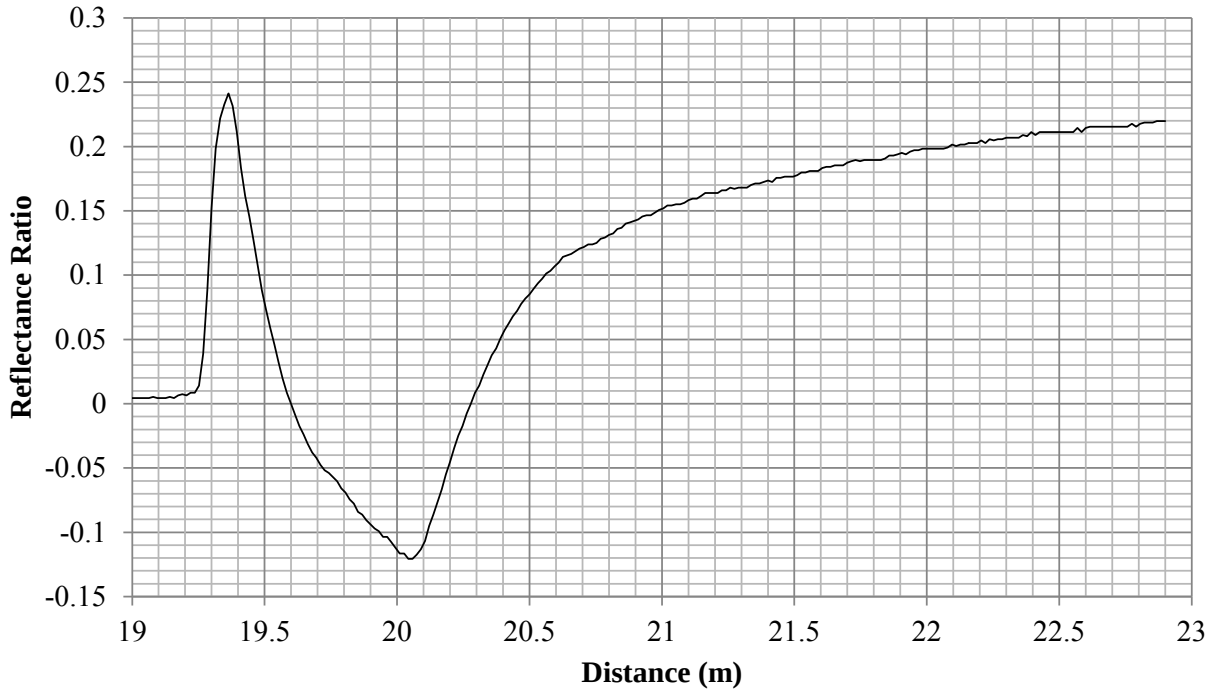

Figure A.24. Captured waveform for test V4.

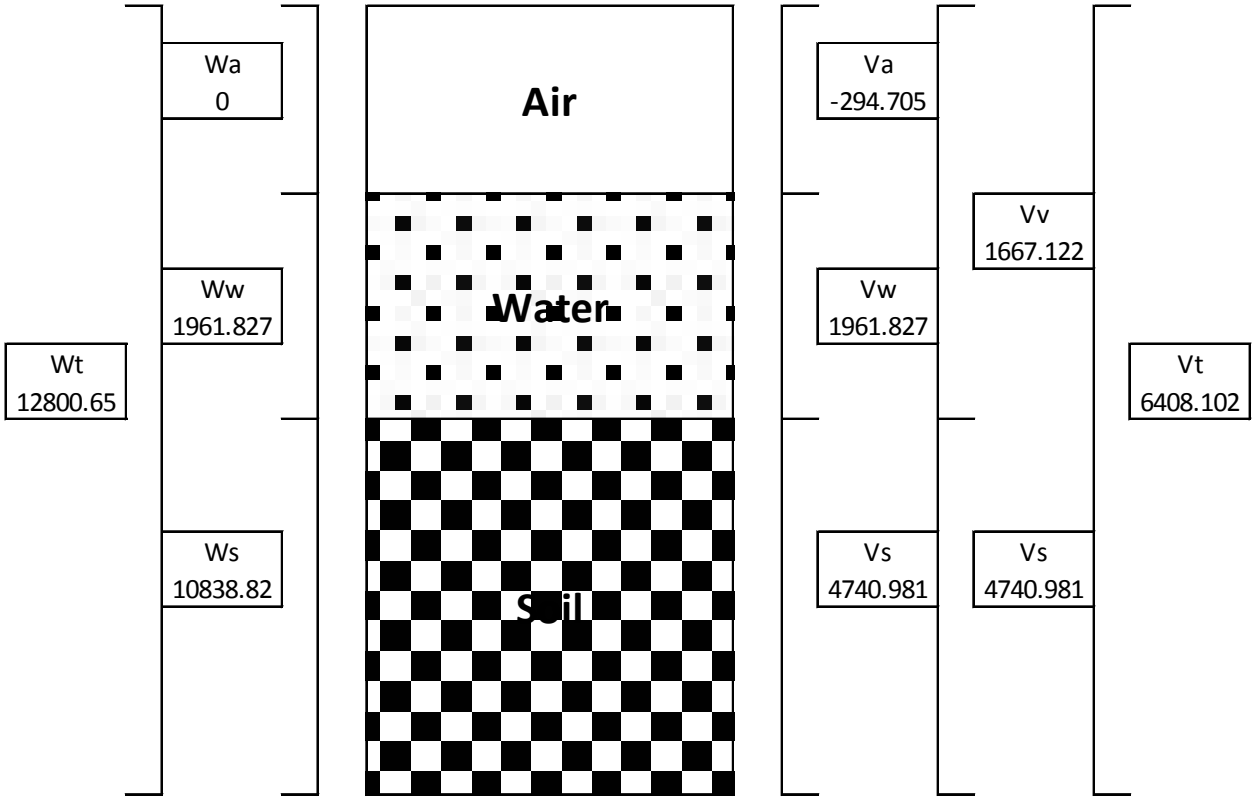

Figure A.25. Phase diagram for test V5 (weights in grams and volumes in cm).

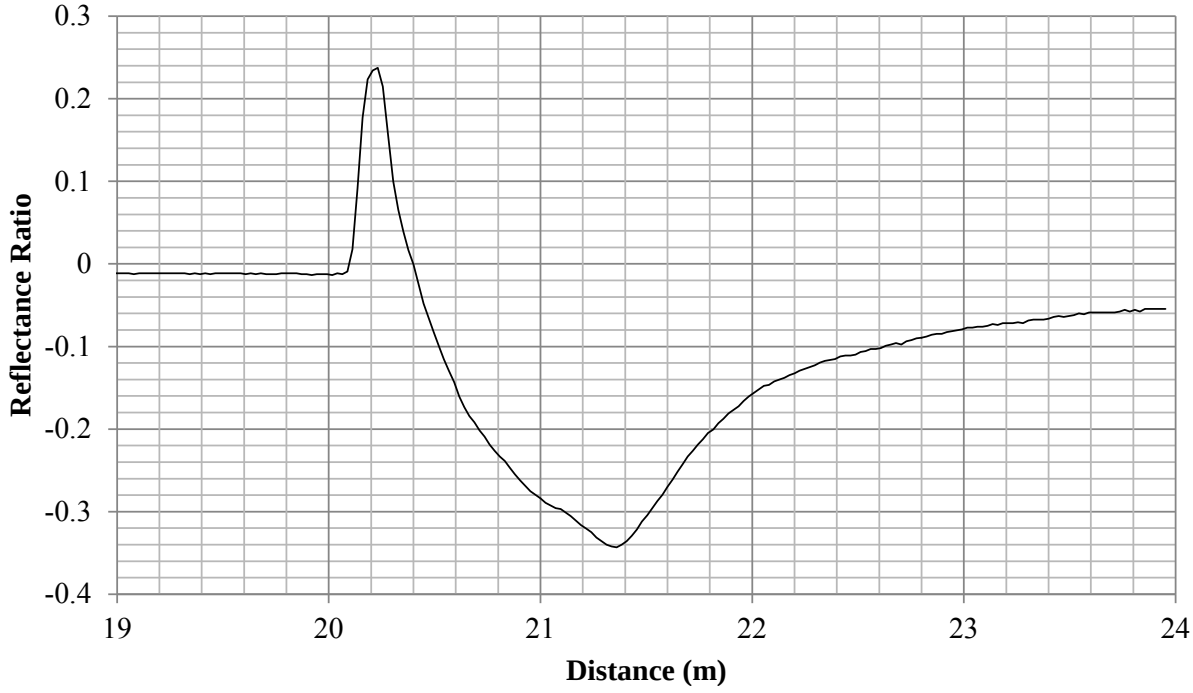

Figure A.26. Captured waveform for test V5.

Appendix B

B.1. . CR10X Datalogger Program (Phase 2)

This appendix contains the CR basic program developed to conduct the remote monitoring of the in-situ instrumentation in the field. The program was created using the PC-400 software suite from Campbell Scientific. The operating interval is every 3600 seconds.

```
;{CR10X}
;COMBINED PROGRAM TO RUN ALL OF MBTC-3031 FIELD OBSERVATIONS
;PROGRAM TO MEASURE WC, EC, AND WAVEFORM FOR TWENTY TDR PROBES
;CYRUS GARNER BASED ON EXAMPLE PROGRAM IN TDR100 DOCUMENTATION
;30-May-2012

;TESTING PROGRAM PROBE MUX
;PROBE ARRAY PROBE ## -- MUX
;PROBE 01--1101  ;PROBE 02--1201  ;PROBE 03--1301  ;PROBE 04--1101
;PROBE 05--1201  ;PROBE 06--1301  ;PROBE 07--1101  ;PROBE 08--1201
;PROBE 09--2101  ;PROBE 10--2201  ;PROBE 11--2301  ;PROBE 12--2101
;PROBE 13--2201  ;PROBE 14--2301  ;PROBE 15--2101  ;PROBE 16--2201
;PROBE 17--3001  ;PROBE 18--4001  ;PROBE 19--3001  ;PROBE 20--4001

;MEMORY ARRAY
;1-1 =     [BAT_VOLT]
;2-2 =     [DL_TEMP]
;3-3 =     [LAL_CH1]
;4-4 =     [WC_CH1]
;5-5 =     [EC_CH1]
;6 - 264 = [WF_CH1]

;266     = [LAL_CH2]
;267     = [WC_CH2]
;268     = [EC_CH2]
;269-527 = [WF_CH2]

;529     = [LAL_CH3]
;530     = [WC_CH3]
```

;531 = [EC_CH3]
;532-790 = [WF_CH3]

;792 = [LAL_CH4]
;793 = [WC_CH4]
;794 = [EC_CH4]
;795-1053 = [WF_CH4]

;1055 = [LAL_CH5]
;1056 = [WC_CH5]
;1057 = [EC_CH5]
;1058-1316 = [WF_CH5]

;1318 = [LAL_CH6]
;1319 = [WC_CH6]
;1320 = [EC_CH6]
;1321-1579 = [WF_CH6]

;1581 = [LAL_CH7]
;1582 = [WC_CH7]
;1583 = [EC_CH7]
;1584-1842 = [WF_CH7]

;1844 = [LAL_CH8]
;1845 = [WC_CH8]
;1846 = [EC_CH8]
;1847-2105 = [WF_CH8]

;2107 = [LAL_CH9]
;2108 = [WC_CH9]
;2109 = [EC_CH9]
;2110-2368 = [WF_CH9]

;2370 = [LAL_CH10]
;2371 = [WC_CH10]
;2372 = [EC_CH10]
;2373-2631 = [WF_CH10]

;2633 = [LAL_CH11]
;2634 = [WC_CH11]
;2635 = [EC_CH11]
;2636-2894 = [WF_CH11]

;2896 = [LAL_CH12]
;2897 = [WC_CH12]
;2898 = [EC_CH12]

```
;2899-3157= [WF_CH12]

;3159     = [LAL_CH13]
;3160     = [WC_CH13]
;3161     = [EC_CH13]
;3162-3420 = [WF_CH13]

;3422     = [LAL_CH14]
;3423     = [WC_CH14]
;3424     = [EC_CH14]
;3425-3683 = [WF_CH14]

;3685     = [LAL_CH15]
;3686     = [WC_CH15]
;3687     = [EC_CH15]
;3688-3946 = [WF_CH15]

;3948     = [LAL_CH16]
;3949     = [WC_CH16]
;3950     = [EC_CH16]
;3951-4209 = [WF_CH16]
;4211-4224 = IRR_1-14
;4226 = TB
;4227 = PV_1
;4228 = PV_2
;4229 = RELAY_1
;4230 = RELAY_2
;4231-4234 = TC_1-3

*Table 1 Program
  01: 120       Execution Interval (seconds)

1:  Do (P86)
 1: 45       Set Port 5 High

2:  Batt Voltage (P10)
 1: 1        Loc [ BAT_VOLT  ]

3:  Internal Temperature (P17)
 1: 2        Loc [ DL_TEMP   ]

; FOR EACH TDR PROBE TAKE THREE MEASUREMENTS
;1 - WATER CONTENT
;2 - BULK ELECTRICAL CONDUCTIVITY
;3 - CAPTURE WAVEFORM
```

```
; MEASURE P1
4:  TDR100 Measurement (P119)
 1: 00       SDM Address
 2: 00       Output Option
 3: 1101     MMMP Mux & Probe Selection
 4: 4        Waveform Averaging
 5: 1        Vp
 6: 250      Points
 7: 18       Cable Length (meters)
 8: 6        Window Length (meters)
 9: .4       Probe Length (meters)
10: .085     Probe Offset (meters)
11: 3        Loc [ LAL_CH1   ]
12: 1.0      Multiplier
13: 0.0      Offset

;IMPLEMENT TOPPS (1980) EQN
5:  Z=X*Y (P36)
 1: 3        X Loc [ LAL_CH1   ]
 2: 3        Y Loc [ LAL_CH1   ]
 3: 4        Z Loc [ WC_CH1    ]

6:  Z=X*F (P37)
 1: 4        X Loc [ WC_CH1    ]
 2: 0.1      F
 3: 4        Z Loc [ WC_CH1    ]

7:  Polynomial (P55)
 1: 1        Reps
 2: 4        X Loc [ WC_CH1    ]
 3: 4        F(X) Loc [ WC_CH1    ]
 4: -0.053   C0
 5: 0.292    C1
 6: -0.055   C2
 7: 0.0043   C3
 8: 0.0      C4
 9: 0.0      C5


8:  TDR100 Measurement (P119)
 1: 00       SDM Address
 2: 3        Electrical Conductivity
 3: 1101     MMMP Mux & Probe Selection
 4: 4        Waveform Averaging
 5: 1        Vp
 6: 250      Points
```

```
 7: 18       Cable Length (meters)
 8: 6        Window Length (meters)
 9: .3       Probe Length (meters)
10: .085     Probe Offset (meters)
11: 5        Loc [ EC_CH1    ]
12: 1.0      Multiplier
13: 0.0      Offset

9:  TDR100 Measurement (P119)
 1: 00       SDM Address
 2: 1        Waveform
 3: 1101     MMMP Mux & Probe Selection
 4: 4        Waveform Averaging
 5: 1        Vp
 6: 250      Points
 7: 18       Cable Length (meters)
 8: 6        Window Length (meters)
 9: .3       Probe Length (meters)
10: .085     Probe Offset (meters)
11: 6        Loc [ WFCH1_1   ]
12: 1.0      Multiplier
13: 0        O

; MEASURE P2
10:  TDR100 Measurement (P119)
 1: 00       SDM Address
 2: 00       Output Option
 3: 1201     MMMP Mux & Probe Selection
 4: 4        Waveform Averaging
 5: 1        Vp
 6: 250      Points
 7: 18       Cable Length (meters)
 8: 8        Window Length (meters)
 9: .3       Probe Length (meters)
10: .085     Probe Offset (meters)
11: 266      Loc [ LAL_CH2   ]
12: 1.0      Multiplier
13: 0.0      Offset

11:  Z=X*Y (P36)
 1: 266      X Loc [ LAL_CH2   ]
 2: 266      Y Loc [ LAL_CH2   ]
 3: 267      Z Loc [ WC_CH2    ]

12:  Z=X*F (P37)
 1: 267      X Loc [ WC_CH2    ]
```

```
 2: 0.1      F
 3: 267      Z Loc [ WC_CH2    ]

13:  Polynomial (P55)
 1: 1        Reps
 2: 267      X Loc [ WC_CH2    ]
 3: 267      F(X) Loc [ WC_CH2    ]
 4: -0.053   C0
 5: 0.292    C1
 6: -0.055   C2
 7: 0.0043   C3
 8: 0.0      C4
 9: 0.0      C5

14:  TDR100 Measurement (P119)
 1: 00       SDM Address
 2: 3        Electrical Conductivity
 3: 1201     MMMP Mux & Probe Selection
 4: 4        Waveform Averaging
 5: 1        Vp
 6: 250      Points
 7: 18       Cable Length (meters)
 8: 6        Window Length (meters)
 9: .3       Probe Length (meters)
10: .085     Probe Offset (meters)
11: 268      Loc [ EC_CH2    ]
12: 1.0      Multiplier
13: 0.0      Offset

15:  TDR100 Measurement (P119)
 1: 00       SDM Address
 2: 1        Waveform
 3: 1201     MMMP Mux & Probe Selection
 4: 4        Waveform Averaging
 5: 1        Vp
 6: 250      Points
 7: 18       Cable Length (meters)
 8: 6        Window Length (meters)
 9: .3       Probe Length (meters)
10: .085     Probe Offset (meters)
11: 269      Loc [ WFCH2_1   ]
12: 1.0      Multiplier
13: 0        O

; MEASURE P3
16:  TDR100 Measurement (P119)
```

```
 1: 00       SDM Address
 2: 00       Output Option
 3: 1301     MMMP Mux & Probe Selection
 4: 4        Waveform Averaging
 5: 1        Vp
 6: 250      Points
 7: 18       Cable Length (meters)
 8: 8        Window Length (meters)
 9: .3       Probe Length (meters)
10: .085     Probe Offset (meters)
11: 529      Loc [ LAL_CH3   ]
12: 1.0      Multiplier
13: 0.0      Offset

17:  Z=X*Y (P36)
 1: 529      X Loc [ LAL_CH3   ]
 2: 529      Y Loc [ LAL_CH3   ]
 3: 530      Z Loc [ WC_CH3    ]


18:  Z=X*F (P37)
 1: 530      X Loc [ WC_CH3    ]
 2: 0.1      F
 3: 530      Z Loc [ WC_CH3    ]

19:  Polynomial (P55)
 1: 1        Reps
 2: 530      X Loc [ WC_CH3    ]
 3: 530      F(X) Loc [ WC_CH3    ]
 4: -0.053   C0
 5: 0.292    C1
 6: -0.055   C2
 7: 0.0043   C3
 8: 0.0      C4
 9: 0.0      C5

20:  TDR100 Measurement (P119)
 1: 00       SDM Address
 2: 3        Electrical Conductivity
 3: 1301     MMMP Mux & Probe Selection
 4: 4        Waveform Averaging
 5: 1        Vp
 6: 250      Points
 7: 18       Cable Length (meters)
 8: 6        Window Length (meters)
 9: .3       Probe Length (meters)
```

```
10: .085     Probe Offset (meters)
11: 531      Loc [ EC_CH3    ]
12: 1.0      Multiplier
13: 0.0      Offset

21:  TDR100 Measurement (P119)
 1: 00       SDM Address
 2: 1        Waveform
 3: 1301     MMMP Mux & Probe Selection
 4: 4        Waveform Averaging
 5: 1        Vp
 6: 250      Points
 7: 18       Cable Length (meters)
 8: 6        Window Length (meters)
 9: .3       Probe Length (meters)
10: .085     Probe Offset (meters)
11: 532      Loc [ WFCH3_1   ]
12: 1.0      Multiplier
13: 0        O

; MEASURE P4
22:  TDR100 Measurement (P119)
 1: 00       SDM Address
 2: 00       Output Option
 3: 1401     MMMP Mux & Probe Selection
 4: 4        Waveform Averaging
 5: 1        Vp
 6: 250      Points
 7: 18       Cable Length (meters)
 8: 8        Window Length (meters)
 9: .3       Probe Length (meters)
10: .085     Probe Offset (meters)
11: 792      Loc [ LAL_CH4   ]
12: 1.0      Multiplier
13: 0.0      Offset

23:  Z=X*Y (P36)
 1: 792      X Loc [ LAL_CH4   ]
 2: 792      Y Loc [ LAL_CH4   ]
 3: 793      Z Loc [ WC_CH4    ]

24:  Z=X*F (P37)
 1: 793      X Loc [ WC_CH4    ]
 2: 0.1      F
 3: 793      Z Loc [ WC_CH4    ]
```

```
25:  Polynomial (P55)
 1: 1        Reps
 2: 793      X Loc [ WC_CH4    ]
 3: 793      F(X) Loc [ WC_CH4    ]
 4: -0.053   C0
 5: 0.292    C1
 6: -0.055   C2
 7: 0.0043   C3
 8: 0.0      C4
 9: 0.0      C5

26:  TDR100 Measurement (P119)
 1: 00       SDM Address
 2: 3        Electrical Conductivity
 3: 1401     MMMP Mux & Probe Selection
 4: 4        Waveform Averaging
 5: 1        Vp
 6: 250      Points
 7: 18       Cable Length (meters)
 8: 6        Window Length (meters)
 9: .3       Probe Length (meters)
10: .085     Probe Offset (meters)
11: 794      Loc [ EC_CH4    ]
12: 1.0      Multiplier
13: 0.0      Offset

27:  TDR100 Measurement (P119)
 1: 00       SDM Address
 2: 1        Waveform
 3: 1401     MMMP Mux & Probe Selection
 4: 4        Waveform Averaging
 5: 1        Vp
 6: 250      Points
 7: 18       Cable Length (meters)
 8: 6        Window Length (meters)
 9: .3       Probe Length (meters)
10: .085     Probe Offset (meters)
11: 795      Loc [ WFCH4_1   ]
12: 1.0      Multiplier
13: 0        O

; MEASURE P5
28:  TDR100 Measurement (P119)
 1: 00       SDM Address
 2: 00       Output Option
 3: 1501     MMMP Mux & Probe Selection
```

```
 4: 4        Waveform Averaging
 5: 1        Vp
 6: 250      Points
 7: 18       Cable Length (meters)
 8: 6        Window Length (meters)
 9: .3       Probe Length (meters)
10: .085     Probe Offset (meters)
11: 1055     Loc [ LAL_CH5   ]
12: 1.0      Multiplier
13: 0.0      Offset

29:  Z=X*Y (P36)
 1: 1055     X Loc [ LAL_CH5   ]
 2: 1055     Y Loc [ LAL_CH5   ]
 3: 1056     Z Loc [ WC_CH5    ]

30:  Z=X*F (P37)
 1: 1056     X Loc [ WC_CH5    ]
 2: 0.1      F
 3: 1056     Z Loc [ WC_CH5    ]

31:  Polynomial (P55)
 1: 1        Reps
 2: 1056     X Loc [ WC_CH5    ]
 3: 1056     F(X) Loc [ WC_CH5    ]
 4: -0.053   C0
 5: 0.292    C1
 6: -0.055   C2
 7: 0.0043   C3
 8: 0.0      C4
 9: 0.0      C5

32:  TDR100 Measurement (P119)
 1: 00       SDM Address
 2: 3        Electrical Conductivity
 3: 1501     MMMP Mux & Probe Selection
 4: 4        Waveform Averaging
 5: 1        Vp
 6: 250      Points
 7: 18       Cable Length (meters)
 8: 6        Window Length (meters)
 9: .3       Probe Length (meters)
10: .085     Probe Offset (meters)
11: 1057     Loc [ EC_CH5    ]
12: 1.0      Multiplier
13: 0.0      Offset
```

```
33:  TDR100 Measurement (P119)
 1: 00       SDM Address
 2: 1        Waveform
 3: 1501     MMMP Mux & Probe Selection
 4: 4        Waveform Averaging
 5: 1        Vp
 6: 250      Points
 7: 18       Cable Length (meters)
 8: 6        Window Length (meters)
 9: .3       Probe Length (meters)
10: .085     Probe Offset (meters)
11: 1058     Loc [ WFCH5_1   ]
12: 1.0      Multiplier
13: 0        O

; MEASURE P6
34:  TDR100 Measurement (P119)
 1: 00       SDM Address
 2: 00       Output Option
 3: 1601     MMMP Mux & Probe Selection
 4: 4        Waveform Averaging
 5: 1        Vp
 6: 250      Points
 7: 18       Cable Length (meters)
 8: 6        Window Length (meters)
 9: 3        Probe Length (meters)
10: .085     Probe Offset (meters)
11: 1318     Loc [ LAL_CH6   ]
12: 1.0      Multiplier
13: 0.0      Offset

35:  Z=X*Y (P36)
 1: 1318     X Loc [ LAL_CH6   ]
 2: 1318     Y Loc [ LAL_CH6   ]
 3: 1319     Z Loc [ WC_CH6    ]


36:  Z=X*F (P37)
 1: 1319     X Loc [ WC_CH6    ]
 2: 0.1      F
 3: 1319     Z Loc [ WC_CH6    ]

37:  Polynomial (P55)
 1: 1        Reps
 2: 1319     X Loc [ WC_CH6    ]
```

```
 3: 1319     F(X) Loc [ WC_CH6    ]
 4: -0.053   C0
 5: 0.292    C1
 6: -0.055   C2
 7: 0.0043   C3
 8: 0.0      C4
 9: 0.0      C5

38:  TDR100 Measurement (P119)
 1: 00       SDM Address
 2: 3        Electrical Conductivity
 3: 1601     MMMP Mux & Probe Selection
 4: 4        Waveform Averaging
 5: 1        Vp
 6: 250      Points
 7: 18       Cable Length (meters)
 8: 6        Window Length (meters)
 9: .3       Probe Length (meters)
10: .085     Probe Offset (meters)
11: 1320     Loc [ EC_CH6    ]
12: 1.0      Multiplier
13: 0.0      Offset

39:  TDR100 Measurement (P119)
 1: 00       SDM Address
 2: 1        Waveform
 3: 1601     MMMP Mux & Probe Selection
 4: 4        Waveform Averaging
 5: 1        Vp
 6: 250      Points
 7: 18       Cable Length (meters)
 8: 6        Window Length (meters)
 9: .3       Probe Length (meters)
10: .085     Probe Offset (meters)
11: 1321     Loc [ WFCH6_1   ]
12: 1.0      Multiplier
13: 0        O

; MEASURE P7
40:  TDR100 Measurement (P119)
 1: 00       SDM Address
 2: 00       Output Option
 3: 1701     MMMP Mux & Probe Selection
 4: 4        Waveform Averaging
 5: 1        Vp
 6: 250      Points
```

```
 7: 18       Cable Length (meters)
 8: 6        Window Length (meters)
 9: .3       Probe Length (meters)
10: .085     Probe Offset (meters)
11: 1581     Loc [ LAL_CH7   ]
12: 1.0      Multiplier
13: 0.0      Offset

41:  Z=X*Y (P36)
 1: 1581     X Loc [ LAL_CH7   ]
 2: 1581     Y Loc [ LAL_CH7   ]
 3: 1582     Z Loc [ WC_CH7    ]

42:  Z=X*F (P37)
 1: 1582     X Loc [ WC_CH7    ]
 2: 0.1      F
 3: 1582     Z Loc [ WC_CH7    ]

43:  Polynomial (P55)
 1: 1        Reps
 2: 1582     X Loc [ WC_CH7    ]
 3: 1582     F(X) Loc [ WC_CH7    ]
 4: -0.053   C0
 5: 0.292    C1
 6: -0.055   C2
 7: 0.0043   C3
 8: 0.0      C4
 9: 0.0      C5

44:  TDR100 Measurement (P119)
 1: 00       SDM Address
 2: 3        Electrical Conductivity
 3: 1701     MMMP Mux & Probe Selection
 4: 4        Waveform Averaging
 5: 1        Vp
 6: 250      Points
 7: 18       Cable Length (meters)
 8: 6        Window Length (meters)
 9: .3       Probe Length (meters)
10: .085     Probe Offset (meters)
11: 1583     Loc [ EC_CH7    ]
12: 1.0      Multiplier
13: 0.0      Offset

45:  TDR100 Measurement (P119)
 1: 00       SDM Address
```

```
 2: 1        Waveform
 3: 1701     MMMP Mux & Probe Selection
 4: 4        Waveform Averaging
 5: 1        Vp
 6: 250      Points
 7: 18       Cable Length (meters)
 8: 6        Window Length (meters)
 9: .3       Probe Length (meters)
10: .085     Probe Offset (meters)
11: 1584     Loc [ WFCH7_1   ]
12: 1.0      Multiplier
13: 0        O

; MEASURE P8
46:  TDR100 Measurement (P119)
 1: 00       SDM Address
 2: 00       Output Option
 3: 1801     MMMP Mux & Probe Selection
 4: 4        Waveform Averaging
 5: 1        Vp
 6: 250      Points
 7: 18       Cable Length (meters)
 8: 6        Window Length (meters)
 9: .3       Probe Length (meters)
10: .085     Probe Offset (meters)
11: 1844     Loc [ LAL_CH8   ]
12: 1.0      Multiplier
13: 0.0      Offset

47:  Z=X*Y (P36)
 1: 1844     X Loc [ LAL_CH8   ]
 2: 1844     Y Loc [ LAL_CH8   ]
 3: 1845     Z Loc [ WC_CH8    ]

48:  Z=X*F (P37)
 1: 1845     X Loc [ WC_CH8    ]
 2: 0.1      F
 3: 1845     Z Loc [ WC_CH8    ]

49:  Polynomial (P55)
 1: 1        Reps
 2: 1845     X Loc [ WC_CH8    ]
 3: 1845     F(X) Loc [ WC_CH8    ]
 4: -0.053   C0
 5: 0.292    C1
 6: -0.055   C2
```

```
 7: 0.0043   C3
 8: 0.0      C4
 9: 0.0      C5

50:  TDR100 Measurement (P119)
 1: 00       SDM Address
 2: 3        Electrical Conductivity
 3: 1801     MMMP Mux & Probe Selection
 4: 4        Waveform Averaging
 5: 1        Vp
 6: 250      Points
 7: 26       Cable Length (meters)
 8: 6        Window Length (meters)
 9: .3       Probe Length (meters)
10: .085     Probe Offset (meters)
11: 1846     Loc [ EC_CH8    ]
12: 1.0      Multiplier
13: 0.0      Offset

51:  TDR100 Measurement (P119)
 1: 00       SDM Address
 2: 1        Waveform
 3: 1801     MMMP Mux & Probe Selection
 4: 4        Waveform Averaging
 5: 1        Vp
 6: 250      Points
 7: 28       Cable Length (meters)
 8: 6        Window Length (meters)
 9: .3       Probe Length (meters)
10: .085     Probe Offset (meters)
11: 1847     Loc [ WFCH8_1   ]
12: 1.0      Multiplier
13: 0        O

; MEASURE P9
52:  TDR100 Measurement (P119)
 1: 00       SDM Address
 2: 00       Output Option
 3: 2101     MMMP Mux & Probe Selection
 4: 4        Waveform Averaging
 5: 1        Vp
 6: 250      Points
 7: 26       Cable Length (meters)
 8: 8        Window Length (meters)
 9: .3       Probe Length (meters)
10: .085     Probe Offset (meters)
```

11: 2107 Loc [LAL_CH9]
12: 1.0 Multiplier
13: 0.0 Offset

53: Z=X*Y (P36)
1: 2107 X Loc [LAL_CH9]
2: 2107 Y Loc [LAL_CH9]
3: 2108 Z Loc [WC_CH9]

54: Z=X*F (P37)
1: 2108 X Loc [WC_CH9]
2: 0.1 F
3: 2108 Z Loc [WC_CH9]

55: Polynomial (P55)
1: 1 Reps
2: 2108 X Loc [WC_CH9]
3: 2108 F(X) Loc [WC_CH9]
4: -0.053 C0
5: 0.292 C1
6: -0.055 C2
7: 0.0043 C3
8: 0.0 C4
9: 0.0 C5

56: TDR100 Measurement (P119)
1: 00 SDM Address
2: 3 Electrical Conductivity
3: 2101 MMMP Mux & Probe Selection
4: 4 Waveform Averaging
5: 1 Vp
6: 250 Points
7: 26 Cable Length (meters)
8: 6 Window Length (meters)
9: .3 Probe Length (meters)
10: .085 Probe Offset (meters)
11: 2109 Loc [EC_CH9]
12: 1.0 Multiplier
13: 0.0 Offset

57: TDR100 Measurement (P119)
1: 00 SDM Address
2: 1 Waveform
3: 2101 MMMP Mux & Probe Selection
4: 4 Waveform Averaging
5: 1 Vp

```
 6: 250      Points
 7: 26       Cable Length (meters)
 8: 6        Window Length (meters)
 9: .3       Probe Length (meters)
10: .085     Probe Offset (meters)
11: 2110     Loc [ WFCH9_1   ]
12: 1.0      Multiplier
13: 0        O

; MEASURE P10
58:  TDR100 Measurement (P119)
 1: 00       SDM Address
 2: 00       Output Option
 3: 2201     MMMP Mux & Probe Selection
 4: 4        Waveform Averaging
 5: 1        Vp
 6: 250      Points
 7: 26       Cable Length (meters)
 8: 6        Window Length (meters)
 9: .3       Probe Length (meters)
10: .085     Probe Offset (meters)
11: 2370     Loc [ LAL_CH10  ]
12: 1.0      Multiplier
13: 0.0      Offset

59:  Z=X*Y (P36)
 1: 2370     X Loc [ LAL_CH10  ]
 2: 2370     Y Loc [ LAL_CH10  ]
 3: 2371     Z Loc [ WC_CH10   ]

60:  Z=X*F (P37)
 1: 2371     X Loc [ WC_CH10   ]
 2: 0.1      F
 3: 2371     Z Loc [ WC_CH10   ]

61:  Polynomial (P55)
 1: 1        Reps
 2: 2371     X Loc [ WC_CH10   ]
 3: 2371     F(X) Loc [ WC_CH10   ]
 4: -0.053   C0
 5: 0.292    C1
 6: -0.055   C2
 7: 0.0043   C3
 8: 0.0      C4
 9: 0.0      C5
```

```
62:  TDR100 Measurement (P119)
 1: 00       SDM Address
 2: 3        Electrical Conductivity
 3: 2201     MMMP Mux & Probe Selection
 4: 4        Waveform Averaging
 5: 1        Vp
 6: 250      Points
 7: 26       Cable Length (meters)
 8: 6        Window Length (meters)
 9: .33      Probe Length (meters)
10: .09      Probe Offset (meters)
11: 2372     Loc [ EC_CH10   ]
12: 1.0      Multiplier
13: 0.0      Offset

63:  TDR100 Measurement (P119)
 1: 00       SDM Address
 2: 1        Waveform
 3: 2201     MMMP Mux & Probe Selection
 4: 4        Waveform Averaging
 5: 1        Vp
 6: 250      Points
 7: 26       Cable Length (meters)
 8: 6        Window Length (meters)
 9: .3       Probe Length (meters)
10: .085     Probe Offset (meters)
11: 2373     Loc [ WFC10_1   ]
12: 1.0      Multiplier
13: 0        O

; MEASURE P11
64:  TDR100 Measurement (P119)
 1: 00       SDM Address
 2: 00       Output Option
 3: 2301     MMMP Mux & Probe Selection
 4: 4        Waveform Averaging
 5: 1        Vp
 6: 250      Points
 7: 26       Cable Length (meters)
 8: 6        Window Length (meters)
 9: .3       Probe Length (meters)
10: .085     Probe Offset (meters)
11: 2633     Loc [ LAL_CH11  ]
12: 1.0      Multiplier
13: 0.0      Offset
```

```
65:  Z=X*Y (P36)
 1: 2633     X Loc [ LAL_CH11  ]
 2: 2633     Y Loc [ LAL_CH11  ]
 3: 2634     Z Loc [ WC_CH11   ]

66:  Z=X*F (P37)
 1: 2634     X Loc [ WC_CH11   ]
 2: 0.1      F
 3: 2634     Z Loc [ WC_CH11   ]

67:  Polynomial (P55)
 1: 1        Reps
 2: 2634     X Loc [ WC_CH11   ]
 3: 2634     F(X) Loc [ WC_CH11   ]
 4: -0.053   C0
 5: 0.292    C1
 6: -0.055   C2
 7: 0.0043   C3
 8: 0.0      C4
 9: 0.0      C5

68:  TDR100 Measurement (P119)
 1: 00       SDM Address
 2: 3        Electrical Conductivity
 3: 2301     MMMP Mux & Probe Selection
 4: 4        Waveform Averaging
 5: 1        Vp
 6: 250      Points
 7: 18       Cable Length (meters)
 8: 6        Window Length (meters)
 9: .3       Probe Length (meters)
10: .085     Probe Offset (meters)
11: 2635     Loc [ EC_CH11   ]
12: 1.0      Multiplier
13: 0.0      Offset

69:  TDR100 Measurement (P119)
 1: 00       SDM Address
 2: 1        Waveform
 3: 2301     MMMP Mux & Probe Selection
 4: 4        Waveform Averaging
 5: 1        Vp
 6: 250      Points
 7: 18       Cable Length (meters)
 8: 6        Window Length (meters)
 9: .3       Probe Length (meters)
```

```
10: .085     Probe Offset (meters)
11: 2636     Loc [ WFC11_1   ]
12: 1.0      Multiplier
13: 0        O

; MEASURE P12
70:  TDR100 Measurement (P119)
 1: 00       SDM Address
 2: 00       Output Option
 3: 2401     MMMP Mux & Probe Selection
 4: 4        Waveform Averaging
 5: 1        Vp
 6: 250      Points
 7: 18       Cable Length (meters)
 8: 6        Window Length (meters)
 9: .3       Probe Length (meters)
10: .085     Probe Offset (meters)
11: 2896     Loc [ LAL_CH12  ]
12: 1.0      Multiplier
13: 0.0      Offset


71:  Z=X*Y (P36)
 1: 2896     X Loc [ LAL_CH12  ]
 2: 2896     Y Loc [ LAL_CH12  ]
 3: 2897     Z Loc [ WC_CH12   ]

72:  Z=X*F (P37)
 1: 2897     X Loc [ WC_CH12   ]
 2: 0.1      F
 3: 2897     Z Loc [ WC_CH12   ]

73:  Polynomial (P55)
 1: 1        Reps
 2: 2897     X Loc [ WC_CH12   ]
 3: 2897     F(X) Loc [ WC_CH12   ]
 4: -0.053   C0
 5: 0.292    C1
 6: -0.055   C2
 7: 0.0043   C3
 8: 0.0      C4
 9: 0.0      C5

74:  TDR100 Measurement (P119)
 1: 00       SDM Address
 2: 3        Electrical Conductivity
```

```
 3: 2401     MMMP Mux & Probe Selection
 4: 4        Waveform Averaging
 5: 1        Vp
 6: 250      Points
 7: 26       Cable Length (meters)
 8: 6        Window Length (meters)
 9: .3       Probe Length (meters)
10: .085     Probe Offset (meters)
11: 2898     Loc [ EC_CH12   ]
12: 1.0      Multiplier
13: 0.0      Offset

75:  TDR100 Measurement (P119)
 1: 00       SDM Address
 2: 1        Waveform
 3: 2401     MMMP Mux & Probe Selection
 4: 4        Waveform Averaging
 5: 1        Vp
 6: 250      Points
 7: 26       Cable Length (meters)
 8: 6        Window Length (meters)
 9: .3       Probe Length (meters)
10: .085     Probe Offset (meters)
11: 2899     Loc [ WFC12_1   ]
12: 1.0      Multiplier
13: 0        O

; MEASURE P13
76:  TDR100 Measurement (P119)
 1: 00       SDM Address
 2: 00       Output Option
 3: 2501     MMMP Mux & Probe Selection
 4: 4        Waveform Averaging
 5: 1        Vp
 6: 250      Points
 7: 26       Cable Length (meters)
 8: 6        Window Length (meters)
 9: .3       Probe Length (meters)
10: .085     Probe Offset (meters)
11: 3159     Loc [ LAL_CH13  ]
12: 1.0      Multiplier
13: 0.0      Offset

77:  Z=X*Y (P36)
 1: 3159     X Loc [ LAL_CH13  ]
 2: 3159     Y Loc [ LAL_CH13  ]
```

```
 3: 3160     Z Loc [ WC_CH13   ]

78:  Z=X*F (P37)
 1: 3160     X Loc [ WC_CH13   ]
 2: 0.1      F
 3: 3160     Z Loc [ WC_CH13   ]

79:  Polynomial (P55)
 1: 1        Reps
 2: 3160     X Loc [ WC_CH13   ]
 3: 3160     F(X) Loc [ WC_CH13   ]
 4: -0.053   C0
 5: 0.292    C1
 6: -0.055   C2
 7: 0.0043   C3
 8: 0.0      C4
 9: 0.0      C5

80:  TDR100 Measurement (P119)
 1: 00       SDM Address
 2: 3        Electrical Conductivity
 3: 2501     MMMP Mux & Probe Selection
 4: 4        Waveform Averaging
 5: 1        Vp
 6: 250      Points
 7: 26       Cable Length (meters)
 8: 6        Window Length (meters)
 9: .3       Probe Length (meters)
10: .085     Probe Offset (meters)
11: 3161     Loc [ EC_CH13   ]
12: 1.0      Multiplier
13: 0.0      Offset

81:  TDR100 Measurement (P119)
 1: 00       SDM Address
 2: 1        Waveform
 3: 2501     MMMP Mux & Probe Selection
 4: 4        Waveform Averaging
 5: 1        Vp
 6: 250      Points
 7: 26       Cable Length (meters)
 8: 6        Window Length (meters)
 9: .3       Probe Length (meters)
10: .085     Probe Offset (meters)
11: 3162     Loc [ WFC13_1   ]
12: 1.0      Multiplier
```

```
13: 0       O

; MEASURE P14
82:  TDR100 Measurement (P119)
 1: 00      SDM Address
 2: 00      Output Option
 3: 2601    MMMP Mux & Probe Selection
 4: 4       Waveform Averaging
 5: 1       Vp
 6: 250     Points
 7: 26      Cable Length (meters)
 8: 6       Window Length (meters)
 9: .3      Probe Length (meters)
10: .085    Probe Offset (meters)
11: 3422    Loc [ LAL_CH14  ]
12: 1.0     Multiplier
13: 0.0     Offset

83:  Z=X*Y (P36)
 1: 3422    X Loc [ LAL_CH14  ]
 2: 3422    Y Loc [ LAL_CH14  ]
 3: 3423    Z Loc [ WC_CH14   ]

84:  Z=X*F (P37)
 1: 3423    X Loc [ WC_CH14   ]
 2: 0.1     F
 3: 3423    Z Loc [ WC_CH14   ]

85:  Polynomial (P55)
 1: 1       Reps
 2: 3423    X Loc [ WC_CH14   ]
 3: 3423    F(X) Loc [ WC_CH14   ]
 4: -0.053  C0
 5: 0.292   C1
 6: -0.055  C2
 7: 0.0043  C3
 8: 0.0     C4
 9: 0.0     C5

86:  TDR100 Measurement (P119)
 1: 00      SDM Address
 2: 3       Electrical Conductivity
 3: 2601    MMMP Mux & Probe Selection
 4: 4       Waveform Averaging
 5: 1       Vp
 6: 250     Points
```

```
 7: 26       Cable Length (meters)
 8: 6        Window Length (meters)
 9: .3       Probe Length (meters)
10: .085     Probe Offset (meters)
11: 3424     Loc [ EC_CH14   ]
12: 1.0      Multiplier
13: 0.0      Offset

87:  TDR100 Measurement (P119)
 1: 00       SDM Address
 2: 1        Waveform
 3: 2601     MMMP Mux & Probe Selection
 4: 4        Waveform Averaging
 5: 1        Vp
 6: 250      Points
 7: 26       Cable Length (meters)
 8: 6        Window Length (meters)
 9: .3       Probe Length (meters)
10: .085     Probe Offset (meters)
11: 3425     Loc [ WFC14_1   ]
12: 1.0      Multiplier
13: 0        O

; MEASURE P15
88:  TDR100 Measurement (P119)
 1: 00       SDM Address
 2: 00       Output Option
 3: 2701     MMMP Mux & Probe Selection
 4: 4        Waveform Averaging
 5: 1        Vp
 6: 250      Points
 7: 26       Cable Length (meters)
 8: 6        Window Length (meters)
 9: .3       Probe Length (meters)
10: .085     Probe Offset (meters)
11: 3685     Loc [ LAL_CH15  ]
12: 1.0      Multiplier
13: 0.0      Offset


89:  Z=X*Y (P36)
 1: 3685     X Loc [ LAL_CH15  ]
 2: 3685     Y Loc [ LAL_CH15  ]
 3: 3686     Z Loc [ WC_CH15   ]

90:  Z=X*F (P37)
```

```
 1: 3686     X Loc [ WC_CH15   ]
 2: 0.1      F
 3: 3686     Z Loc [ WC_CH15   ]

91:  Polynomial (P55)
 1: 1        Reps
 2: 3686     X Loc [ WC_CH15   ]
 3: 3686     F(X) Loc [ WC_CH15   ]
 4: -0.053   C0
 5: 0.292    C1
 6: -0.055   C2
 7: 0.0043   C3
 8: 0.0      C4
 9: 0.0      C5

92:  TDR100 Measurement (P119)
 1: 00       SDM Address
 2: 3        Electrical Conductivity
 3: 2701     MMMP Mux & Probe Selection
 4: 4        Waveform Averaging
 5: 1        Vp
 6: 250      Points
 7: 26       Cable Length (meters)
 8: 6        Window Length (meters)
 9: .3       Probe Length (meters)
10: .085     Probe Offset (meters)
11: 3687     Loc [ EC_CH15   ]
12: 1.0      Multiplier
13: 0.0      Offset

93:  TDR100 Measurement (P119)
 1: 00       SDM Address
 2: 1        Waveform
 3: 2701     MMMP Mux & Probe Selection
 4: 4        Waveform Averaging
 5: 1        Vp
 6: 250      Points
 7: 26       Cable Length (meters)
 8: 6        Window Length (meters)
 9: .3       Probe Length (meters)
10: .085     Probe Offset (meters)
11: 3688     Loc [ WFC15_1   ]
12: 1.0      Multiplier
13: 0        O

; MEASURE P16
```

```
94:  TDR100 Measurement (P119)
 1: 00       SDM Address
 2: 00       Output Option
 3: 2801     MMMP Mux & Probe Selection
 4: 4        Waveform Averaging
 5: 1        Vp
 6: 250      Points
 7: 26       Cable Length (meters)
 8: 6        Window Length (meters)
 9: .3       Probe Length (meters)
10: .085     Probe Offset (meters)
11: 3948     Loc [ LAL_CH16  ]
12: 1.0      Multiplier
13: 0.0      Offset

95:  Z=X*Y (P36)
 1: 3948     X Loc [ LAL_CH16  ]
 2: 3948     Y Loc [ LAL_CH16  ]
 3: 3949     Z Loc [ WC_CH16   ]

96:  Z=X*F (P37)
 1: 3949     X Loc [ WC_CH16   ]
 2: 0.1      F
 3: 3949     Z Loc [ WC_CH16   ]


97:  Polynomial (P55)
 1: 1        Reps
 2: 3949     X Loc [ WC_CH16   ]
 3: 3949     F(X) Loc [ WC_CH16   ]
 4: -0.053   C0
 5: 0.292    C1
 6: -0.055   C2
 7: 0.0043   C3
 8: 0.0      C4
 9: 0.0      C5

98:  TDR100 Measurement (P119)
 1: 00       SDM Address
 2: 3        Electrical Conductivity
 3: 2801     MMMP Mux & Probe Selection
 4: 4        Waveform Averaging
 5: 1        Vp
 6: 250      Points
 7: 26       Cable Length (meters)
 8: 6        Window Length (meters)
```

```
 9: .3       Probe Length (meters)
10: .085     Probe Offset (meters)
11: 3950     Loc [ EC_CH16   ]
12: 1.0      Multiplier
13: 0.0      Offset

99:  TDR100 Measurement (P119)
 1: 00       SDM Address
 2: 1        Waveform
 3: 2801     MMMP Mux & Probe Selection
 4: 4        Waveform Averaging
 5: 1        Vp
 6: 250      Points
 7: 26       Cable Length (meters)
 8: 6        Window Length (meters)
 9: .3       Probe Length (meters)
10: .085     Probe Offset (meters)
11: 3951     Loc [ WFC16_1   ]
12: 1.0      Multiplier
13: 0        O


100:  Do (P86)
 1: 45       Set Port 5 High

;END OF TDR100 MEASUREMENT SEQUENCE
;START MEASUREMENT OF 14 IRROMETERS ON AM416

101:  Beginning of Loop (P87)
 1: 0        Delay
 2: 14       Loop Count

    102:  Do (P86)
     1: 46       Set Port 6 High

    103:  Excitation with Delay (P22)
     1: 1        Ex Channel
     2: 0000     Delay W/Ex (0.01 sec units)
     3: 10       Delay After Ex (0.01 sec units)
     4: 0000     mV Excitation

    104:  Step Loop Index (P90)
     1: 1        Step

    105:  Do (P86)
     1: 74       Pulse Port 4
```

```
    106:  Excitation with Delay (P22)
     1: 1        Ex Channel
     2: 0000     Delay W/Ex (0.01 sec units)
     3: 1        Delay After Ex (0.01 sec units)
     4: 0000     mV Excitation

    107:  3W Half Bridge (P7)
     1: 1        Reps
     2: 12       7.5 mV Fast Range
     3: 1        SE Channel
     4: 1        Excite all reps w/Exchan 1
     5: 2500     mV Excitation
     6: 4211  -- Loc [ IRR_1     ]
     7: 1.0      Multiplier
     8: 0.0      Offset

    108:  Do (P86)
     1: 56       Set Port 6 Low

    109:  Excitation with Delay (P22)
     1: 1        Ex Channel
     2: 0000     Delay W/Ex (0.01 sec units)
     3: 10       Delay After Ex (0.01 sec units)
     4: 0000     mV Excitation

110:  End (P95)

111:  Do (P86)
 1: 55       Set Port 5 Low

; END IRROMETER MEASUREMENT
; MEASURE PRECIPITATION THROUGH TIPPING BUCKET

112:  Pulse (P3)
 1: 1        Reps
 2: 1        Pulse Channel 1
 3: 2        Switch Closure, All Counts
 4: 4226     Loc [ TB        ]
 5: 1.0      Multiplier
 6: 0.0      Offset

113:  Volt (Diff) (P2)
 1: 1        Reps
 2: 12       7.5 mV Fast Range
 3: 6        DIFF Channel
```

4: 4229 Loc [RELAY1]
5: 1.0 Multiplier
6: 0.0 Offset

114: Do (P86)
1: 46 Set Port 6 High

115: Excitation with Delay (P22)
1: 1 Ex Channel
2: 0000 Delay W/Ex (0.01 sec units)
3: 10 Delay After Ex (0.01 sec units)
4: 0000 mV Excitation

116: Volt (Diff) (P2)
1: 1 Reps
2: 12 7.5 mV Fast Range
3: 6 DIFF Channel
4: 4230 Loc [RELAY2]
5: 1.0 Multiplier
6: 0.0 Offset

117: Do (P86)
1: 56 Set Port 6 Low

118: Volt (Diff) (P2)
1: 1 Reps
2: 12 7.5 mV Fast Range
3: 4 DIFF Channel
4: 4234 Loc [PV1]
5: 1.0 Multiplier
6: 0.0 Offset

119: Volt (Diff) (P2)
1: 1 Reps
2: 12 7.5 mV Fast Range
3: 5 DIFF Channel
4: 4235 Loc [PV2]
5: 1.0 Multiplier
6: 0.0 Offset

120: Thermocouple Temp (DIFF) (P14)
1: 1 Reps
2: 21 2.5 mV 60 Hz Rejection Range
3: 2 DIFF Channel
4: 1 Type T (Copper-Constantan)

```
 5: 2       Ref Temp (Deg. C) Loc [ DL_TEMP   ]
 6: 4231    Loc [ TC_1      ]
 7: 1.0     Multiplier
 8: 0.0     Offset

121:  Thermocouple Temp (DIFF) (P14)
 1: 1       Reps
 2: 21      2.5 mV 60 Hz Rejection Range
 3: 3       DIFF Channel
 4: 1       Type T (Copper-Constantan)
 5: 2       Ref Temp (Deg. C) Loc [ DL_TEMP   ]
 6: 4232    Loc [ TC_2      ]
 7: 1.0     Multiplier
 8: 0.0     Offset

; BEGIN OUTPUT SEQUENCE
122:  Do (P86)
 1: 10      Set Output Flag High (Flag 0)

123:  Real Time (P77)^1629
 1: 1220    Year,Day,Hour/Minute (midnight = 2400)

124:  Sample (P70)^1597
 1: 1       Reps
 2: 1       Loc [ BAT_VOLT  ]

125:  Sample (P70)^5787
 1: 1       Reps
 2: 2       Loc [ DL_TEMP   ]

;OUTPUT P1
126:  Sample (P70)^3245
 1: 1       Reps
 2: 3       Loc [ LAL_CH1   ]

127:  Sample (P70)^15516
 1: 1       Reps
 2: 4       Loc [ WC_CH1    ]

128:  Sample (P70)^4658
 1: 1       Reps
 2: 5       Loc [ EC_CH1    ]


129:  Sample (P70)^12137
 1: 259     Reps
```

```
 2: 6       Loc [ WFCH1_1   ]

;OUTPUT P2
130:  Sample (P70)^30144
 1: 1       Reps
 2: 266     Loc [ LAL_CH2   ]

131:  Sample (P70)^15514
 1: 1       Reps
 2: 267     Loc [ WC_CH2    ]

132:  Sample (P70)^21565
 1: 1       Reps
 2: 268     Loc [ EC_CH2    ]

133:  Sample (P70)^8107
 1: 259     Reps
 2: 269     Loc [ WFCH2_1   ]

;OUTPUT P3
134:  Sample (P70)^27090
 1: 1       Reps
 2: 529     Loc [ LAL_CH3   ]

135:  Sample (P70)^31181
 1: 1       Reps
 2: 530     Loc [ WC_CH3    ]

136:  Sample (P70)^19532
 1: 1       Reps
 2: 531     Loc [ EC_CH3    ]

137:  Sample (P70)^18295
 1: 259     Reps
 2: 532     Loc [ WFCH3_1   ]

;OUTPUT P4
138:  Sample (P70)^26740
 1: 1       Reps
 2: 792     Loc [ LAL_CH4   ]

139:  Sample (P70)^17209
 1: 1       Reps
 2: 793     Loc [ WC_CH4    ]

140:  Sample (P70)^32649
```

```
 1: 1        Reps
 2: 794      Loc [ EC_CH4    ]

141:  Sample (P70)^31370
 1: 259      Reps
 2: 795      Loc [ WFCH4_1   ]

;OUTPUT P5
142:  Sample (P70)^28776
 1: 1        Reps
 2: 1055     Loc [ LAL_CH5   ]

143:  Sample (P70)^22150
 1: 1        Reps
 2: 1056     Loc [ WC_CH5    ]

144:  Sample (P70)^21664
 1: 1        Reps
 2: 1057     Loc [ EC_CH5    ]

145:  Sample (P70)^4377
 1: 259      Reps
 2: 1058     Loc [ WFCH5_1   ]

;OUTPUT P6
146:  Sample (P70)^10936
 1: 1        Reps
 2: 1318     Loc [ LAL_CH6   ]


147:  Sample (P70)^28123
 1: 1        Reps
 2: 1319     Loc [ WC_CH6    ]

148:  Sample (P70)^10747
 1: 1        Reps
 2: 1320     Loc [ EC_CH6    ]

149:  Sample (P70)^5253
 1: 259      Reps
 2: 1321     Loc [ WFCH6_1   ]

;OUTPUT P7
150:  Sample (P70)^12435
 1: 1        Reps
 2: 1581     Loc [ LAL_CH7   ]
```

```
151:  Sample (P70)^17248
 1: 1        Reps
 2: 1582     Loc [ WC_CH7    ]

152:  Sample (P70)^13991
 1: 1        Reps
 2: 1583     Loc [ EC_CH7    ]

153:  Sample (P70)^122
 1: 259      Reps
 2: 1584     Loc [ WFCH7_1   ]

;OUTPUT P8
154:  Sample (P70)^13371
 1: 1        Reps
 2: 1844     Loc [ LAL_CH8   ]

155:  Sample (P70)^1337
 1: 1        Reps
 2: 1845     Loc [ WC_CH8    ]

156:  Sample (P70)^8852
 1: 1        Reps
 2: 1846     Loc [ EC_CH8    ]

157:  Sample (P70)^12762
 1: 259      Reps
 2: 1847     Loc [ WFCH8_1   ]

;OUTPUT P9
158:  Sample (P70)^4528
 1: 1        Reps
 2: 2107     Loc [ LAL_CH9   ]

159:  Sample (P70)^670
 1: 1        Reps
 2: 2108     Loc [ WC_CH9    ]

160:  Sample (P70)^14563
 1: 1        Reps
 2: 2109     Loc [ EC_CH9    ]

161:  Sample (P70)^18001
 1: 259      Reps
 2: 2110     Loc [ WFCH9_1   ]
```

```
;OUTPUT P10
162:  Sample (P70)^5690
 1: 1        Reps
 2: 2370     Loc [ LAL_CH10  ]

163:  Sample (P70)
 1: 1        Reps
 2: 2371     Loc [ WC_CH10   ]

164:  Sample (P70)^27061
 1: 1        Reps
 2: 2372     Loc [ EC_CH10   ]

165:  Sample (P70)^27547
 1: 259      Reps
 2: 2373     Loc [ WFC10_1   ]

;OUTPUT P11
166:  Sample (P70)^16681
 1: 1        Reps
 2: 2633     Loc [ LAL_CH11  ]

167:  Sample (P70)^115
 1: 1        Reps
 2: 2634     Loc [ WC_CH11   ]

168:  Sample (P70)^11785
 1: 1        Reps
 2: 2635     Loc [ EC_CH11   ]

169:  Sample (P70)^13428
 1: 259      Reps
 2: 2636     Loc [ WFC11_1   ]

;OUTPUT P12
170:  Sample (P70)^7285
 1: 1        Reps
 2: 2896     Loc [ LAL_CH12  ]

171:  Sample (P70)^2651
 1: 1        Reps
 2: 2897     Loc [ WC_CH12   ]

172:  Sample (P70)^3475
 1: 1        Reps
```

```
 2: 2898     Loc [ EC_CH12   ]

173:  Sample (P70)^23147
 1: 259      Reps
 2: 2899     Loc [ WFC12_1   ]

;OUTPUT P13
174:  Sample (P70)^21109
 1: 1        Reps
 2: 3159     Loc [ LAL_CH13  ]


175:  Sample (P70)^31613
 1: 1        Reps
 2: 3160     Loc [ WC_CH13   ]

176:  Sample (P70)^27084
 1: 1        Reps
 2: 3161  -- Loc [ EC_CH13   ]

177:  Sample (P70)^23142
 1: 259      Reps
 2: 3162     Loc [ WFC13_1   ]

;OUTPUT P14
178:  Sample (P70)^9977
 1: 1        Reps
 2: 3422     Loc [ LAL_CH14  ]

179:  Sample (P70)^29405
 1: 1        Reps
 2: 3423     Loc [ WC_CH14   ]

180:  Sample (P70)^5257
 1: 1        Reps
 2: 3424     Loc [ EC_CH14   ]

181:  Sample (P70)^1689
 1: 259      Reps
 2: 3425     Loc [ WFC14_1   ]

;OUTPUT P15
182:  Sample (P70)^3082
 1: 1        Reps
 2: 3685     Loc [ LAL_CH15  ]
```

183: Sample (P70)^28183
1: 1 Reps
2: 3686 Loc [WC_CH15]

184: Sample (P70)^23020
1: 1 Reps
2: 3687 Loc [EC_CH15]

185: Sample (P70)^14099
1: 259 Reps
2: 3688 Loc [WFC15_1]

;OUTPUT P16
186: Sample (P70)^29026
1: 1 Reps
2: 3948 Loc [LAL_CH16]

187: Sample (P70)^17387
1: 1 Reps
2: 3949 Loc [WC_CH16]

188: Sample (P70)^5979
1: 1 Reps
2: 3950 Loc [EC_CH16]

189: Sample (P70)^2035
1: 259 Reps
2: 3951 Loc [WFC16_1]

190: Sample (P70)^11131
1: 14 Reps
2: 4211 Loc [IRR_1]

191: Sample (P70)^2506
1: 1 Reps
2: 4226 Loc [TB]

192: Sample (P70)^21101
1: 1 Reps
2: 4227 Loc [PV_1]

193: Sample (P70)^25522
1: 1 Reps
2: 4228 Loc [PV_2]

```
194:  Sample (P70)^19223
 1: 1        Reps
 2: 4229     Loc [ RELAY1    ]

195:  Sample (P70)^25219
 1: 1        Reps
 2: 4230     Loc [ RELAY2    ]

196:  Sample (P70)^1621
 1: 1        Reps
 2: 4231     Loc [ TC_1      ]

197:  Sample (P70)^24304
 1: 1        Reps
 2: 4232     Loc [ TC_2      ]

*Table 2 Program
  02: 0.0000    Execution Interval (seconds)

*Table 3 Subroutines

End Program
```

Appendix C

C.1. . Example of CR-10X output file.

Contained in this section of the appendix is a sample data file extracted from the in-situ instrumentation for the MBTC-3031 project. This datafile is then ingested using the MATLAB program presented in Appendix D and then analysized using MATLAB and Microsoft excel.

222,2012,1,12,12.07,24.88,8.54,.82,.001,4,1,250,18,6,.3,.085,1,0,.974,.974,.974,.974,.974
,.974,.974,.974,.974,.974,.974,.974,.974,.974,.974,.974,.974,.974,.974,.974,.974,.974,.974,.974,.9
74,.974,.974,.974,.974,.974,.974,.974,.974,.974,.974,.974,.974,.974,.974,.973,.973,.974,.974,.974
,.974,.974,.974,.974,.974,.974,.974,.974,.974,.974,.974,.974,.974,.974,.974,.974,.974,.974,.974,.9
74,.973,.974,.974,.974,.974,.974,.974,.974,.974,.973,.974,.973,.973,.974,.974,.974,.974,.974,.974
,.974,.974,.974,.974,.974,.974,.973,.973,.974,.974,.974,.974,.974,.974,.974,.974,.973,.974,.974,.9
74,.974,.974,.974,.974,.974,.974,.974,.974,.974,.973,.974,.973,.974,.973,.973,.974,.973,.973,.974
,.974,.974,.974,.974,.974,.974,.974,.974,.974,.974,.974,.974,.974,.973,.974,.974,.974,.974,.974,.9
74,.973,.973,.974,.973,.973,.974,.974,.974,.974,.974,.974,.973,.973,.974,.973,.973,.974,.974,.974
,.974,.974,.974,.974,.974,.974,.974,.973,.973,.973,.974,.974,.974,.974,.974,.973,.974,.974,.974,.9
73,.974,.974,.974,.973,.974,.974,.974,.974,.974,.974,.973,.973,.974,.973,.973,.973,.973,.974,.974
,.974,.974,.974,.974,.973,.973,.973,.973,.973,.973,.974,.974,.973,.974,.973,.973,.973,.973,.973,.9
73,.973,.974,.974,.973,.974,.973,.973,.973,.973,.972,.973,.971,.971,.973,.973,.973,.973,.973,.974
,.974,.974,.974,.974,.973,.973,.974,.973,.973,.972,.972,13.3,11.73,.001,4,1,250,18,6,.3,.085,1,0,.
974,.974,.974,.974,.974,.974,.974,.974,.974,.974,.974,.974,.974,.974,.974,.974,.974,.974,.974,.97
4,.974,.974,.974,.974,.974,.974,.974,.974,.974,.974,.974,.974,.974,.974,.974,.974,.974,.974,.974,.
974,.974,.974,.974,.974,.974,.974,.974,.974,.974,.974,.974,.974,.974,.974,.974,.974,.974,.974,.97

4,.974,.974,.974,.974,.974,.974,.974,.974,.974,.974,.974,.974,.974,.974,.974,.974,.974,.974,.974,.
974,.974,.974,.974,.974,.974,.974,.974,.974,.974,.974,.974,.974,.974,.974,.974,.974,.974,.974,.97
4,.974,.974,.974,.974,.974,.974,.974,.974,.974,.974,.974,.974,.974,.974,.973,.974,.974,.974,.974,.
974,.974,.974,.974,.974,.974,.974,.974,.974,.973,.974,.974,.974,.974,.974,.974,.974,.974,.974,.97
4,.974,.974,.974,.974,.974,.973,.974,.974,.974,.974,.974,.974,.974,.974,.974,.974,.974,.973,.974,.
974,.974,.974,.974,.974,.974,.974,.974,.974,.974,.974,.974,.974,.974,.974,.974,.974,.974,.974,.97
4,.974,.974,.974,.973,.973,.974,.974,.974,.974,.974,.974,.974,.974,.974,.974,.974,.974,.974,.974,.
974,.974,.974,.974,.974,.974,.974,.974,.973,.974,.974,.974,.974,.973,.974,.974,.974,.974,.974,.97
4,.974,.974,.974,.974,.974,.974,.974,.974,.974,.974,.974,.974,.974,.974,.973,.97,.973,.97,.973,.97
3,.973,.974,.974,.974,.974,.974,.974,.974,.974,.973,.974,.973,.974,.973,.973,-.103,-
.053,.001,4,1,250,18,6,.3,.085,1,0,.974,.975,.974,.974,.974,.974,.974,.974,.974,.975,.976,.974,.97
5,.974,.974,.975,.974,.977,.974,.974,.974,.976,.975,.974,.974,.974,.974,.974,.974,.974,.974,.976,.
974,.974,.974,.974,.974,.974,.974,.974,.974,.974,.975,.977,.977,.974,.974,.974,.974,.974,.974,.97
4,.974,.974,.974,.975,.975,.974,.974,.974,.974,.974,.974,.974,.974,.974,.975,.975,.976,.974,.974,.
974,.974,.974,.974,.974,.974,.974,.975,.974,.974,.974,.974,.974,.974,.974,.974,.974,.974,.974,.97
4,.975,.975,.974,.974,.974,.974,.974,.974,.974,.974,.974,.974,.974,.974,.974,.974,.974,.974,.974,.
974,.974,.974,.974,.974,.974,.974,.974,.974,.974,.974,.974,.974,.974,.974,.974,.974,.974,.974,.97
4,.974,.974,.974,.974,.975,.974,.975,.974,.974,.974,.974,.974,.974,.974,.974,.974,.974,.974,.974,.
974,.974,.974,.974,.974,.974,.974,.974,.974,.974,.974,.974,.974,.974,.974,.974,.974,.974,.974,.97
4,.974,.974,.974,.974,.974,.974,.974,.974,.974,.974,.974,.974,.974,.974,.974,.974,.974,.974,.974,.
974,.974,.974,.974,.974,.974,.974,.974,.974,.974,.974,.974,.974,.974,.974,.974,.974,.974,.974,.97
4,.974,.974,.974,.974,.974,.974,.974,.974,.974,.974,.974,.974,.974,.974,.974,.974,.974,.974,.974,.
974,.974,.973,.974,.974,.974,.974,.973,.974,.974,.974,.974,.974,.974,.975,.976,.974,.973,.974,.97

4,.974,.974,.974,.744,-

.037,.001,4,1,250,18,6,.3,.085,1,0,.978,.979,.978,.979,.978,.978,.978,.978,.978,.979,.977,.979,.97

9,.976,.978,.977,.979,.977,.978,.979,.979,.978,.978,.976,.977,.976,.977,.979,.979,.979,.979,.979,.

979,.978,.976,.976,.976,.976,.976,.976,.976,.978,.979,.979,.979,.976,.979,.976,.978,.976,.976,.97

6,.977,.979,.977,.979,.979,.978,.977,.976,.976,.976,.976,.976,.977,.977,.979,.979,.979,.979,.979,.

977,.976,.977,.976,.976,.976,.978,.978,.977,.979,.979,.978,.978,.976,.976,.976,.976,.976,.977,.97

7,.977,.979,.978,.977,.978,.977,.976,.976,.976,.976,.976,.977,.976,.976,.976,.977,.976,.977,.977,.

977,.978,.977,.976,.976,.976,.976,.976,.976,.976,.976,.977,.978,.977,.978,.976,.976,.976,.976,.97

6,.976,.976,.976,.976,.976,.976,.976,.976,.978,.976,.976,.976,.976,.976,.976,.976,.976,.977,.979,.

976,.976,.976,.977,.976,.976,.976,.976,.976,.976,.976,.977,.977,.976,.976,.976,.976,.976,.976,.97

6,.976,.977,.976,.976,.976,.976,.976,.976,.976,.976,.976,.976,.976,.976,.976,.976,.976,.978,.

976,.976,.976,.976,.976,.976,.976,.976,.976,.976,.976,.976,.976,.976,.976,.976,.976,.976,.976,.97

6,.976,.976,.976,.978,.976,.976,.976,.976,.976,.976,.976,.976,.976,.976,.976,.976,.976,.976,.976,.

976,.976,.976,.976,.976,.976,.976,.976,.976,.976,.976,.976,.976,.976,.976,.976,.976,.976,.976,.97

6,.976,.976,.976,-

12.43,7.19,.056,4,1,250,18,6,.3,.085,1,0,.03,.03,.03,.03,.03,.03,.031,.031,.03,.03,.03,.031,.03,.031

,.031,.031,.031,.031,.031,.031,.031,.031,.03,.03,.03,.03,.031,.031,.031,.031,.031,.03,.031,.03,.031

,.03,.03,.031,.03,.031,.031,.031,.031,.031,.031,.031,.03,.031,.03,.03,.03,.03,.03,.03,.03,.03,.031,.0

31,.031,.03,.031,.03,.031,.031,.031,.031,.031,.031,.031,.031,.031,.031,.031,.031,.031,.031,.031,.0

3,.03,.03,.03,.03,.03,.031,.031,.031,.031,.03,.031,.03,.031,.03,.03,.03,.03,.03,.03,.031,.03,.03,.031

,.03,.029,.027,.028,.029,.03,.03,.03,.031,.031,.03,.031,.03,.031,.031,.03,.03,.031,.031,.031,.032,.0

31,.031,.031,.031,.031,.031,.031,.03,.031,.031,.031,.031,.032,.033,.031,.031,.031,.031,.031,.031,.

031,.031,.031,.031,.031,.031,.031,.032,.036,.047,.071,.113,.165,.213,.244,.266,.284,.29,.269,.215

,.144,.072,.015,-.022,-.046,-.066,-.084,-.106,-.136,-.166,-.188,-.206,-.22,-.234,-.251,-.268,-.28,-
.288,-.297,-.301,-.306,-.308,-.308,-.314,-.316,-.317,-.316,-.319,-.321,-.327,-.332,-.335,-.338,-
.342,-.347,-.354,-.361,-.371,-.377,-.38,-.386,-.393,-.398,-.399,-.403,-.408,-.415,-.418,-.42,-.422,-
.425,-.428,-.432,-.433,-.438,-.444,-.451,-.459,-.466,-.473,-.483,-.492,-.502,-.511,-.519,-.526,-
.53,-.536,-.54,-.544,-.547,-.551,-.555,-.559,-.561,-.567,-.57,-.574,-.578,-.582,-.586,-.59,-.596,-
.602,-.605,-.609,-.612,-
.616,1.417,.003,.001,4,1,250,18,6,.3,.085,1,0,.974,.975,.975,.975,.974,.974,.974,.974,.975,.975,.9
75,.975,.975,.975,.975,.975,.975,.974,.975,.975,.975,.975,.975,.975,.974,.974,.974,.974,.975,.975
,.975,.975,.974,.974,.975,.974,.974,.974,.974,.974,.975,.974,.975,.975,.975,.975,.974,.974,.974,.9
74,.974,.974,.974,.974,.974,.975,.975,.975,.975,.974,.974,.974,.974,.974,.974,.974,.974,.975,.975
,.975,.975,.974,.974,.974,.974,.974,.974,.975,.975,.975,.975,.975,.975,.974,.974,.974,.974,.974,.9
74,.974,.974,.974,.974,.974,.975,.974,.974,.974,.974,.974,.974,.975,.974,.974,.974,.975,.974,.975
,.974,.974,.974,.974,.974,.975,.974,.974,.974,.974,.974,.974,.974,.974,.975,.974,.974,.974,.9
74,.973,.971,.973,.974,.974,.974,.974,.974,.974,.974,.974,.974,.974,.974,.974,.972,.974,.974,.974
,.974,.974,.975,.974,.975,.975,.975,.974,.972,.974,.974,.974,.974,.974,.975,.974,.974,.974,.973,.9
72,.974,.974,.974,.974,.973,.974,.974,.974,.974,.974,.973,.973,.972,.973,.974,.974,.974,.973,.974
,.974,.974,.974,.974,.974,.974,.973,.974,.973,.974,.974,.974,.974,.974,.974,.974,.974,.974,.974,.9
73,.974,.973,.974,.973,.973,.974,.972,.973,.972,.973,.974,.973,.974,.974,.974,.973,.974,.974,.974
,.974,.972,.972,.971,.971,.971,.971,.971,.971,.971,.971,.973,.974,.971,.973,.974,.974,.974,.974,.9
74,.972,.971,.972,.971,.971,16.8,61.08,.001,4,1,250,18,6,.3,.085,1,0,.974,.974,.973,.974,.974,.97
4,.974,.974,.974,.974,.974,.974,.974,.974,.974,.974,.974,.974,.974,.974,.974,.974,.974,.974,.974,.
973,.974,.974,.974,.974,.974,.974,.974,.974,.974,.974,.973,.974,.973,.973,.974,.974,.974,.97
4,.974,.973,.974,.974,.974,.973,.973,.974,.974,.974,.974,.974,.974,.974,.974,.974,.974,.974,.974,.

974,.974,.974,.974,.974,.974,.974,.974,.974,.973,.973,.974,.974,.974,.974,.974,.974,.974,.974,.974,.97
4,.974,.974,.973,.974,.974,.973,.974,.974,.974,.974,.974,.974,.974,.974,.974,.974,.973,.974,.974,.
974,.974,.974,.974,.974,.974,.974,.974,.974,.973,.974,.974,.974,.973,.974,.974,.973,.974,.974,.97
4,.974,.974,.974,.974,.973,.973,.973,.973,.973,.974,.974,.974,.974,.974,.974,.974,.973,.973,.973,.
973,.974,.973,.973,.974,.974,.974,.974,.974,.973,.974,.974,.973,.973,.973,.973,.974,.974,.974,.97
4,.974,.973,.974,.974,.973,.973,.974,.973,.973,.974,.974,.973,.974,.973,.973,.973,.973,.973,.973,.
973,.974,.973,.973,.973,.973,.974,.973,.973,.973,.973,.973,.974,.973,.973,.973,.974,.974,.973,.97
3,.973,.973,.973,.973,.974,.974,.973,.973,.973,.973,.973,.973,.973,.973,.973,.973,.973,.973,.973,.
973,.973,.973,.973,.973,.973,.972,.973,.972,.973,.972,.971,.972,.973,.973,.973,.973,.973,.973,.97
4,.974,.974,.972,.973,.973,.973,.973,.971,.972,.972,11.64,4.49,.001,4,1,250,28,6,.3,.085,1,0,.973,
.973,.97,.971,.973,.97,.97,.969,.971,.971,.973,.973,.97,.973,.973,.973,.97,.973,.973,.973,.973,.97,
.971,.973,.971,.97,.971,.971,.97,.971,.973,.973,.973,.973,.971,.973,.973,.971,.969,.97,.97,.973,.9
73,.973,.971,.973,.969,.973,.969,.969,.969,.969,.97,.971,.971,.973,.97,.971,.97,.969,.97,.969,.971
,.97,.97,.971,.97,.969,.97,.971,.971,.973,.97,.969,.969,.969,.97,.97,.969,.973,.969,.969,.969,.969,.
969,.969,.97,.969,.969,.97,.973,.969,.969,.969,.969,.969,.969,.969,.973,.973,.971,.97,.971,.969,.9
69,.969,.969,.969,.97,.971,.969,.971,.973,.97,.969,.969,.969,.969,.969,.969,.969,.97,.971,.973,.97
3,.97,.973,.969,.969,.969,.969,.973,.969,.973,.973,.973,.973,.969,.969,.969,.969,.969,.969,.969,.9
69,.971,.971,.973,.973,.973,.969,.969,.969,.969,.969,.969,.969,.97,.969,.971,.971,.97,.969,.969,.9
69,.969,.969,.969,.969,.969,.971,.973,.969,.969,.969,.969,.969,.969,.969,.97,.97,.97,.97,.969,.969
,.969,.97,.97,.969,.969,.969,.969,.969,.969,.969,.969,.969,.969,.969,.969,.969,.969,.969,.969,.969
,.969,.969,.969,.969,.969,.969,.969,.969,.97,.969,.969,.969,.969,.969,.969,.969,.969,.969,.969,.96
9,.969,.969,.969,.969,.969,.969,.969,.969,.969,.969,.969,.969,.969,.97,.969,.97,.969,.969,.969,.96
9,.969,.969,.969,.969,.969,16.05,44.43,0,4,1,250,26,6,.3,.085,1,0,.974,.974,.974,.974,.974,.974,.9

74,.974,.974,.974,.974,.974,.974,.974,.974,.974,.974,.974,.974,.974,.974,.974,.974,.974,.974,.974
,.974,.974,.974,.973,.974,.974,.974,.974,.974,.974,.974,.974,.974,.974,.974,.974,.974,.974,.974,.9
74,.974,.974,.974,.974,.974,.974,.974,.974,.974,.974,.974,.974,.974,.974,.974,.974,.974,.974,.974
,.974,.974,.974,.974,.974,.974,.974,.974,.974,.974,.974,.974,.974,.974,.974,.974,.974,.974,.974,.9
74,.974,.974,.974,.973,.974,.974,.974,.973,.974,.973,.974,.974,.974,.974,.974,.974,.974,.974,.973
,.973,.974,.974,.974,.974,.974,.974,.974,.974,.974,.974,.974,.973,.974,.974,.974,.974,.973,.973,.9
73,.973,.974,.973,.973,.974,.974,.973,.974,.974,.974,.973,.973,.973,.973,.973,.973,.974,.974,.974
,.974,.974,.974,.973,.973,.973,.974,.973,.973,.974,.974,.974,.973,.973,.974,.973,.973,.974,.974,.9
74,.973,.973,.973,.973,.973,.973,.973,.973,.973,.974,.974,.974,.974,.973,.973,.973,.973,.973,.973
,.973,.973,.974,.974,.973,.973,.973,.973,.973,.974,.974,.974,.973,.974,.973,.973,.973,.973,.973,.9
73,.973,.973,.973,.973,.973,.973,.974,.974,.974,.973,.973,.973,.973,.973,.973,.974,.974,.974,.973
,.973,.971,.97,.969,.971,.971,.973,.973,.973,.974,.974,.974,.974,.973,.97,.969,.969,.973,.973,.973
,.973,.973,.973,.974,.973,.973,.973,.973,.973,14.79,25.04,.001,4,1,250,26,6,.3,.085,1,0,.974,.974,
.974,.974,.974,.974,.974,.974,.974,.974,.974,.974,.974,.974,.974,.974,.974,.974,.974,.974,.974,.9
74,.974,.974,.974,.974,.974,.974,.974,.974,.974,.974,.974,.974,.974,.974,.974,.974,.974,.974,.974
,.974,.974,.974,.974,.974,.974,.974,.974,.974,.974,.974,.974,.974,.974,.974,.974,.974,.974,.974,.9
74,.974,.974,.974,.974,.974,.974,.974,.974,.974,.974,.974,.974,.974,.974,.974,.974,.974,.974,.974
,.974,.974,.974,.974,.974,.974,.974,.974,.974,.974,.974,.974,.974,.974,.974,.974,.974,.974,.974,.9
74,.974,.974,.974,.974,.974,.974,.974,.974,.974,.974,.974,.974,.973,.974,.973,.973,.974,.974,.974
,.974,.974,.974,.974,.974,.974,.974,.974,.974,.974,.974,.974,.974,.974,.974,.974,.974,.974,.974,.9
74,.974,.974,.974,.974,.974,.974,.973,.974,.974,.973,.973,.974,.974,.974,.974,.974,.974,.974,.974
,.974,.974,.974,.974,.974,.974,.973,.973,.973,.974,.974,.974,.973,.974,.974,.974,.974,.974,.974,.9
74,.973,.974,.974,.974,.974,.974,.974,.973,.974,.974,.973,.973,.974,.974,.974,.974,.974,.974,.974

,.973,.973,.974,.973,.973,.973,.974,.974,.974,.974,.974,.974,.973,.973,.973,.973,.974,.974,.974,.9
74,.974,.974,.974,.973,.973,.972,.973,.973,.973,.973,.973,.973,.974,.974,.974,.974,.974,.973,.973
,.97,.972,.973,.973,.973,.973,.974,.973,.974,.974,.974,.973,.973,.973,7.97,.684,.056,4,1,250,18,6,
.3,.085,1,0,.042,.042,.043,.042,.043,.042,.042,.042,.042,.042,.042,.042,.042,.042,.042,.042,.041,.
042,.044,.043,.043,.042,.042,.042,.042,.042,.042,.041,.042,.043,.043,.042,.042,.042,.043,.043,.04
2,.043,.042,.042,.041,.043,.043,.042,.043,.044,.045,.042,.042,.042,.042,.043,.045,.042,.042,.042,.
042,.041,.041,.042,.042,.042,.042,.041,.042,.042,.043,.042,.044,.042,.042,.043,.042,.042,.043,.04
2,.042,.043,.045,.042,.045,.042,.044,.044,.042,.042,.042,.042,.045,.045,.043,.044,.043,.042,.045,.
045,.042,.043,.045,.045,.045,.045,.043,.042,.042,.042,.042,.043,.044,.045,.042,.042,.042,.042,.04
3,.043,.042,.042,.043,.043,.042,.045,.042,.042,.044,.044,.043,.042,.042,.043,.044,.045,.042,.043,.
042,.044,.044,.044,.042,.042,.043,.042,.042,.042,.043,.044,.043,.042,.042,.043,.042,.041,.041,.04
1,.042,.042,.042,.044,.044,.042,.042,.042,.042,.042,.042,.043,.042,.044,.042,.045,.042,.042,.042,.
043,.044,.042,.044,.043,.044,.043,.042,.042,.042,.045,.045,.042,.043,.045,.045,.045,.045,.043,.04
4,.043,.045,.046,.046,.045,.045,.046,.045,.044,.046,.046,.045,.045,.045,.044,.045,.046,.045,.043,.
044,.045,.045,.045,.045,.045,.045,.045,.043,.042,.042,.042,.045,.045,.044,.045,.042,.042,.043,.04
5,.045,.045,.045,.042,.044,.045,.046,.045,.045,.047,.046,.046,.044,.043,.042,.042,.045,.045,8.71,.
875,0,4,1,250,26,6,.3,.085,1,0,.975,.974,.975,.974,.976,.974,.973,.973,.973,.973,.973,.974,.973,.9
73,.973,.973,.973,.973,.973,.973,.973,.973,.973,.974,.973,.973,.974,.973,.973,.975,.973,.973,.973
,.973,.973,.973,.973,.974,.975,.973,.973,.973,.973,.973,.973,.973,.973,.974,.975,.974,.974,.974,.9
73,.973,.973,.973,.973,.973,.973,.973,.973,.975,.974,.973,.973,.973,.973,.973,.973,.973,.973,.973
,.973,.973,.973,.973,.973,.973,.973,.973,.973,.973,.973,.973,.973,.973,.973,.973,.973,.973,.973,.9
73,.973,.973,.973,.973,.973,.973,.973,.973,.973,.973,.973,.973,.973,.973,.973,.973,.973,.973,.973
,.973,.973,.973,.973,.973,.973,.973,.973,.973,.973,.973,.973,.973,.973,.973,.973,.973,.973,.973,.9

73,.973,.973,.973,.973,.973,.973,.973,.973,.973,.973,.973,.973,.973,.973,.973,.973,.973,.973,.973,.973,.973

,.973,.973,.973,.973,.973,.973,.973,.973,.973,.973,.973,.973,.973,.973,.973,.973,.973,.973,.973,.973,.9

73,.973,.973,.973,.973,.973,.973,.973,.973,.973,.973,.973,.973,.973,.973,.973,.973,.973,.973,.973,.973

,.973,.973,.973,.973,.973,.973,.973,.973,.973,.973,.973,.973,.973,.973,.973,.973,.973,.973,.973,.973,.9

73,.973,.973,.973,.972,.973,.973,.973,.973,.973,.973,.973,.973,.973,.973,.972,.972,.973,.973,.973

,.973,.974,.973,.973,.973,.973,.973,.972,.972,.972,.972,.973,.973,.973,.973,.973,.973,.973,.973,.973,.9

73,.973,.973,2.497,.109,0,4,1,250,26,6,.3,.085,1,0,.974,.975,.975,.973,.973,.974,.972,.975,.973,.9

74,.974,.973,.973,.974,.975,.975,.975,.974,.975,.974,.972,.974,.973,.972,.974,.975,.975,.974,.974

,.975,.973,.974,.972,.973,.972,.972,.974,.973,.974,.975,.974,.972,.973,.974,.972,.973,.972,.974,.9

74,.974,.974,.973,.972,.973,.972,.973,.973,.974,.974,.973,.974,.974,.973,.973,.972,.972,.975,.974

,.973,.972,.973,.972,.972,.973,.972,.972,.973,.972,.974,.975,.972,.972,.972,.972,.972,.973,.973,.9

73,.972,.972,.972,.973,.974,.972,.972,.972,.972,.972,.972,.972,.972,.972,.972,.972,.972,.972,.972

,.972,.972,.972,.972,.972,.973,.972,.972,.972,.972,.972,.972,.972,.972,.972,.974,.972,.972,.9

72,.972,.972,.972,.972,.972,.972,.972,.972,.972,.972,.972,.972,.972,.972,.972,.972,.972,.972,.972

,.972,.972,.972,.972,.972,.972,.972,.972,.972,.972,.972,.972,.972,.972,.972,.972,.972,.972,.9

72,.972,.972,.972,.972,.972,.972,.972,.972,.972,.972,.972,.972,.972,.972,.972,.972,.972,.972,.972

,.972,.972,.972,.972,.972,.972,.972,.972,.973,.972,.972,.972,.972,.972,.972,.972,.972,.972,.972,.9

72,.972,.972,.972,.972,.972,.972,.972,.972,.972,.972,.974,.972,.972,.972,.972,.972,.972,.972,.972

,.971,.972,.972,.972,.972,.972,.973,.972,.972,.972,.972,.972,.972,.972,.972,.972,.972,.972,.972,.9

72,.972,.972,.972,.972,.972,.972,3.297,.205,0,4,1,250,26,6,.3,.085,1,0,.974,.973,.973,.974,.974,.9

74,.972,.972,.972,.974,.973,.974,.974,.974,.974,.974,.974,.971,.973,.973,.974,.974,.974,.974,.974

,.973,.974,.974,.974,.971,.974,.973,.974,.973,.974,.971,.973,.973,.974,.974,.974,.974,.974,.974,.9

74,.974,.973,.974,.973,.974,.973,.974,.973,.972,.972,.973,.974,.973,.974,.974,.974,.972,.971,.973

,.974,.973,.971,.973,.971,.973,.973,.972,.973,.973,.971,.971,.973,.973,.973,.974,.974,.973,.972,.9
73,.972,.972,.971,.971,.971,.973,.972,.973,.973,.972,.973,.971,.972,.973,.971,.971,.974,.972,.971
,.971,.972,.973,.973,.972,.972,.971,.971,.971,.971,.972,.971,.974,.971,.973,.971,.971,.971,.971,.9
72,.971,.973,.973,.971,.971,.972,.971,.971,.971,.971,.971,.972,.971,.971,.971,.971,.971,.971,.971
,.971,.972,.972,.971,.971,.973,.971,.971,.971,.971,.971,.971,.971,.971,.972,.971,.971,.971,.971,.9
71,.971,.971,.971,.971,.971,.971,.971,.971,.971,.973,.971,.971,.971,.971,.971,.971,.971,.971,.973
,.971,.972,.974,.971,.972,.971,.971,.971,.971,.971,.971,.971,.973,.974,.972,.971,.971,.971,.971,.9
71,.971,.971,.972,.971,.971,.971,.971,.971,.971,.971,.971,.971,.971,.971,.972,.971,.971,.973,.971
,.971,.971,.971,.971,.971,.971,.971,.971,.971,.972,.972,.971,.971,.971,.971,.971,.971,.971,.971,.9
71,.971,.971,.971,.971,.971,.971,.971,.971,.971,.971,15.22,30.63,0,4,1,250,26,6,.3,.085,1,0,.973,.
973,.973,.973,.973,.973,.973,.974,.973,.973,.973,.973,.973,.974,.974,.973,.973,.973,.973,.973,.97
3,.973,.973,.973,.973,.974,.973,.973,.972,.973,.972,.973,.973,.973,.973,.973,.974,.973,.973,.973,.
973,.973,.973,.973,.973,.973,.973,.973,.973,.973,.973,.973,.972,.973,.973,.973,.972,.973,.973,.97
3,.973,.973,.973,.973,.971,.973,.973,.973,.973,.973,.973,.973,.973,.973,.973,.973,.974,.973,.973,.
973,.973,.973,.973,.973,.971,.973,.972,.973,.973,.972,.973,.973,.973,.971,.972,.972,.973,.972,.97
3,.971,.971,.971,.973,.973,.972,.972,.972,.972,.97,.972,.972,.972,.971,.972,.971,.973,.972,.973,.9
7,.971,.97,.97,.97,.973,.97,.97,.972,.972,.973,.973,.972,.971,.972,.972,.972,.97,.971,.972,.97,.972
,.972,.972,.972,.973,.971,.97,.971,.97,.971,.973,.973,.972,.973,.972,.971,.97,.971,.973,.971,.971,.
972,.972,.971,.97,.97,.971,.97,.971,.972,.973,.971,.972,.971,.973,.971,.971,.97,.97,.97,.97,.97,.97
2,.973,.973,.97,.97,.97,.97,.97,.97,.97,.971,.971,.972,.973,.97,.973,.972,.97,.97,.97,.97,.97,.97,.97
,.973,.972,.971,.973,.97,.97,.97,.97,.97,.97,.971,.973,.973,.971,.97,.97,.97,.97,.97,.97,.97,.97,.97,.
972,.973,.973,.971,.97,.97,.97,.97,.97,.97,.97,.97,.97,.971,.971,.97,.97,.97,.97,.97,.97,6.097,.4
93,0,4,1,250,26,6,.3,.085,1,0,.973,.974,.974,.973,.973,.973,.974,.974,.973,.973,.973,.974,.974,.97

4,.974,.974,.973,.973,.973,.973,.973,.974,.973,.973,.974,.973,.974,.974,.973,.973,.973,.973,.973,.973,.973,.974,.974,.974,.974,.973,.974,.973,.973,.973,.973,.974,.974,.974,.973,.974,.974,.973,.973,.973,.974,.973,.973,.973,.973,.973,.974,.973,.974,.974,.973,.973,.973,.973,.973,.973,.973,.973,.973,.973,.973,.973,.974,.973,.973,.973,.973,.973,.973,.973,.973,.973,.973,.972,.973,.972,.973,.973,.973,.973,.973,.973,.973,.973,.973,.973,.973,.974,.973,.973,.973,.973,.972,.973,.973,.973,.973,.973,.973,.973,.972,.973,.973,.973,.973,.971,.973,.973,.972,.973,.973,.972,.973,.97,.972,.97,.972,.972,.973,.973,.973,.973,.972,.973,.972,.973,.972,.973,.973,.973,.973,.971,.972,.973,.973,.972,.973,.973,.973,.972,.973,.972,.973,.973,.973,.973,.973,.973,.972,.973,.972,.971,.971,.973,.972,.973,.973,.973,.973,.973,.973,.971,.973,.971,.972,.973,.973,.973,.973,.973,.973,.97,.971,.97,.971,.973,.973,.973,.973,.973,.973,.973,.973,.973,.97,.971,.97,.971,.971,.971,.972,.973,.973,.971,.97,.97,.971,.97,.971,.972,.973,.973,.972,.973,.973,.97,.97,.97,.97,.97,.97,.971,.973,.973,.973,.973,.973,.973,.97,.97,.97,.97,.97,.97,.97,.972,.972,.972,.973,.97,.972,.971,.973,.972,.971,-6999,-6999,-6999,-6999,-6999,-6999,-6999,-6999,-6999,-6999,-6999,-6999,-6999,-6999,-6999,-6999,-6999,-6999,-6999,0,0,0,.256,-6999,24.06,-6999

Appendix D

D.1. MATLAB data extraction program

Contained in this section of the appendices is the MATLAB data extraction program used to extract and process the exported datalogger data files. Data is ingested in the form of a comma delinated text file and then is output as MATLAB variable arrays for importation into Microsoft Excel.

```
%%DATA LOGGER .DAT EXTRACTION FOR PROCESSING
%CYRUS GARNER
%%
%%OUTPUT ARRAY FOR .DAT FROM CR10X AS A,XXXX ARRAY
%ARRAY POSITION - VAR
%0001 -
%0002 - YEAR
%0003 - DAY
%0004 - SECOND
%0005 - BATTERY_VOLTAGE (BAT_VOLT)
%0006 - DL_TEMPERATURE (DL_TEMP)
%0007 - TDR_PROBE_01 LA_L VALUE (BY TDR100)
%0008 - TDR_PROBE_01 WATER_CONTENT (BY TDR100 AND TOPPS)
%0009 - TDR_PROBE_01 E_VALUE
%0010 - TDR_PROBE_01 WAVE_FORM_01 PARAMETER_1 - AVERAGING
%0011 - TDR_PROBE_01 WAVE_FORM_01 PARAMETER_2 - DATA_AQ_MODE
%0012 - TDR_PROBE_01 WAVE_FORM_01 PARAMETER_3 - NUMBER SAMPLES
%0013 - TDR_PROBE_01 WAVE_FORM_01 PARAMETER_4 - WINDOW START
%0014 - TDR_PROBE_01 WAVE_FORM_01 PARAMETER_5 - WINDOW LENGTH
%0015 - TDR_PROBE_01 WAVE_FORM_01 PARAMETER_6 - PROBE LENGTH
%0016 - TDR_PROBE_01 WAVE_FORM_01 PARAMETER_7 - PROBE OFFSET
%0017 - TDR_PROBE_01 WAVE_FORM_01 PARAMETER_8 - MULTIPLIER
%0018 - TDR_PROBE_01 WAVE_FORM_01 PARAMETER_9 - OFFSET
%0019-0268 - TDR_PROBE_1 WAVE_FORM_1
%0269 - TDR_PROBE_02 LA_L VALUE (BY TDR100)
%0270 - TDR_PROBE_02 WATER_CONTENT (BY TDR100 AND TOPPS)
%0271 - TDR_PROBE_02 E_VALUE
%0272 - TDR_PROBE_02 WAVE_FORM_02 PARAMETER_1 - AVERAGING
%0273 - TDR_PROBE_02 WAVE_FORM_02 PARAMETER_2 - DATA_AQ_MODE
%0274 - TDR_PROBE_02 WAVE_FORM_02 PARAMETER_3 - NUMBER SAMPLES
%0275 - TDR_PROBE_02 WAVE_FORM_02 PARAMETER_4 - WINDOW START
```

```
%0276 - TDR_PROBE_02 WAVE_FORM_02 PARAMETER_5 - WINDOW LENGTH
%0277 - TDR_PROBE_02 WAVE_FORM_02 PARAMETER_6 - PROBE LENGTH
%0278 - TDR_PROBE_02 WAVE_FORM_02 PARAMETER_7 - PROBE OFFSET
%0279 - TDR_PROBE_02 WAVE_FORM_02 PARAMETER_8 - MULTIPLIER
%0280 - TDR_PROBE_02 WAVE_FORM_02 PARAMETER_9 - OFFSET
%0281-0530 - TDR_PROBE_02 WAVE_FORM_02
%0531-0792 - TDR_PROBE_03 READINGS / PARAMETERS / WAVE_FORM
%0793-1054 - TDR_PROBE_04 READINGS / PARAMETERS / WAVE_FORM
%1055-1316 - TDR_PROBE_05 READINGS / PARAMETERS / WAVE_FORM
%1317-1578 - TDR_PROBE_06 READINGS / PARAMETERS / WAVE_FORM
%1579-1840 - TDR_PROBE_07 READINGS / PARAMETERS / WAVE_FORM
%1841-2102 - TDR_PROBE_08 READINGS / PARAMETERS / WAVE_FORM
%2103-2364 - TDR_PROBE_09 READINGS / PARAMETERS / WAVE_FORM
%2365-2626 - TDR_PROBE_10 READINGS / PARAMETERS / WAVE_FORM
%2627-2888 - TDR_PROBE_11 READINGS / PARAMETERS / WAVE_FORM
%2889-3150 - TDR_PROBE_12 READINGS / PARAMETERS / WAVE_FORM
%3151-3412 - TDR_PROBE_13 READINGS / PARAMETERS / WAVE_FORM
%3413-3674 - TDR_PROBE_14 READINGS / PARAMETERS / WAVE_FORM
%3675-3936 - TDR_PROBE_15 READINGS / PARAMETERS / WAVE_FORM
%3937-4198 - TDR_PROBE_16 READINGS / PARAMETERS / WAVE_FORM
%4199 - IRROMETER_01
%4200 - IRROMETER_02
%4201 - IRROMETER_03
%4202 - IRROMETER_04
%4203 - IRROMETER_05
%4204 - IRROMETER_06
%4205 - IRROMETER_07
%4206 - IRROMETER_08
%4207 - IRROMETER_09
%4208 - IRROMETER_10
%4209 - IRROMETER_11
%4210 - IRROMETER_12
%4211 - IRROMETER_13
%4212 - IRROMETER_14
%4213 - THERMOCOUPLE_1
%4214 - THERMOCOUPLE_2
%4215 - THERMOCOUPLE_3
%4216 - THERMOCOUPLE_4
%4217 - TIPPING BUCKET
%4218 - PV_VOLTAGE 1
%4219 - PV_VOLTAGE 2
%%
clear
clc
%raw_name = input('name of .dat file? ','s');
raw_name = 'datatest.dat';
```

```
lv1_path = 'C:\Users\cxg021\Desktop\';
raw_path = strcat(lv1_path,raw_name);
data_raw = load(raw_path);
[a b] = size(data_raw);
mkdir(lv1_path,date);
lv2_path = strcat(lv1_path,date,'\');
disp(strcat('Readings Recorded','_',num2str(b)))
if b == 4219
   disp('Proper Array Length Detected')
else
   disp('Unexpected Array Length Detected!')
   error_array_size = strcat('Expected 4219 Locs, Found_',num2str(b),' Locs');
   disp(error_array_size);
end

for i = 1:a
data_sgl = zeros(1,b);
data_sgl(:) = data_raw(i,:);
y = num2str(data_sgl(1,2));
d = num2str(data_sgl(1,3));
h = num2str(data_sgl(1,4));
proc_path = strcat(y,'_',d,'_',h);
[sucess, message, messageid] = mkdir(lv2_path,proc_path);
lv3_path = strcat(lv2_path,proc_path,'\');
   if sucess == 0
      disp(strcat('File Error-',message,messageid));
   else
      for ii = 1:15
         ini_pos = 10+(ii-1)*262;
         if ii < 10;
         probe_path = strcat('tdr_0',num2str(ii));
         else
         probe_path = strcat('tdr_',num2str(ii));
         end
         mkdir(lv3_path,probe_path);
         lv4_path = strcat(lv3_path,probe_path,'\');
         for jj = 1:258
          wave_form(jj)=data_sgl(ini_pos+(jj-1));
         end
         tdr_lal_cs(a,ii) = data_sgl(ini_pos-3);
         tdr_vwc_cs(a,ii) = data_sgl(ini_pos-2);
         tdr_bec_cs(a,ii) = data_sgl(ini_pos-1);
         [tdr_lal_tn(a,ii)  fun_check  wave_x  wave_y]  =
tan_method(wave_form,lv4_path,tdr_lal_cs);
         if fun_check == 0
         disp('Wave Form Error. Min Value Detected Before Max Value!')
```

```
        disp(strcat('Error at...',probe_path,'...Verify Plot'))
        figure
        plot(wave_x(:),wave_y(:));
        input('Continue ? 1/0 ')
        else
          figure
        plot(wave_x(:),wave_y(:));
        end

      end
   end
end
```

Appendix E

```
%%DATA LOGGER .DAT EXTRACTION FOR PROCESSING
%CYRUS GARNER
%%
%%OUTPUT ARRAY FOR .DAT FROM CR10X AS A,4235 ARRAY
%ARRAY POSITION - VAR
%0001 -
%0002 - YEAR
%0003 - DAY
%0004 - SECOND
%0005 - BATTERY_VOLTAGE (BAT_VOLT)
%0006 - DL_TEMPERATURE (DL_TEMP)
%0007 - TDR_PROBE_01 LA_L VALUE (BY TDR100)
%0008 - TDR_PROBE_01 WATER_CONTENT (BY TDR100 AND TOPPS)
%0009 - TDR_PROBE_01 E_VALUE
%0010 - TDR_PROBE_01 WAVE_FORM_01 PARAMETER_1 - AVERAGING
%0011 - TDR_PROBE_01 WAVE_FORM_01 PARAMETER_2 - DATA_AQ_MODE
%0012 - TDR_PROBE_01 WAVE_FORM_01 PARAMETER_3 - NUMBER SAMPLES
%0013 - TDR_PROBE_01 WAVE_FORM_01 PARAMETER_4 - WINDOW START
%0014 - TDR_PROBE_01 WAVE_FORM_01 PARAMETER_5 - WINDOW LENGTH
%0015 - TDR_PROBE_01 WAVE_FORM_01 PARAMETER_6 - PROBE LENGTH
%0016 - TDR_PROBE_01 WAVE_FORM_01 PARAMETER_7 - PROBE OFFSET
%0017 - TDR_PROBE_01 WAVE_FORM_01 PARAMETER_8 - MULTIPLIER
%0018 - TDR_PROBE_01 WAVE_FORM_01 PARAMETER_9 - OFFSET
%0019-0268 - TDR_PROBE_1 WAVE_FORM_1
%0269 - TDR_PROBE_02 LA_L VALUE (BY TDR100)
%0270 - TDR_PROBE_02 WATER_CONTENT (BY TDR100 AND TOPPS)
%0271 - TDR_PROBE_02 E_VALUE
%0272 - TDR_PROBE_02 WAVE_FORM_02 PARAMETER_1 - AVERAGING
%0273 - TDR_PROBE_02 WAVE_FORM_02 PARAMETER_2 - DATA_AQ_MODE
%0274 - TDR_PROBE_02 WAVE_FORM_02 PARAMETER_3 - NUMBER SAMPLES
%0275 - TDR_PROBE_02 WAVE_FORM_02 PARAMETER_4 - WINDOW START
%0276 - TDR_PROBE_02 WAVE_FORM_02 PARAMETER_5 - WINDOW LENGTH
%0277 - TDR_PROBE_02 WAVE_FORM_02 PARAMETER_6 - PROBE LENGTH
%0278 - TDR_PROBE_02 WAVE_FORM_02 PARAMETER_7 - PROBE OFFSET
%0279 - TDR_PROBE_02 WAVE_FORM_02 PARAMETER_8 - MULTIPLIER
%0280 - TDR_PROBE_02 WAVE_FORM_02 PARAMETER_9 - OFFSET
%0281-0530 - TDR_PROBE_02 WAVE_FORM_02
%0531-0792 - TDR_PROBE_03 READINGS / PARAMETERS / WAVE_FORM
%0793-1054 - TDR_PROBE_04 READINGS / PARAMETERS / WAVE_FORM
%1055-1316 - TDR_PROBE_05 READINGS / PARAMETERS / WAVE_FORM
%1317-1578 - TDR_PROBE_06 READINGS / PARAMETERS / WAVE_FORM
%1579-1840 - TDR_PROBE_07 READINGS / PARAMETERS / WAVE_FORM
%1841-2102 - TDR_PROBE_08 READINGS / PARAMETERS / WAVE_FORM
%2103-2364 - TDR_PROBE_09 READINGS / PARAMETERS / WAVE_FORM
%2365-2626 - TDR_PROBE_10 READINGS / PARAMETERS / WAVE_FORM
%2627-2888 - TDR_PROBE_11 READINGS / PARAMETERS / WAVE_FORM
%2889-3150 - TDR_PROBE_12 READINGS / PARAMETERS / WAVE_FORM
%3151-3412 - TDR_PROBE_13 READINGS / PARAMETERS / WAVE_FORM
%3413-3674 - TDR_PROBE_14 READINGS / PARAMETERS / WAVE_FORM
%3675-3936 - TDR_PROBE_15 READINGS / PARAMETERS / WAVE_FORM
%3937-4198 - TDR_PROBE_16 READINGS / PARAMETERS / WAVE_FORM
%4199 - IRROMETER_01
%4200 - IRROMETER_02
%4201 - IRROMETER_03
```

```
%4202 - IRROMETER_04
%4203 - IRROMETER_05
%4204 - IRROMETER_06
%4205 - IRROMETER_07
%4206 - IRROMETER_08
%4207 - IRROMETER_09
%4208 - IRROMETER_10
%4209 - IRROMETER_11
%4210 - IRROMETER_12
%4211 - IRROMETER_13
%4212 - IRROMETER_14
%4213 - THERMOCOUPLE_1
%4214 - THERMOCOUPLE_2
%4215 - THERMOCOUPLE_3
%4216 - THERMOCOUPLE_4
%4217 - TIPPING BUCKET
%4218 - PV_VOLTAGE 1
%4219 - PV_VOLTAGE 2
%%
function [output] = data_extraction(raw_name,lv2_path_s);
%clear, close all, clc
%warning off MATLAB:MKDIR:DirectoryExists
%  raw_name = input('name of .dat file? ','s');
raw_name = raw_name
lv1_path = 'lv2_path_s';
raw_path = strcat(lv1_path,raw_name);
data_raw = load(raw_name);
[a b] = size(data_raw);

tdr_lal_tm = zeros(a,14);
tdr_vwc_tm = zeros(a,14);
tdr_lal_cs = zeros(a,14);
tdr_vwc_cs = zeros(a,14);
tdr_bec_cs = zeros(a,14);
wave_1y = zeros(249,a);
wave_2y = zeros(249,a);
wave_3y = zeros(249,a);
wave_4y = zeros(249,a);
wave_5y = zeros(249,a);
wave_6y = zeros(249,a);
wave_7y = zeros(249,a);
wave_8y = zeros(249,a);
wave_9y = zeros(249,a);
wave_10y = zeros(249,a);
wave_11y = zeros(249,a);
wave_12y = zeros(249,a);
wave_13y = zeros(249,a);
wave_14y = zeros(249,a);
wave_form = zeros(1,259);
precip = zeros(a,1);
tc_s = zeros(1,a);
tc_a = zeros(1,a);
pv_1 = zeros(1,a);
pv_2 = zeros(1,a);

irr = zeros(a,14);
```

```
irr_gr = zeros(a,14);


mkdir(lv1_path,date);
lv2_path = strcat(lv1_path,date,'\');
disp(strcat('Readings Recorded','_',num2str(b)))
if b == 4235
    disp('Proper Array Length Detected')
else
    disp('Unexpected Array Length Detected!')
    error_array_size = strcat('Expected 4235 Locs, Found_',num2str(b),'
Locs');
    disp(error_array_size);
end

for i = 1:a
data_sgl = zeros(1,b);
data_sgl(:) = data_raw(i,:);
y = num2str(data_sgl(1,2));
d = num2str(data_sgl(1,3));
h = num2str(data_sgl(1,4));
proc_path = strcat(y,'_',d,'_',h);
[sucess, message, messageid] = mkdir(lv2_path,proc_path);
lv3_path = strcat(lv2_path,proc_path,'\');
    if sucess == 0
        disp(strcat('File Error-',message,messageid));
    else
        for ii = 1:14
            ii;
            ini_pos = 10+(ii-1)*262;
            if ii < 10;
            probe_path = strcat('tdr_0',num2str(ii));
            else
            probe_path = strcat('tdr_',num2str(ii));
            end
            mkdir(lv3_path,probe_path);
            lv4_path = strcat(lv3_path,probe_path,'\');
            for jj = 1:258
             wave_form(jj)=data_sgl(ini_pos+(jj-1));
            end
            if ii == 1
             %   wave_six(:,i)=wave_form(ii);
             del_x = wave_form(5)/wave_form(3);
                for k = 1:wave_form(3)-1
                wave_1x(k,1) = wave_form(4)+k*del_x;
                wave_1y(k,i) = wave_form(+8);
                end
                [tdr_lal_tm(i,1) fun_check wave_x wave_y] =
tan_method5(wave_1x(:,1), wave_1y(:,i), wave_form,lv4_path,probe_path);
            elseif ii == 2
                del_x = wave_form(5)/wave_form(3);
              %  wave_seven(:,i)=wave_form(ii);
                 for k = 1:wave_form(3)-1
                wave_2x(k,1) = wave_form(4)+k*del_x;
                wave_2y(k,i) = wave_form(k+8);
                 end
```

```
                [tdr_lal_tm(i,2) fun_check wave_x wave_y] =
tan_method5(wave_2x(:,1), wave_2y(:,i), wave_form,lv4_path,probe_path);
             elseif ii == 3
                del_x = wave_form(5)/wave_form(3);
              %  wave_seven(:,i)=wave_form(ii);
                 for k = 1:wave_form(3)-1
                wave_3x(k,1) = wave_form(4)+k*del_x;
                wave_3y(k,i) = wave_form(k+8);
                 end
                 [tdr_lal_tm(i,3) fun_check wave_x wave_y] =
tan_method5(wave_3x(:,1), wave_3y(:,i), wave_form,lv4_path,probe_path);
            elseif ii == 4
               % wave_eight(:,i)=wave_form(ii);
               del_x = wave_form(5)/wave_form(3);
                for k = 1:wave_form(3)-1
                wave_4x(k,1) = wave_form(4)+k*del_x;
                wave_4y(k,i) = wave_form(k+8);
                end
                [tdr_lal_tm(i,4) fun_check wave_x wave_y] =
tan_method5(wave_4x(:,1), wave_4y(:,i), wave_form,lv4_path,probe_path);
            elseif ii == 5
                del_x = wave_form(5)/wave_form(3);
               % wave_five(:,i)=wave_form(ii);
                for k = 1:wave_form(3)-1
                wave_5x(k,1) = wave_form(4)+k*del_x;
                wave_5y(k,i) = wave_form(k+8);
                end
                [tdr_lal_tm(i,5) fun_check wave_x wave_y] =
tan_method5(wave_5x(:,1), wave_5y(:,i), wave_form,lv4_path,probe_path);
             elseif ii == 6
                del_x = wave_form(5)/wave_form(3);
              %  wave_seven(:,i)=wave_form(ii);
                 for k = 1:wave_form(3)-1
                wave_6x(k,1) = wave_form(4)+k*del_x;
                wave_6y(k,i) = wave_form(k+8);
                 end
                 [tdr_lal_tm(i,6) fun_check wave_x wave_y] =
tan_method5(wave_6x(:,1), wave_6y(:,i), wave_form,lv4_path,probe_path);
             elseif ii == 7
                del_x = wave_form(5)/wave_form(3);
              %  wave_seven(:,i)=wave_form(ii);
                 for k = 1:wave_form(3)-1
                wave_7x(k,1) = wave_form(4)+k*del_x;
                wave_7y(k,i) = wave_form(k+8);
                 end
                 [tdr_lal_tm(i,7) fun_check wave_x wave_y] =
tan_method5(wave_7x(:,1), wave_7y(:,i), wave_form,lv4_path,probe_path);
            elseif ii == 8
               % wave_eight(:,i)=wave_form(ii);
               del_x = wave_form(5)/wave_form(3);
                for k = 1:wave_form(3)-1
                wave_8x(k,1) = wave_form(4)+k*del_x;
                wave_8y(k,i) = wave_form(k+8);
                end
                [tdr_lal_tm(i,8) fun_check wave_x wave_y] =
tan_method5(wave_8x(:,1), wave_8y(:,i), wave_form,lv4_path,probe_path);
            elseif ii == 9
```

```
                del_x = wave_form(5)/wave_form(3);
               % wave_five(:,i)=wave_form(ii);
                for k = 1:wave_form(3)-1
                wave_9x(k,1) = wave_form(4)+k*del_x;
                wave_9y(k,i) = wave_form(k+8);
                end
                [tdr_lal_tm(i,9) fun_check , ~, wave_y] =
tan_method5(wave_9x(:,1), wave_9y(:,i), wave_form,lv4_path,probe_path);
            elseif ii == 10
                del_x = wave_form(5)/wave_form(3);
              %  wave_seven(:,i)=wave_form(ii);
                 for k = 1:wave_form(3)-1
                wave_10x(k,1) = wave_form(4)+k*del_x;
                wave_10y(k,i) = wave_form(k+8);
                 end
                 [tdr_lal_tm(i,10) fun_check wave_x wave_y] =
tan_method5(wave_10x(:,1), wave_10y(:,i), wave_form,lv4_path,probe_path);
             elseif ii == 11
                del_x = wave_form(5)/wave_form(3);
              %  wave_seven(:,i)=wave_form(ii);
                 for k = 1:wave_form(3)-1
                wave_11x(k,1) = wave_form(4)+k*del_x;
                wave_11y(k,i) = wave_form(k+8);
                end
                 [tdr_lal_tm(i,11) fun_check wave_x wave_y] =
tan_method5(wave_11x(:,1), wave_11y(:,i), wave_form,lv4_path,probe_path);
            elseif ii == 12
               % wave_eight(:,i)=wave_form(ii);
               del_x = wave_form(5)/wave_form(3);
                for k = 1:wave_form(3)-1
                wave_12x(k,1) = wave_form(4)+k*del_x;
                wave_12y(k,i) = wave_form(k+8);
                end
                [tdr_lal_tm(i,12) fun_check wave_x wave_y] =
tan_method5(wave_12x(:,1), wave_12y(:,i), wave_form,lv4_path,probe_path);
            elseif ii == 13
                del_x = wave_form(5)/wave_form(3);
               % wave_five(:,i)=wave_form(ii);
                for k = 1:wave_form(3)-1
                wave_13x(k,1) = wave_form(4)+k*del_x;
                wave_13y(k,i) = wave_form(k+8);
                end
                [tdr_lal_tm(i,13) fun_check wave_x wave_y] =
tan_method5(wave_13x(:,1), wave_13y(:,i), wave_form,lv4_path,probe_path);
            elseif ii == 14
                del_x = wave_form(5)/wave_form(3);
               % wave_five(:,i)=wave_form(ii);
                for k = 1:wave_form(3)-1
                wave_14x(k,1) = wave_form(4)+k*del_x;
                wave_14y(k,i) = wave_form(k+8);
                end
                [tdr_lal_tm(i,14) fun_check wave_x wave_y] =
tan_method5(wave_14x(:,1), wave_14y(:,i), wave_form,lv4_path,probe_path);
            end
            tdr_lal_cs(i,ii) = data_sgl(ini_pos-3);
            tdr_vwc_cs(i,ii) = data_sgl(ini_pos-2);
            tdr_bec_cs(i,ii) = data_sgl(ini_pos-1);
```

```
       if tdr_lal_tm(i,ii) >= 3.57
                                tdr_vwc_tm(i,ii) =
            (tdr_lal_tm(i,ii)^2)^3*(4.3e-6)-(5.5e-
            4)*(tdr_lal_tm(i,ii)^2)^2+(2.92e-2)*(tdr_lal_tm(i,ii)^2)-(5.3e-
            2);
       else
             %tdr_vwc_tm(i,ii) = 5e-05*(tdr_lal_tm(i,ii)^2)^5-
0.0027*(tdr_lal_tm(i,ii)^2)^4+0.0519*%(tdr_lal_tm(i,ii)^2)^3-
.4275*(tdr_lal_tm(i,ii)^2)^2+1.2614*(tdr_lal_tm(i,ii)^2)^1-.0727;
       end


            if tdr_vwc_tm(i,ii) <= 0
                tdr_vwc_tm(i,ii) = 0;
        elseif tdr_vwc_tm(i,ii) >= 0.6
        tdr_vwc_tim(i,ii) = 0.6
            end
        end
    end
    disp(strcat('Percent Complete_',num2str(i/a*100),'_%'))
end
et = 0;
for i=1:a
    et = 1+et;
    for ii=1:16

        irr(i,ii) = data_raw(i,ii+4198);
        rel(i,ii) = data_raw(i,ii+4214);
        if irr(i,ii) == 0;
         irr_gr(i,ii) = 0;
        else
         irr_gr(i,ii) = (2*rel(i,ii)/1000-
2*irr(i,ii)/1000)/((265*.01110)/100);
        end
    end
end
figure

for i=1:a
    precip(i) = data_raw(i,4233)*1;
end
for i =1:a
    tc_s(i) = data_raw(i,4234);
    tc_a(i) = data_raw(i,4235);
end
for i=1:a
    pv_1(i) = data_raw(i,4231);
    if pv_1(i) <= 0
        pv_1(i) = 0;
    end
    pv_2(i) = data_raw(i,4232);
    if pv_2(i) <= 0
        pv_2(i) = 0;
    end
end
```

```
for i=1:a
    rec_yr(i) = data_raw(i,2);
    rec_dy(i) = data_raw(i,3);
    rec_hr(i) = floor(data_raw(i,4)/100);
    rec_mn(i) = data_raw(i,4)-rec_hr(i)*100;
    %note will have to be updated for 2013
    rec_time(i) = rec_dy(i)*24+rec_hr(i)+rec_mn(i)/60;
end
th_e(:,1) = tc_s';
th_e(:,2) = tc_a';
pv_e(:,1) = pv_1';
pv_e(:,2) = pv_2';
rain(:,1) = precip';
bv_e(:,1) = data_raw(:,5);
rt_e(:,1) = rec_time';
%CORRECT IRROMETER FOR LAND LOCS ON AM416
ir_e(:,1) = irr_gr(:,13)';
ir_e(:,2) = irr_gr(:,16)';
ir_e(:,3) = irr_gr(:,11)';
ir_e(:,4) = irr_gr(:,12)';
ir_e(:,5) = irr_gr(:,9)';
ir_e(:,6) = irr_gr(:,6)';
ir_e(:,7) = irr_gr(:,15)';
ir_e(:,8) = irr_gr(:,10)';
ir_e(:,9) = irr_gr(:,1)';
ir_e(:,10) = irr_gr(:,8)';
ir_e(:,11) = irr_gr(:,3)';
ir_e(:,12) = irr_gr(:,4)';
ir_e(:,13) = irr_gr(:,7)';
ir_e(:,14) = irr_gr(:,2)';

output(:,1) = rt_e(:,1);
output(:,2) = rt_e(:,1)-rt_e(1,1);
output(:,3) = rec_dy(:)';
output(:,4) = rec_hr(:)';
output(:,5) = bv_e(:,1)';
output(:,6) = th_e(:,1)';
output(:,7) = th_e(:,2)';
output(:,8) = pv_e(:,1)';
output(:,9) = pv_e(:,2)';
output(:,10) = pv_e(:,1)*11/1000';
output(:,11) = pv_e(:,2)*11/1000';
output(:,12) = rain(:,1);
output(:,13) = ir_e(:,1)-22.77;
output(:,14) = ir_e(:,2)-22.77;
output(:,15) = ir_e(:,3)-22.77;
output(:,16) = ir_e(:,4)-22.77;
output(:,17) = ir_e(:,5)-22.77;
output(:,18) = ir_e(:,6)-22.77;
output(:,19) = ir_e(:,7)-22.77;
output(:,20) = ir_e(:,8)-22.77;
output(:,21) = ir_e(:,11)-22.77;
output(:,22) = ir_e(:,10)-22.77;
output(:,23) = ir_e(:,9)-22.77;
output(:,24) = ir_e(:,12)-22.77;
output(:,25) = ir_e(:,13)-22.77;
output(:,26) = ir_e(:,14)-22.77;
```

```
output(:,27) = tdr_vwc_tm(:,1);
output(:,28) = tdr_vwc_tm(:,2);
output(:,29) = tdr_vwc_tm(:,3);
output(:,30) = tdr_vwc_tm(:,4);
output(:,31) = tdr_vwc_tm(:,5);
output(:,32) = tdr_vwc_tm(:,6);
output(:,33) = tdr_vwc_tm(:,7);
output(:,34) = tdr_vwc_tm(:,8);
output(:,35) = tdr_vwc_tm(:,9);
output(:,36) = tdr_vwc_tm(:,10);
output(:,37) = tdr_vwc_tm(:,11);
output(:,38) = tdr_vwc_tm(:,12);
output(:,39) = tdr_vwc_tm(:,13);
output(:,40) = tdr_vwc_tm(:,14);
output(:,41) = tdr_lal_tm(:,1);
output(:,42) = tdr_lal_tm(:,2);
output(:,43) = tdr_lal_tm(:,3);
output(:,44) = tdr_lal_tm(:,4);
output(:,45) = tdr_lal_tm(:,5);
output(:,46) = tdr_lal_tm(:,6);
output(:,47) = tdr_lal_tm(:,7);
output(:,48) = tdr_lal_tm(:,8);
output(:,49) = tdr_lal_tm(:,9);
output(:,50) = tdr_lal_tm(:,10);
output(:,51) = tdr_lal_tm(:,11);
output(:,24) = tdr_lal_tm(:,12);
output(:,25) = tdr_lal_tm(:,13);
output(:,26) = tdr_lal_tm(:,14);
```

Appendix E

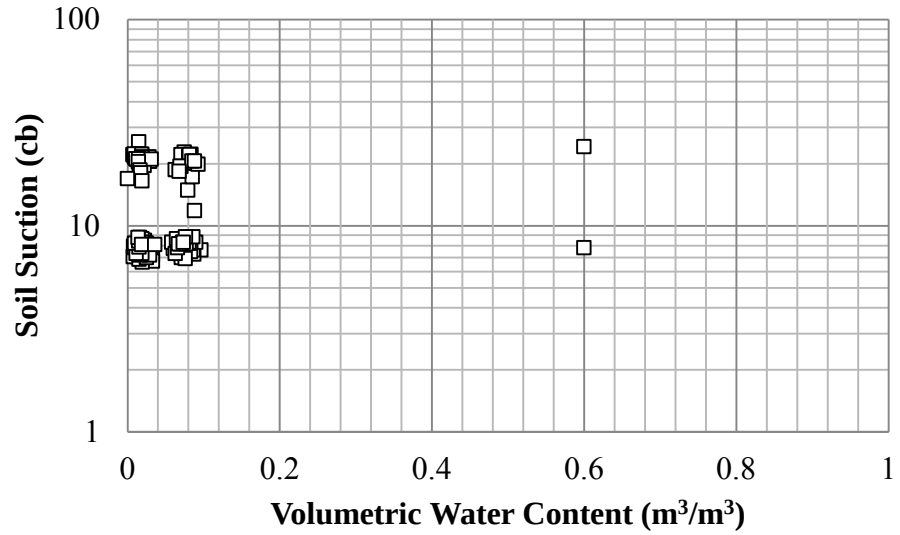

Figure E.1. Soil suction vs. volumetric water content for station 1.

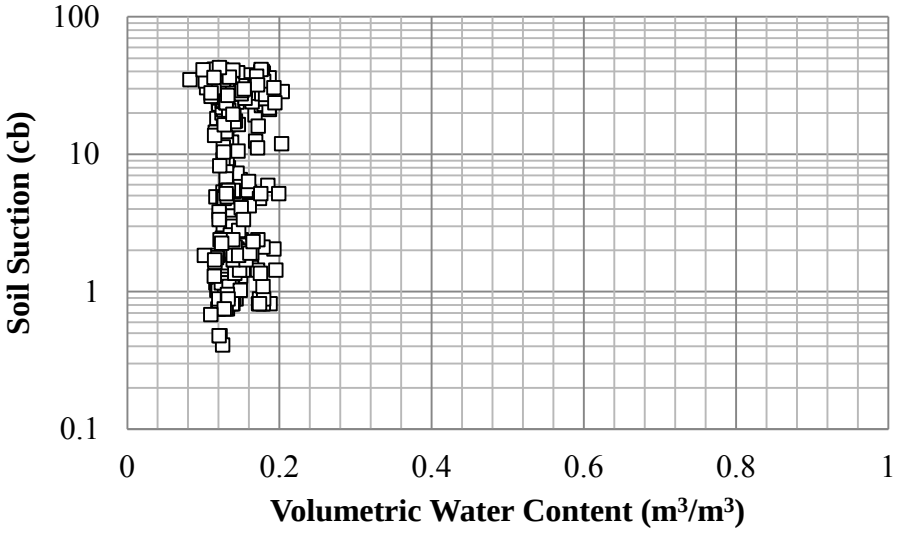

Figure E.2. Soil suction vs. volumetric water content for station 2.

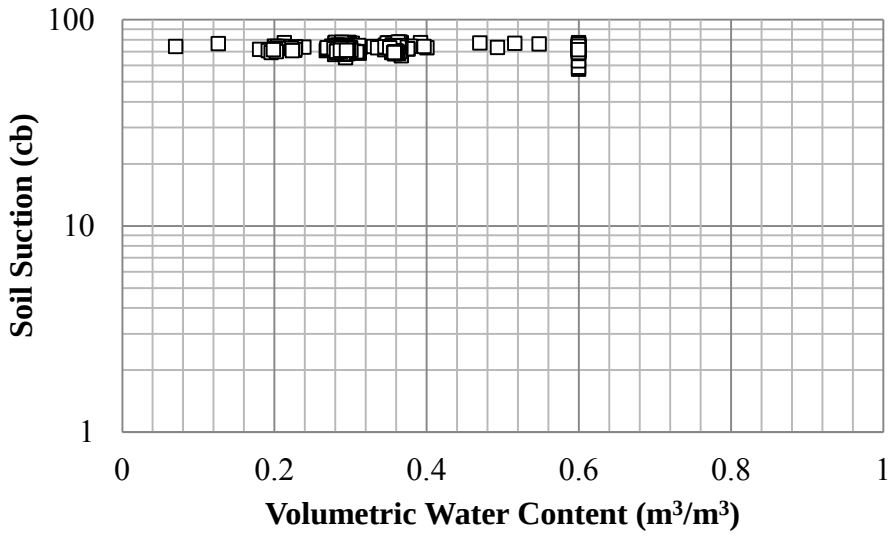

Figure E.3. Soil suction vs. volumetric water content for station 3.

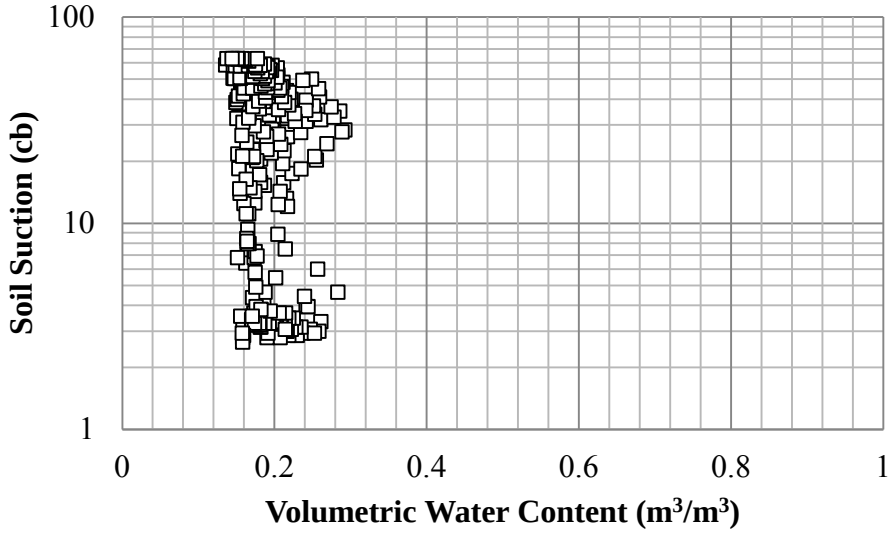

Figure E.4. Soil suction vs. volumetric water content for station 4.

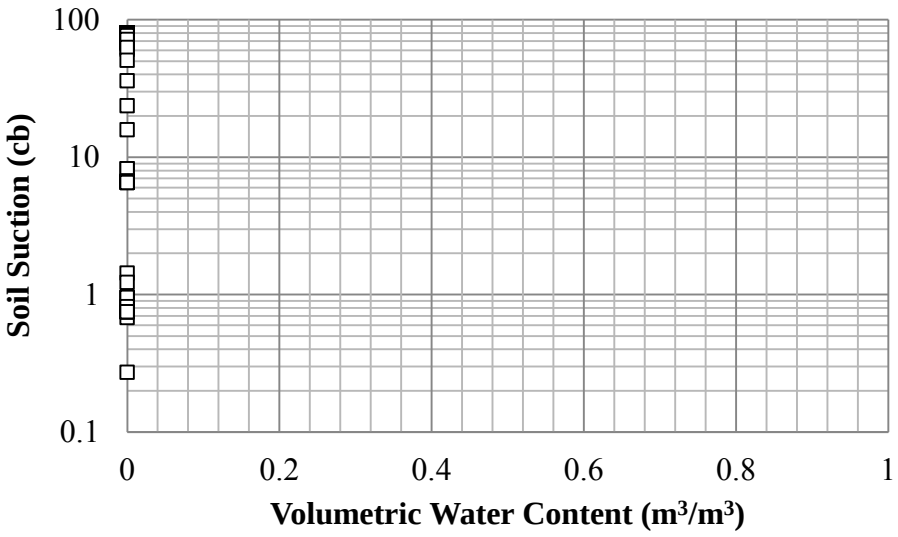

Figure E.5. Soil suction vs. volumetric water content for station 5.

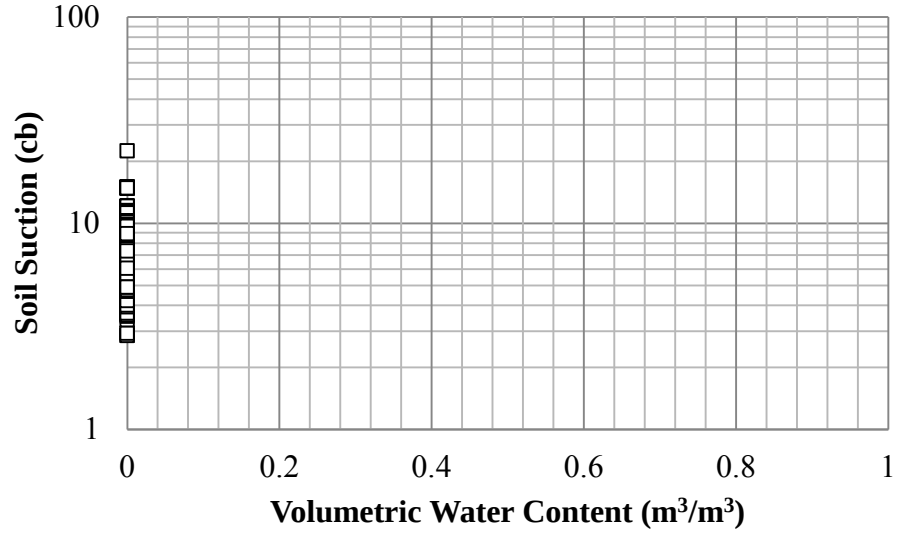

Figure E.6. Soil suction vs. volumetric water content for station 6.

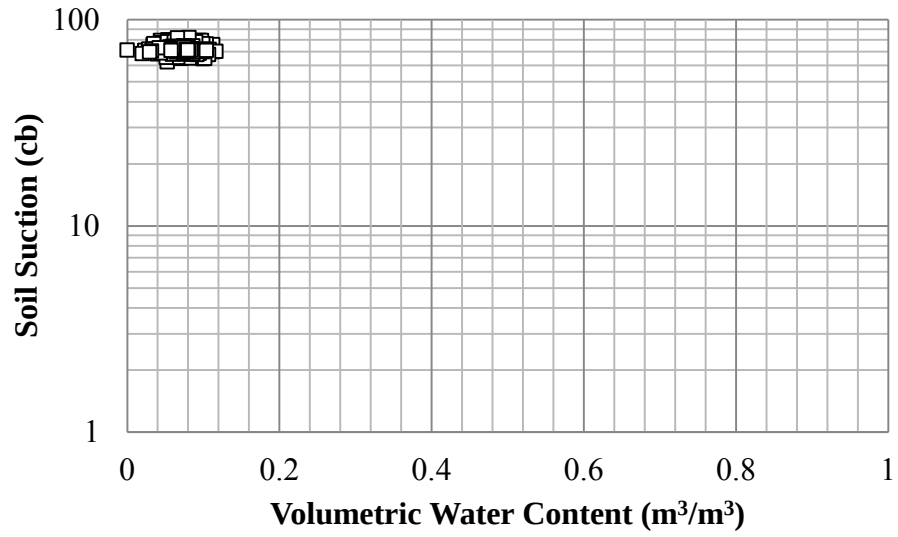

Figure E.7. Soil suction vs. volumetric water content for station 7.

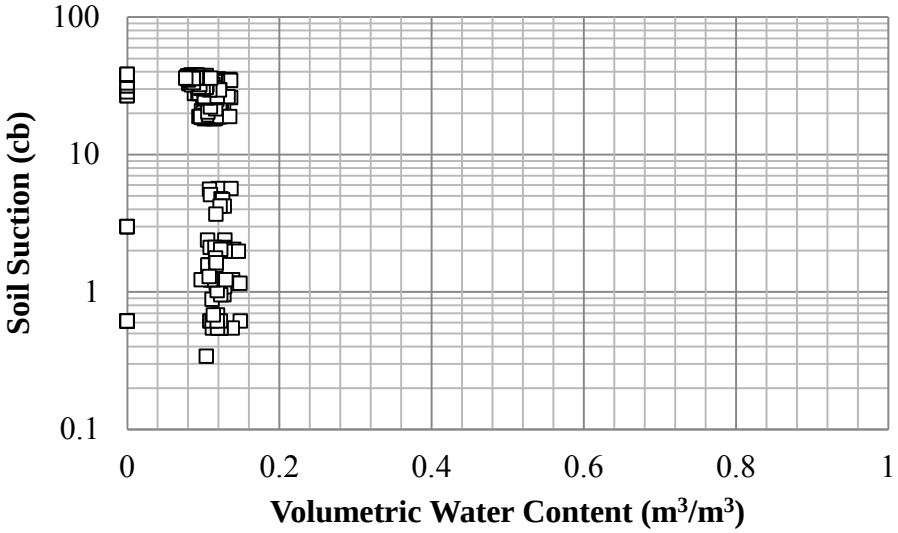

Figure E.8. Soil suction vs. volumetric water content for station 8.

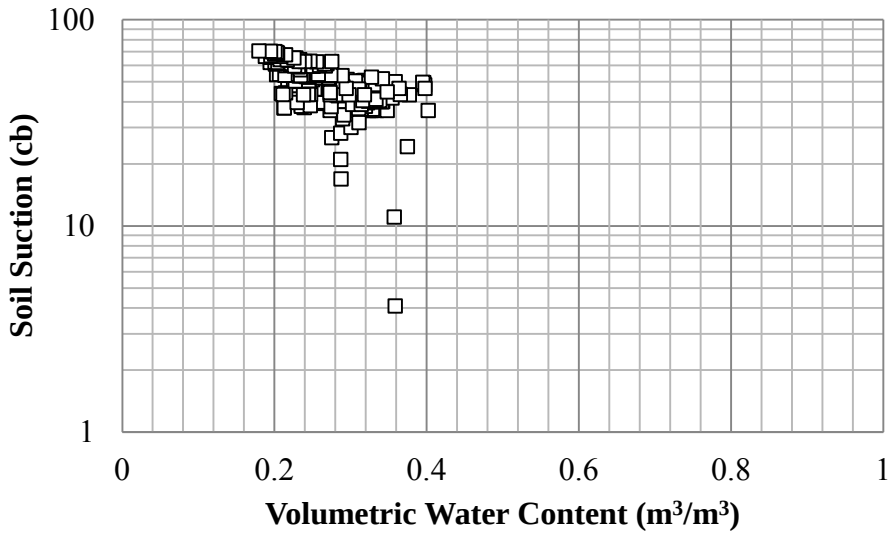

Figure E.9. Soil suction vs. volumetric water content for station 9.

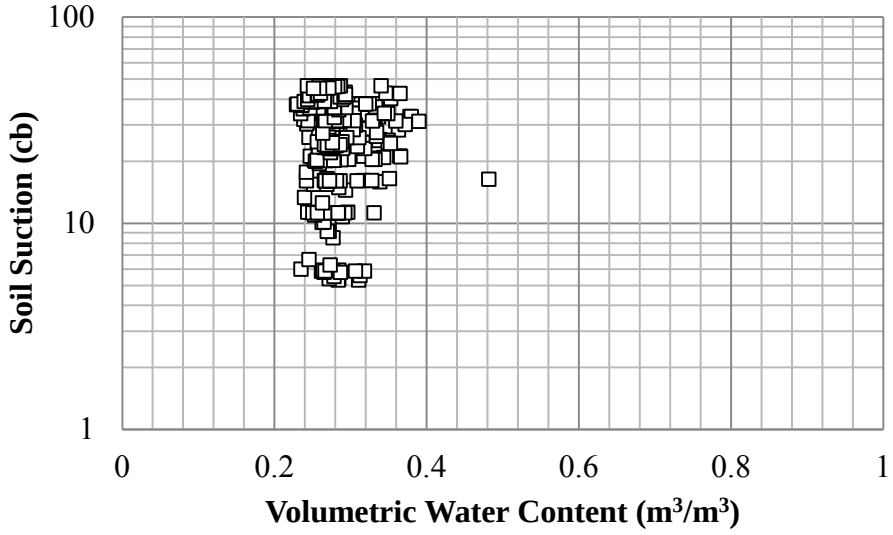

Figure E.10. Soil suction vs. volumetric water content for station 10.

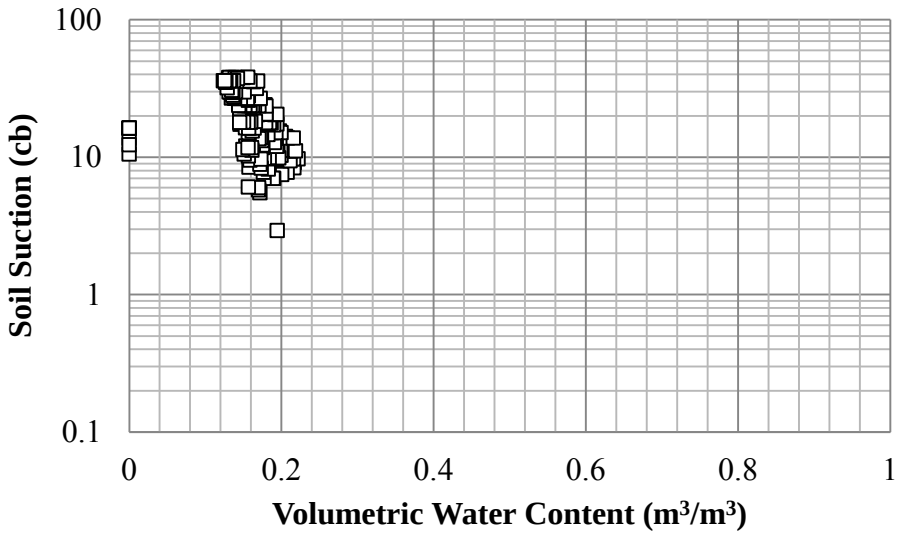

Figure E.11. Soil suction vs. volumetric water content for station 11.

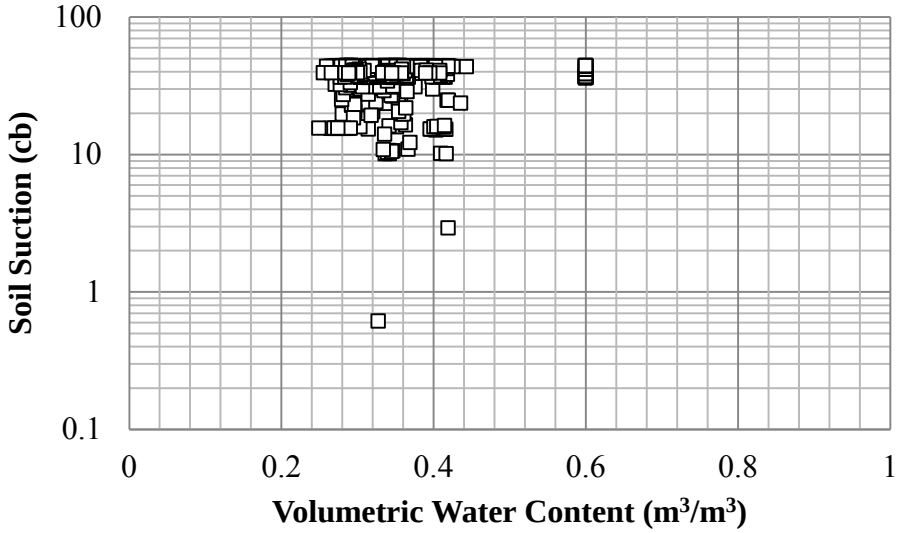

Figure E.12. Soil suction vs. volumetric water content for station 12.

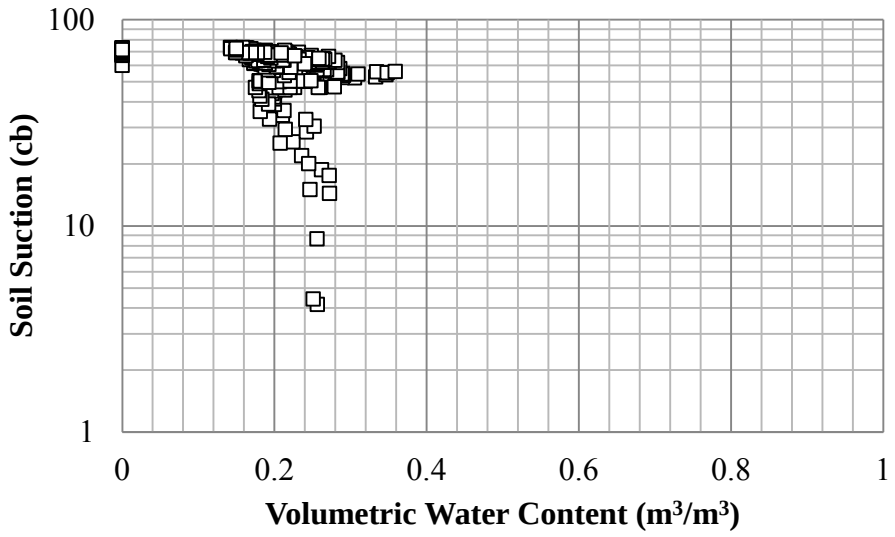

Figure E.13. Soil suction vs. volumetric water content for station 13.

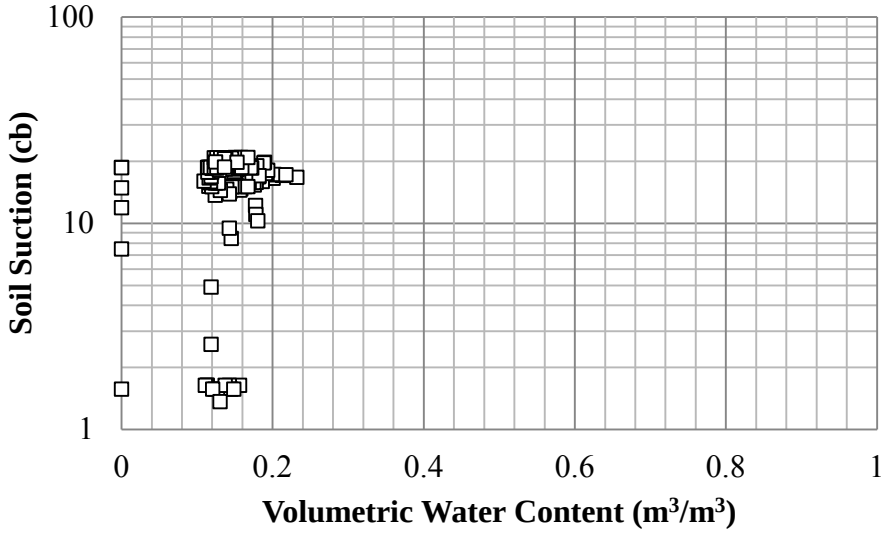

Figure E.14. Soil suction vs. volumetric water content for station 14.